UNCLASSIFIED

SECURITY CLASSIFICATION OF THIS PAGE *(When Data Entered)*

REPORT DOCUMENTATION PAGE		READ INSTRUCTIONS BEFORE COMPLETING FORM
1. REPORT NUMBER NAVENVPREDRSCHFAC Contractor Report CR 84-10	2. GOVT ACCESSION NO.	3. RECIPIENT'S CATALOG NUMBER
4. TITLE *(and Subtitle)* Parameterization of Subgrid-Scale Fluxes in Mesoscale Meteorological Models		5. TYPE OF REPORT & PERIOD COVERED Final Report
		6. PERFORMING ORG. REPORT NUMBER ARAP A-535
7. AUTHOR(s) W.S. Lewellen, R.I. Sykes, S.F. Parker		8. CONTRACT OR GRANT NUMBER(s) N00228-83-C-3073
9. PERFORMING ORGANIZATION NAME AND ADDRESS Aeronautical Research Assoc. of Princeton, Inc. 50 Washington Rd., P.O. Box 2229 Princeton, NJ 08540		10. PROGRAM ELEMENT, PROJECT, TASK AREA & WORK UNIT NUMBERS PE 62759N PN WF59-551 TA 001 NEPRF WU 6.2-4
11. CONTROLLING OFFICE NAME AND ADDRESS Naval Air Systems Command Department of the Navy Washington, DC 20361		12. REPORT DATE December 1984
		13. NUMBER OF PAGES 122
14. MONITORING AGENCY NAME & ADDRESS*(if different from Controlling Office)* Naval Environmental Prediction Research Facility Monterey, CA 93943-5106		15. SECURITY CLASS. *(of this report)* UNCLASSIFIED
		15a. DECLASSIFICATION/DOWNGRADING SCHEDULE

16. DISTRIBUTION STATEMENT *(of this Report)*

Approved for public release; distribution is unlimited.

17. DISTRIBUTION STATEMENT *(of the abstract entered in Block 20, if different from Report)*

18. SUPPLEMENTARY NOTES

19. KEY WORDS *(Continue on reverse side if necessary and identify by block number)*

Turbulent flux parameterization
Convective scalar diffusion
Free convection surface layer
Cumulus parameterization
Planetary boundary layer

20. ABSTRACT *(Continue on reverse side if necessary and identify by block number)*

The problem of subgrid turbulent flux parameterization for mesoscale meteorological models is considered. A particular scheme is recommended, based on a quasi-equilibrium approximation to the A.R.A.P. second-order closure model of turbulent transport in the atmosphere. Tests of this scheme, as compared with results from a full second-order closure, high resolution, 1-D model, indicate reasonable results when the model grid resolution is adequate to include a few points in the unstable boundary layer. ((Continued on reverse))

DD FORM 1 JAN 73 1473 EDITION OF 1 NOV 65 IS OBSOLETE
S/N 0102-014-6601

UNCLASSIFIED

SECURITY CLASSIFICATION OF THIS PAGE *(When Data Entered)*

Block 20, Abstract, continued.

The scheme incorporates cumulus parameterization as an integral part of the quasi-equilibrium, and suggests that intermittency is a fundemental feature of cumulus cloud environment. Further testing of the scheme is recommended, particularly for the cumulus parameterization.

ROUTINE REPLY, ENDORSEMENT, TRANSMITTAL OR INFORMATION SHEET

OPNAV 5216/158 (Rev. 7-78) *A WINDOW ENVELOPE MAY BE USED*
SN 0107-LF-052-1691 *Formerly NAVEXOS 3789*

CLASSIFICATION (*UNCLASSIFIED when detached from enclosures, unless otherwise indicated*) UNCLASSIFIED

FROM (*Show telephone number in addition to address*)
Commanding Officer, Naval Environmental Prediction Research Facility, Monterey, CA 93943-5106 AVN 878-2928

DATE 18 Mar 85

SUBJECT
FORWARDING OF NAVENVPREDRSCHFAC TECHNICAL PUBLICATION

SERIAL OR FILE NO.
5600
Ser 93

TO:
Distribution
[Encl (1), p. Dist-1]

REFERENCE

ENCLOSURE
(1) NAVENVPREDRSCHFAC Contractor Report CR 84-10, Parameterization of Subgrid-Scale Fluxes in Mesoscale Meteorological Models

VIA:

ENDORSEMENT ON

[X] FORWARDED [ ] RETURNED [ ] FOLLOW-UP, OR TRACER [ ] REQUEST [ ] SUBMIT [ ] CERTIFY [ ] MAIL [ ] FILE

GENERAL ADMINISTRATION	CONTRACT ADMINISTRATION	PERSONNEL
[ ] FOR APPROPRIATE ACTION	[ ] NAME & LOCATION OF SUPPLIER OF SUBJECT ITEMS	[ ] REPORTED TO THIS COMMAND:
[ ] UNDER YOUR COGNIZANCE	[ ] SUBCONTRACT NO. OF SUBJECT ITEM	
[X] INFORMATION & retention	[ ] APPROPRIATION SYMBOL, SUBHEAD, AND CHARGEABLE ACTIVITY	[ ] DETACHED FROM THIS COMMAND
[ ] APPROVAL RECOMMENDED [ ] YES [ ] NO	[ ] SHIPPING AT GOVERNMENT EXPENSE [ ] YES [ ] NO	[ ] OTHER
[ ] APPROVED [ ] DISAPPROVED	[ ] A CERTIFICATE, VICE BILL OF LADING	
[ ] COMMENT AND/OR CONCURRENCE	[ ] COPIES OF CHANGE ORDERS, AMENDMENT OR MODIFICATION	
[ ] CONCUR	[ ] CHANGE NOTICE TO SUPPLIER	
[ ] LOANED, RETURN BY:	[ ] STATUS OF MATERIAL ON PURCHASE DOCUMENT	
[ ] SIGN RECEIPT & RETURN		
[ ] REPLY TO THE ABOVE BY:		
[ ] REFERENCE NOT RECEIVED		
[ ] SUBJECT DOCUMENT FORWARDED TO:		
[ ] SUBJECT DOCUMENT RETURNED FOR:		
[ ] SUBJECT DOCUMENT HAS BEEN REQUESTED, AND WILL BE FORWARDED WHEN RECEIVED		
[ ] COPY OF THIS CORRESPONDENCE WITH YOUR REPLY		
[ ] ENCLOSURE NOT RECEIVED		
[ ] ENCLOSURE FORWARDED AS REQUESTED		
[ ] ENCLOSURE RETURNED FOR CORRECTION AS INDICATED		
[ ] CORRECTED ENCLOSURE AS REQUESTED		
[ ] REMOVE FROM DISTRIBUTION LIST		
[ ] REDUCE DISTRIBUTION AMOUNT TO:		

REMARKS (*Continue on reverse*)

Enclosure (1) describes the development and testing of techniques for representing turbulent transfer in mesoscale meteorological models. This will allow more accurate model depiction of the planetary boundary layer.

SIGNATURE & TITLE

By direction

COPY TO:

CLASSIFICATION (*UNCLASSIFIED when detached from enclosures, unless otherwise indicated*) UNCLASSIFIED

★ G.P.O.: 1982-587-016/5340

AN (1) AD-A153 016
FG (2) 040200
CI (3) (U)
CA (5) AERONAUTICAL RESEARCH ASSOCIATES OF PRINCETON INC NJ
TI (6) Parameterization of Subgrid-Scale Fluxes in Mesoscale Meteorological Models.
TC (8) (U)
DN (9) Final rept.,
AU (10) Lewellen,W. S.
AU (10) Sykes,R. I.
AU (10) Parker,S. F.
RD (11) Dec 1984
PG (12) 121p
RS (14) ARAP-535
CT (15) N00228-83-C-3073
PJ (16) F59551
RN (18) NEPRF-CR-84-10
RC (20) Unclassified report
DE (23) *TURBULENCE, MASS TRANSFER, EQUILIBRIUM(GENERAL), CONVECTION(ATMOSPHERIC), TROPOSPHERE, MATHEMATICAL MODELS, GRIDS(COORDINATES), SCALE, CUMULUS CLOUDS, TRANSPORT
DC (24) (U)
ID (25) Parameterization, PE62759N, WU624
IC (26) (U)
AB (27) The problem of subgrid turbulent flux parameterization for mesoscale meteorological models is considered. A particular scheme is recommended, based on a quasi-equilibrium approximation to the A.R.A.P. second-order closure model of turbulent transport in the atmosphere. Tests of this scheme, as compared with results from a full second-order closure, high resolution, 1-D model, indicate reasonable results when the model grid resolution is adequate to include a few points in the unstable boundary layer. The scheme incorporates parameterization as an integral part of the quasi-equilibrium, and suggests that intermittency is a fundamental feature of cumulus cloud environment. Further testing of the scheme is recommended, particularly for the cumulus parameterization. Keywords: Turbulent flux parameterization; Convective scalar diffusion; Free convection surface layer; Cumulus parameterization; Planetary boundary layer.
AC (28) (U)
DL (33) 01
SE (34) F
CC (35) 008400

NAVENVPREDRSCHFAC
CONTRACTOR REPORT
CR 84-10

NAVENVPREDRSCHFAC CR 84-10

PARAMETERIZATION OF SUBGRID-SCALE FLUXES IN MESOSCALE METEOROLOGICAL MODELS

Prepared By:

W. S. Lewellen, R. I. Sykes, S. F. Parker
Aeronautical Research Associates of Princeton, Inc.
Princeton, NJ 08540

Contract No. N00228-83-C-3073

DECEMBER 1984

Prepared For:
NAVAL ENVIRONMENTAL PREDICTION RESEARCH FACILITY
MONTEREY, CALIFORNIA 93943-5106

CONTENTS

1. INTRODUCTION

The grid resolution in any mesoscale meteorological model is inadequate to resolve all the turbulent transport processes likely to be important in the troposphere. Accurate simulation of the physical mechanisms which are controlled by turbulence depend on how faithful the subgrid flux parameterization can represent those turbulent transport processes. In this report we use the A.R.A.P., second-order closure model of turbulent transport in the atmosphere as an aid in developing a practical subgrid flux parameterization scheme. The dynamic equations for the second-order flux quantities of interest are used to suggest practical approximations, and relatively high resolution simulation results from our existing one and two-dimensional models of the atmospheric boundary layer are used to test the accuracy of tentative schemes.

Before developing a subgrid flux parameterization scheme it is desirable to get a clear concept of what motions the parameterization are to represent. The parameterization should represent the effect of the average of the ensemble of motions which are of too fine a scale to be resolved by the mesoscale model. These ensemble average considerations are discussed in Appendix A, a reprint of an AMS Workshop presentation in October, 1983. One needs to make a conscious choice of the scale which is to divide the fluid motions into a resolved mean motion and an unresolved turbulent motion. The unresolved ensemble scale, for most mesoscale models, will include all of the boundary layer scale eddies and most of the individual cloud motions. The most unique feature of our proposed subgrid flux parameterization is the attempt to incorporate cumulus parameterization as an integral part of the turbulent transport model.

We recommend using a quasi-equilibrium approximation to our second-order closure transport model. This approximation combines a prognostic equation for the turbulent kinetic energy with diagnostic equations between local gradients of the mean quantities and the turbulent fluxes and integral surface layer relations. Again, the most attractive feature of this proposed scheme is the incorporation of cumulus parameterization as an integral part of the turbulent transport model.

Results of six different tests of the proposed formulation are described. Further testing of the scheme is required, particularly for the cumulus parameterization, but these preliminary results should justify a continuation of this approach.

2. PROPOSED SCHEME

As discussed in Appendix A, it is necessary to ensemble average over horizontal length scales which are at least 4 times the desired grid length. Thus, in any mesoscale model it will be necessary to ensemble average over length scales which are much bigger than the height of the planetary boundary layer. It follows that vertical gradients of the mean variables will be much larger than horizontal gradients so that a quasi 1-D parameterization of the subgrid turbulent fluxes is appropriate; i.e., although the variables are a function of time and all 3 space coordinates, the subgrid fluxes will be primarily driven by the vertical gradients. After reducing the problem to a quasi 1-D problem, it is still necessary to decide on the level of the turbulent closure to be used. Although full Reynolds stress closure may eventually prove desirable, a reasonable compromise between the desire to provide as much physics in the turbulent transport as possible without unduly increasing the numerical complexity, is to use a quasi-equilibrium approximation for the turbulent flux equations. This approximation combines a prognostic equation for the turbulent kinetic energy with diagnostic relations between local gradients of the mean quantities and the turbulent fluxes.

The equation for the turbulent kinetic energy may be modeled as (Lewellen, 1981):

$$\frac{D(q^2/2)}{Dt} = - \overline{u'w'} \frac{\partial \bar{u}}{\partial z} - \overline{v'w'} \frac{\partial \bar{v}}{\partial z} + \frac{g}{T_o} \overline{w'\theta_v'} + v_c \frac{\partial}{\partial z} \left(\frac{q\Lambda \partial (q^2/2)}{\partial z} \right) - \frac{bq^3}{\Lambda} \tag{2.1}$$

The last 2 modeled terms representing diffusion by turbulent transport and

turbulent dissipation are not specified until the turbulent length scale Λ is specified. Again consistent with our desire to minimize increased complexity we choose the following, relatively simple algebraic specification:

$$\Lambda = \min (0.65\ z,\ \Lambda^*,\ q/2N) \tag{2.2}$$

unless

$$\left|\frac{d\Lambda}{dz}\right| > 0.65, \text{ in which case } \left|\frac{d\Lambda}{dz}\right| = 0.65. \tag{2.3}$$

z is height above the surface, $q^2 = \overline{u_i u_i}$ is twice the turbulent kinetic energy, and $N^2 = \left(g/T_o\right) dT/dz$ is the Brunt-Vaisala frequency if positive, otherwise this term is neglected in the minimization. Λ^* is a measure of the scale of the turbulent region and is set equal to $0.22 z_4$, where z_4 is the height at which q^2 becomes one quarter of the surface value, i.e., the outer edge of the boundary layer. The constant 0.22 was chosen to obtain good agreement with experimental observations of $\overline{w'w'}$. The second restriction on the slope of Λ is used to prevent Λ from decreasing too sharply in any inversion region, since it would be physically unrealistic for the lengthscale to change too abruptly. The scale may be determined by sweeping upward from the surface applying the minimum criterion until the slope bound is exceeded; then the scale is set using the scale at the point below, together with the slope criterion. This simple specification of Λ is probably one of the major limiting factors on our proposed parameterization, but any of the available more complicated formulations do not appear warranted for this level of approximation at the present time.

The diagnostic relations for the vertical turbulent fluxes are obtained by assuming local equilibrium in all of the equations involving second order correlations except the horizontal velocity fluctuations. This yields:

$$\overline{u'w'} = - q\Lambda S_m \frac{\partial \bar{u}}{\partial z} \tag{2.4}$$

$$\overline{v'w'} = - q\Lambda S_m \frac{\partial \bar{v}}{\partial z} \tag{2.5}$$

$$\overline{w'\theta'} = - q\Lambda S_H \frac{\partial \bar{\theta}}{\partial z} \tag{2.6}$$

$$\overline{w'h'} = - q\Lambda S_H \frac{\partial \bar{h}}{\partial z} \tag{2.7}$$

where S_m and S_H are the following stability dependent coefficients:

$$S_H = \frac{(1-2b)}{3[A + (2 + 1/bs)R]} \tag{2.8}$$

$$S_m = S_H \frac{A + (1/bs - 1/A)R}{1 + R/A} \tag{2.9}$$

where $R = \left(g\Lambda^2/q^2T_o\right) \partial T/\partial z$, and A,b, and s are our standard model coefficients (0.75, 0.125, 1.8).

Equations 2.8 and 2.9 are somewhat simpler than the expressions used in Mellor and Yamada's (1974) level 2-1/2 model because we have assumed the vertical velocity variance equation to be in local equilibrium while their relations assumed 1/3rd of the local q^2 imbalance in Equation 2.1 to be apportioned to the $\overline{w'w'}$ balance. Which is more physical is arguable since an imbalance under atmospheric boundary layer conditions appears more likely to persist in the horizontal velocity variance. Our principal reason for choosing local balance in $\overline{w'w'}$ to close the equations is because this leaves S_m and S_H independent of the local velocity gradient.

This quasi-equilibrium parameterization of the subgrid-scale fluxes provides a robust formulation except under conditions which may lead to extreme values of R. Under unstable conditions S_H has a singularity near R = -0.12. Generally, we do not expect this limit to be reached since as S_H becomes large the heat flux production term in Equation 2.1 increases q^2 and thus reduces R. For added robustness, S_H is not allowed to exceed 2, in which

case S_m is also set equal to 2. This limit is set high enough it is rarely invoked, but low enough to not cause problems when it is. Also, R is not allowed to exceed 1, which gives a lower limit of 0.035 for S_H; note that this is only a restriction in the region where the slope criterion governs the choice of Λ, since otherwise

$$\Lambda < q/2N, \text{ i.e., } \Lambda^2 \frac{g}{T_o} \frac{\partial T}{\partial z} < q^2/4 \qquad (2.10)$$

3. SURFACE BOUNDARY CONDITION PARAMETERIZATION

Appropriate surface boundary conditions for any numerical meteorological simulation depend critically on the vertical grid resolution next to the surface. We wish to provide a formulation of the surface transport coefficients which does not require the detailed resolution of a part of the surface layer flow. We would like our formulation to be completely compatible with the standard surface layer relationships but yet sufficiently robust that it can give approximately valid results when the minimal resolution is so coarse as to include the total boundary layer within the model layer adjacent to the surface.

We choose to define the surface transport coefficients by:

$$C_{f_u} = - \overline{u'w'}_o \Big/ qu_1 \tag{3.1}$$

$$C_{f_V} = - \overline{v'w'}_o \Big/ qv_1 \tag{3.2}$$

$$C_\Theta = - \overline{w'\Theta'}_o \Big/ q(\Theta_1 - \Theta_o) \tag{3.3}$$

when the subscript o represents the surface value at z_o and the subscript 1 represents the average of the quantity between the surface and midway between the first two grid points. We designate this height as z_a.

We choose to involve q, in the definitions of Equations 3.1-3.3, rather than use either u, or u_* in the place of this characteristic velocity as is most often done. This removes some of the variation from the transport

coefficients without adding complications since the surface value of q already is needed as a boundary condition on Equation 2.1. With this definition the coefficients are not forced to become very large as free convection conditions are approached. The boundary conditions are now completed by providing a specification for the surface transport coefficients and the turbulent velocity fluctuation q. An expression for q_1 is derived by integrating the turbulent kinetic energy equation between z_o and z_a.

$$1/2\,\frac{\partial q_1^2}{\partial t} = \frac{1}{z_a}\int_{z_o}^{z_a}\left[-\overline{u'w'}\,\frac{\partial \bar{u}}{\partial z} - \overline{v'w'}\,\frac{\partial \bar{v}}{\partial z} + \frac{g}{T_o}\,\overline{w'\theta'} - \frac{q^3}{8\Lambda}\right] dz \qquad (3.4)$$

For purposes of our surface parameterization we will ignore the LHS of Equation 3.4 since the time scale of the turbulence in the surface layer should be short in comparison to the time scale of the mesoscale model simulation. The turbulent scale Λ appearing in the last term can be taken as proportional to z, i.e. αz, up to some height which depends on either stability or the boundary layer thickness. A reasonable representation of Equation 3.4 then should be to take

$$q_1^2 = 8\alpha\left[c_{f_u}u_1^2 + c_{f_v}v_1^2 + \frac{g}{T_o}\,C_\theta\left(\theta_o - \theta_1\right)z_a\right] \Big/ g_1\left(z_a, z_o, z_s\right) \qquad (3.5)$$

where

$$g_1 = \ln\frac{z_a}{z_o} \qquad z_a \le z_s$$

$$= \ln\frac{z_s}{z_o} + \frac{1}{z_s}\left(z_a - z_s\right) \qquad z_a > z_s \qquad (3.6)$$

and z_s is a height based on the maximum value of Λ which is yet to be defined. After some experimentation with this expression we found it desirable also to limit the heat flux term to damp out no more than 20% of the shear flow term under stable conditions. This corresponds to imposing an upper bound on the

flux Richardson number.

Approximations for the transport coefficients may be obtained from integrals of the Reynolds stress and heat flux equations between z_o and z_a. We begin with the Reynolds stress equations as modeled by our second-order closure approach(Lewellen, 1981) and integrate them between z_o and z_a. Under neutral, homogeneous, quasi-steady conditions, these equations may be written as:

$$\int \frac{q}{\Lambda} \overline{u'w'}\, dz = -\int \overline{w'w'} \frac{\partial u}{\partial z}\, dz \tag{3.7}$$

$$\int \frac{q}{\Lambda} \overline{v'w'}\, dz = -\int \overline{w'w'} \frac{\partial v}{\partial z}\, dz \tag{3.8}$$

$$\int \frac{q}{\Lambda} \overline{w'\Theta'}\, dz = -\int \frac{4}{3} \overline{w'w'} \frac{\partial T}{\partial z}\, dz \tag{3.9}$$

When Λ is assumed equal to αz, q and $\overline{w'w'}$ are taken as constant, and $\overline{u'w'}$, $\overline{v'w'}$, and $\overline{\Theta'w'}$ are taken as linear, these equations reduce to

$$C_{f_u} = \left[\alpha \frac{\overline{w'w'}}{q^2} \frac{u_a}{u_1} + \frac{\overline{u'w'}_a}{qu_1} \right] \Big/ \left(\ln \frac{z_a}{z_o} - 1 \right) \tag{3.10}$$

$$C_{f_v} = \left[\alpha \frac{\overline{w'w'}}{q^2} \frac{v_a}{v_1} + \frac{\overline{v'w'}_a}{qv_1} \right] \Big/ \left(\ln \frac{z_a}{z_o} - 1 \right) \tag{3.11}$$

$$C_{\Theta} = \left[\alpha \frac{4\overline{w'w'}}{3q^2} \frac{\Theta_a - \Theta_o}{\Theta_1 - \Theta_o} + \frac{\overline{\Theta'w'}_a}{q\,(\Theta_1 - \Theta_o)} \right] \Big/ \left(\ln \frac{z_a}{z_o} - 1 \right) \tag{3.12}$$

When the turbulent fluxes at z_a are specified by the subgrid flux parameterization between points 1 and 2, the mean value of u,v, and Θ are averaged between their respective values at points 1 and 2, and $\overline{w'w'}/q^2$ is approximated as equal to 1/4; Equations 3.10-3.12 provide approximate expressions for the determination of the surface transport coefficients defined in Equations 3.1-3.3.

If z_a falls within the surface layer where $\overline{u'w'}_a = \overline{u'w'}_o$, u - ln z/z_o, etc., these last 3 equations reduce to.

$$C_{f_u} = C_{f_v} = (0.16) \Big/ \left(\ln \frac{z_a}{z_o} - 1 \right) \tag{3.13}$$

$$C_{\Theta} = (0.22) \Big/ \left(\ln \frac{z_a}{z_o} - 1 \right) \tag{3.14}$$

Where we have given $\alpha\ \overline{w'w'}/q^2$ its neutral value of 0.16.

There are 3 types of modifications which must be considered for Equations 3.13 and 3.14. There are the stability modifications which can be made within the framework of the constant flux surface layer. There are the effects of pressure gradients and heat sinks which force the turbulent transport fluxes to depart from their surface values. Finally, there are modifications required when z_a extends above the height to which the turbulent scale can be taken as proportional to z. Let us consider stability modifications first.

The surface layer relationships are familiarly given in terms of z/L. i.e., for stable conditions

$$U = \frac{U_*}{k} \left[\ln z/z_o + 4.7\ z/L \right] \tag{3.15}$$

$$\Theta_1 - \Theta_o = \frac{\Theta_*}{k} \left[0.74 \ln z/z_o + 4.7\ z/L \right] \tag{3.16}$$

Equations 3.15 and 3.16 may be integrated and inverted to give expressions for the transport coefficients as a function of z_a/L. In order to improve the robustness of the formulation we choose to approximate the stability factor in terms of the layer bulk Richardson number.

$$Ri_B = \frac{g}{To} \frac{\left(\Theta_1 - \Theta_o\right) z_a}{U_1^2 + V_1^2} \tag{3.17}$$

When Equations 3.15 and 3.16 are integrated and order z_o/z_a neglected it is possible to write

$$Ri_B = \left[0.74\chi + \frac{4.7\chi^2}{2}\right] \Big/ \left[1 + \frac{4.7\chi}{2}\right]^2 \tag{3.18}$$

with

$$\chi = \frac{z_a}{L} \left(\ln \frac{z_a}{z_o} - 1\right)^{-1} \tag{3.19}$$

An approximation for the stable modification which agrees very well with the standard surface layer relation is

$$C_f/C_{f_N} = \left[1 + \frac{4.7\ z_a}{2L\left(\ln\frac{z_a}{z_o} - 1\right)}\right]^{-1} \approx \frac{1 - 4.7\ Ri_B/2}{1 + 4.7\ Ri_B/6} \tag{3.20}$$

The 2 expressions for C_f/C_{f_N} in Equation 3.20 are compared in Figure 3.1. The two forms are almost indistinguishable. The compatible expressions for C_Θ are

$$C_\Theta/C_{\Theta_N} = \left[1 + \frac{4.7\ z_a}{(0.74)\,2L\left(\ln \frac{z_a}{z_o} - 1\right)}\right]^{-1} \approx \frac{1 - 4.7\ Ri_B/2}{1 + 1.83\ Ri_B} \tag{3.21}$$

These are compared in Figure 3.2. We expect the Ri_B formulation to be

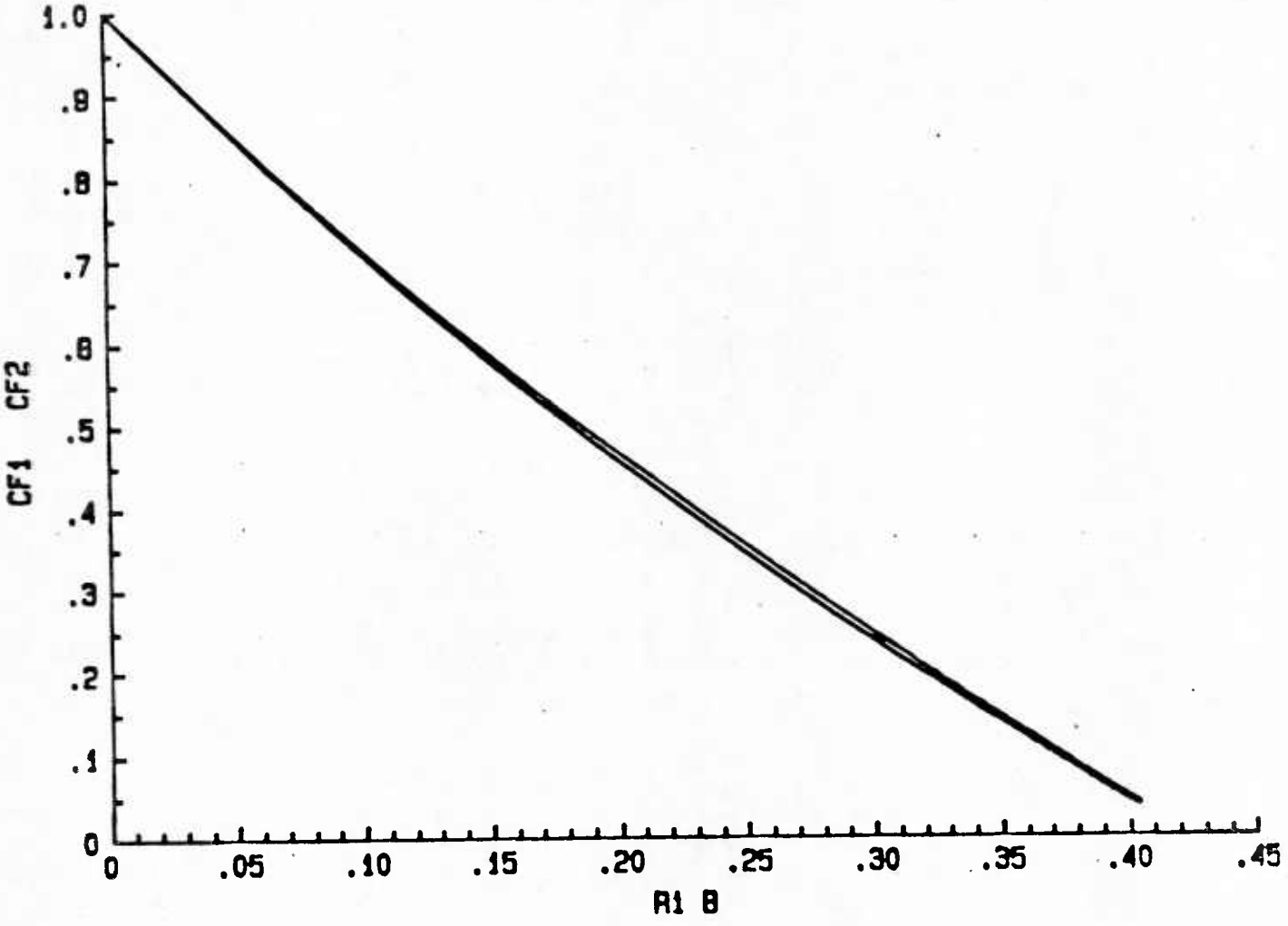

FIGURE 3.1: COMPARISON OF THE TWO EXPRESSIONS FOR C_f/C_{f_n} IN EQUATION 3.20 AS A FUNCTION OF BULK RICHARDSON NUMBER.

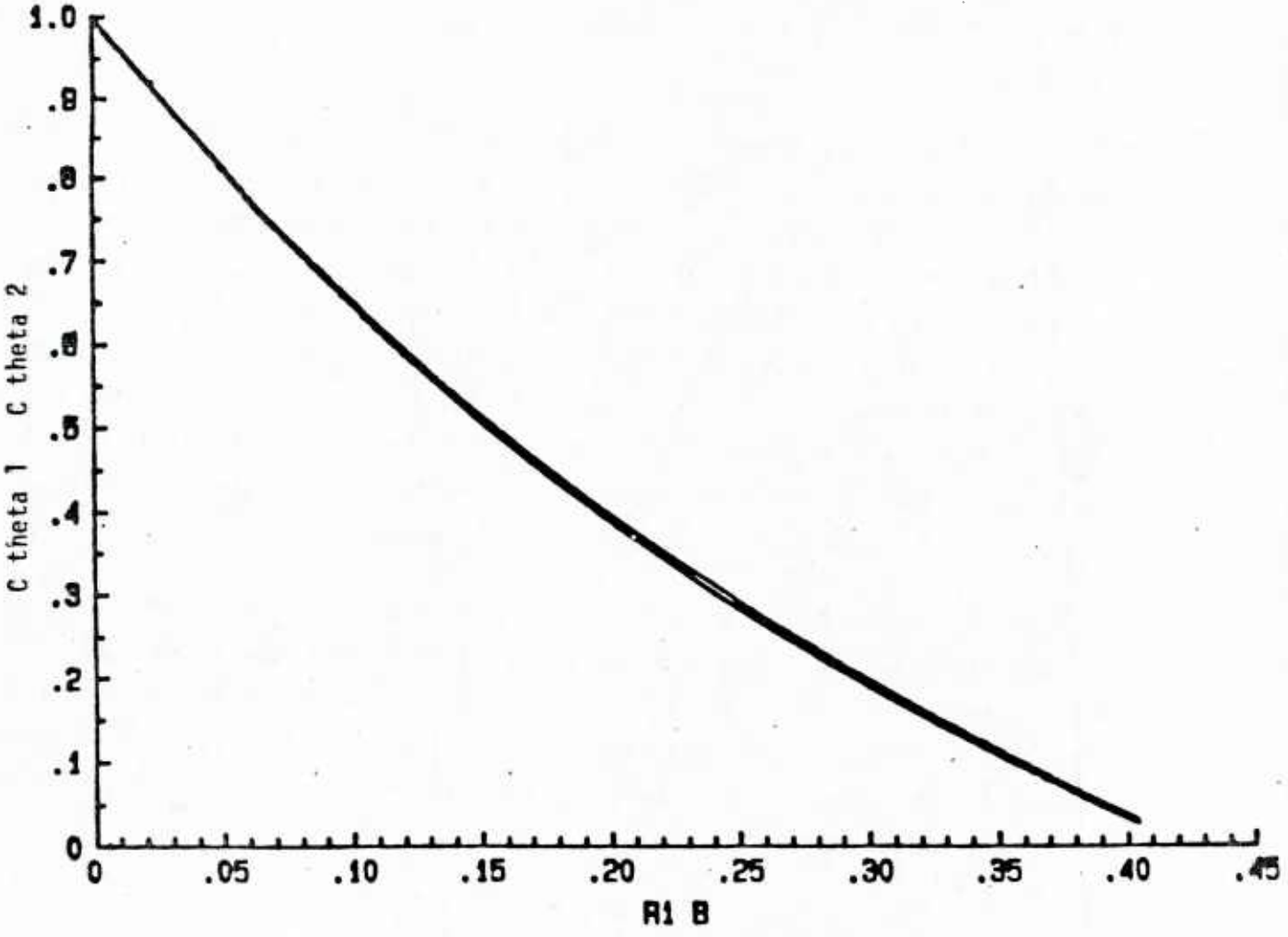

FIGURE 3.2: COMPARISON OF THE TWO EXPRESSIONS FOR C_Θ/C_{Θ_N} IN EQUATION 3.21 AS A FUNCTION OF BULK RICHARDSON NUMBER.

approximately valid even when a coarse grid is used and the model surface layer extends well beyond the actual surface layer. However, in this case, z_a can no longer be determined solely by the grid but also must be a function of the boundary layer thickness which will impose an upper bound on Ri_B to prevent Equations 3.20 and 3.21 from becoming negative. This will be discussed later.

For unstable flow we propose to use essentially the same formulation. We do not anticipate appreciable negative values of Ri_B being maintained for significant times since the strong instability should generate increased turbulence which tends to wipe out the unstable gradients. This change in transport is already accounted for by the presence of q in Equations 3.1 and 3.2. For robustness, we will not let $-Ri_B$ exceed 1/4 which is about as far as the linear form of Equation 3.17 should be expected to hold, and to add q^2, twice the turbulent kinetic energy, to the denominator of Equation 3.17 so that it remains limited even under free convection conditions. The specific limit of free convection is considered in Appendix B.

Let us now look at the effects of pressure gradients and heat sinks which force the turbulent transport fluxes to depart from their surface values. This extension of the neutral surface layer relations beyond the region of constant flux follows the analysis given by Lewellen (1977). At the surface where the advective terms are zero the mean momentum and mean energy equations may be approximated as

$$\frac{\partial \overline{u'w'}}{\partial z} = F_i \tag{3.22}$$

$$\frac{\partial \overline{\theta'w'}}{\partial z} = Q \tag{3.23}$$

where F_i is the pressure gradient vector and Q represents any distribution of heat sources (or sinks). When Equations 3.22 and 3.23 are integrated from z_o to z_a they allow the turbulent fluxes at z_a to be related to those at the

surface. Thus

$$\overline{u'w'}_a = - C_{f_u} q U_1 - F_x \left(z_a - z_o \right) \tag{3.24}$$

$$\overline{v'w'}_a = - C_{f_v} q v_1 - F_y \left(z_a - z_o \right) \tag{3.25}$$

$$\overline{\theta'w'}_a = - C_{\theta} q \left(\theta_1 - \theta_o \right) + Q \left(z_a - z_o \right) \tag{3.26}$$

These last 3 equations can be used in Equations 3.10-3.12 to obtain the influence of F and Q on the surface transfer coefficients. We use these expressions to find approximate expressions for C_{f_N} and C_{θ_N}, namely

$$C_{f_{i_N}} = \left(\frac{\alpha}{4} - \frac{F_i z_a}{q U_a} \right) \Bigg/ \left(\ln \frac{z_a}{z_o} - 1 \right) \tag{3.27}$$

$$C_{\theta_N} = \left(\frac{\alpha}{3} + \frac{Q z_a}{q \left(\theta_a - \theta_o \right)} \right) \Bigg/ \left(\ln \frac{z_a}{z_o} - 1 \right) \tag{3.28}$$

Equations 3.27 and 3.28 are appropriate as long as z_a is less than the height at which the pressure gradient term balances the surface shear stress. If these balance heights are defined as z*, then they are given from Equations 3.24 to 3.26 as:

$$z_u^* = \left| c_{f_u} q u_1 \Big/ \frac{1}{\rho} \frac{\partial p}{\partial x_o} \right| \tag{3.29}$$

$$z_v^* = \left| c_{f_u} q v_1 \Big/ \frac{1}{\rho} \frac{\partial p}{\partial y_o} \right| \tag{3.30}$$

$$z_\theta^* = \left| c_\theta q \left(\theta_1 - \theta_o \right) \Big/ \dot{Q}_o \right| \tag{3.31}$$

Now we are ready to face the problem of extrapolating the formulations to the outer regions of the boundary layer where Λ no longer increases with z and where the turbulence can not be assumed equal to its surface value. These two effects tend to partially cancel each other. In order to account for these effects in any definitive way it would be necessary to estimate the thickness of the boundary layer. We have experimented with integrals of the mean momentum equations, the temperature equation and the turbulent kinetic energy to provide estimates of the boundary layer thickness when the vertical resolution of the model is too coarse to provide a valid estimate. This formulation is presented in Equations 3.35 to 3.51, but the tests results to be presented in the next section suggests that a fairly consistent formulation is possible without adding the complexity of prognostic equations for these boundary layer thicknesses. This simpler formulation is obtained by limiting

$$|Ri_b| \leq 0.2 \tag{3.32}$$

and under stable conditions to set

$$\delta = 0.2 \left(u_1^2 + v_1^2 \right) \Big/ \frac{g}{T_o} \left(\theta_1 - \theta_o \right) \tag{3.33}$$

For purposes of estimating z_s in Equation 3.6, the maximum Λ may be estimated by setting the stable boundary layer thickness as equal to 5L (Deardorff, 1972), and $\Lambda_{max} = 0.2L$ (Lewellen & Teske, 1973). This yields

$$z_s = 0.012 \left(u_1^2 + v_1^2 \right) \Big/ \frac{g}{T_o} \left(\theta_1 - \theta_o \right) \tag{3.34}$$

Equations 3.20 and 3.21 are extrapolated beyond the surface layer by restricting the numerator to be limited as if $Ri_B \leq 0.2$, but not limiting Ri_B in the denominator. On the unstable side Ri_B is everywhere limited to ≤ 0.2.

The effect of the pressure gradient is extended by replacing the surface pressure gradient with $f(v_g - v_1)$ and $f(u_1 - u_g)$ in C_{f_U} and C_{f_V} respectively. We have not attempted to include surface layer radiation. For robustness we have also included the restriction that the angle of the surface shear stress can not depart from arctan v_1 / u_1 by more than 45°.

This completes the formulation required for the tests in the next section.

On the unstable side the tests provided in the next section generally have sufficient grid points to provide a rough estimate of δ. If the formulation is to be used with a much coarser resolution then even the unstable layer is likely to appear as a stable layer. For this coarser grid resolution it would be desirable to include an integral equation for δ. A number of prognostic equations for δ have been published e.g., Deardorff, 1972, Randall, 1979. A consistent formulation of δ may be derived from integrals of the mean momentum, temperature, and turbulent kinetic energy equations. The momentum and temperature equations may be written in the following defect form

$$\frac{\partial}{\partial t}(U_\infty - U) = \frac{\partial}{\partial z}\overline{u'w'} - f(V - V_g) + \frac{\partial}{\partial t} U_\infty \qquad (3.35)$$

$$\frac{\partial}{\partial t}(V_\infty - V) = \frac{\partial}{\partial z}\overline{v'w'} + f(U - U_g) + \frac{\partial}{\partial t} V_\infty \qquad (3.36)$$

$$\frac{\partial}{\partial t}(\Theta_\infty - \Theta) = \frac{\partial}{\partial z}\overline{w'\Theta'} - \dot{Q} + \frac{\partial}{\partial t} \Theta_\infty \qquad (3.37)$$

where by definition the subscript ∞ represents the value of the quantity in the inviscid region above the boundary layer, fV_g and fU_g represent the two components of the pressure gradient, and $\dot{Q}$ is any thermal energy source term. We can replace V_g and U_g in Equations 3.35 and 3.36 with V_∞ and U_∞, after

noting that

$$f\left(V_\infty - V_g\right) = \frac{\partial U_\infty}{\partial t} \tag{3.38}$$

and

$$f\left(U_\infty - U_g\right) = \frac{\partial V_\infty}{\partial t} \tag{3.39}$$

after integrating across the boundary layer Equations 3.35-3.37 may be written as:

$$\frac{\partial}{\partial t}\left(U_\infty \delta_u\right) = U_*^2 + fU_\infty \delta_v \tag{3.40}$$

$$\frac{\partial}{\partial t}\left(U_\infty \delta_v\right) = V_*^2 - fU_\infty \delta_u \tag{3.41}$$

$$\frac{\partial}{\partial t}\left(\theta_r \delta_\theta\right) = \theta_* U_* + S_\theta \tag{3.42}$$

where

$$\delta_u = \frac{1}{U_\infty}\int_o^\delta \left(U_\infty - U\right)\, dz \tag{3.43}$$

$$\delta_v = \frac{1}{U_\infty}\int_o^\delta \left(V_\infty - V\right)\, dz \tag{3.44}$$

$$\delta_\theta = \frac{1}{\theta_r}\int_o^\delta \left(\theta_\infty - \theta\right)\, dz \tag{3.45}$$

and

$$S_\theta = \int_o^\delta \left(Q_\infty - Q\right)\, dz \tag{3.46}$$

$$\theta_r = \theta_\infty - \theta_o = \Gamma\delta + \Delta\,\theta_s \tag{3.47}$$

The turbulent kinetic energy may be written as:

$$\frac{\partial}{\partial t}\int_{z_o}^{\delta} \frac{q^2}{2}\, dz = \int_{z_o}^{\delta} \left[- \overline{u'w'} \frac{\partial u}{\partial z} - \overline{v'w'} \frac{\partial v}{\partial z} + \frac{g}{T_o} \overline{w'\theta'} - \frac{q^3}{8\Lambda} \right] dz \qquad (3.48)$$

When we define

$$\hat{q}^2 = \frac{1}{\delta} \int_{z_o}^{\delta} q^2\, dz \qquad (3.49)$$

and assume the turbulent fluxes vary linearly across the boundary layer Equation 3.48 can be rewritten as:

$$\frac{\partial}{\partial t}\, \hat{q}^2\delta = U_\infty U_*^2 \left(1 - \frac{\delta_u}{\delta}\right) + V_\infty V_*^2 - U_\infty V_*^2 \frac{\delta_v}{\delta} + \frac{g}{T_o} \overline{\theta'w'}_o \frac{\delta}{2} - \varepsilon \qquad (3.50)$$

A reasonable form for the dissipation appears to be

$$\varepsilon = \frac{1}{8}\int_{z_o}^{\delta} \frac{q^3}{\Lambda}\, dz \approx \frac{\hat{q}^3}{8} \left[\frac{1}{\alpha} \ln \frac{z_a}{z_o} + B + AR i_B \right] \qquad (3.51)$$

where A and B are constants to be obtained by fitting high resolution runs.

During high resolution runs none of these last equations 3.40-3.51 should be required but for the general case we need to carry these prognostic equations for δ_u, δ_v, δ_θ, and $\hat{q}^2$ and provide a consistent algorithm for determining δ.

We would like δ to be a valid measure of the height to which the turbulence in the boundary layer extends. Under neutral conditions this can be provided by a simple proportionality constant, i.e.,

$$\delta = C_2 \left(\delta_u^2 + \delta_v^2 \right)^{1/2}. \tag{3.52}$$

However, when strong thermal gradients are present the spread of the turbulence is more likely to be controlled by the thermal thickness than it is by the velocity displacement thickness. A practical scheme for accomplishing this transition will require some numerical experimentation. The unstable transition is the best understood. The inversion at the top of the boundary layer takes over the governing role, with the rate of entrainment across this inversion determining the growth rate for δ. Under these conditions, when θ is nearly uniform across the boundary layer, Equation 3.45 reduces to

$$\delta_\theta = \left(\frac{\Delta\theta_i}{\theta_\infty - \theta_o} \right) \delta \tag{3.53}$$

with $\Delta\theta_i$ equal to the temperature change across the inversion. This temperature jump may be specified or may be estimated by setting the Ri across the inversion equal to a critical value and assuming its thickness to be a set fraction of the boundary layer thickness.

If

$$Ri_i = \frac{g}{To} \left(\frac{\Delta\theta_i \, (\gamma\delta)}{\left(U_\infty - U_m\right)^2 + \left(V_\infty - V_m\right)^2 + q^2} \right) \tag{3.54}$$

is fixed, then

$$\Delta\Theta_i = Ri_i\left[\left(U_\infty - U_m\right)^2 + \left(V_\infty - V_m\right)^2 + q^2\right] \Big/ \frac{g}{To}\left(\gamma\delta\right) \qquad (3.55)$$

To begin with it is safer to specify $\Delta\Theta_i$, but Equation 3.55 should provide a reasonable rough estimate with $Ri_i/\gamma \approx 1.2$. With $\Delta\Theta_i$ fixed Equation 3.53 can be used to eliminate δ_Θ and the temperature equation, Equation 3.42, becomes a prognostic equation for δ. A number of formulations of this equation under these conditions have been given in the literature.

The thermal control of the boundary layer under stable conditions is more subtle. Under stable conditions we expect the velocity gradient and the temperature gradient to be constant over the majority of the boundary layer between the surface and the top of the boundary layer. The essential dynamical control should be obtained by limiting the Ri based on these gradients to a critical value.

$$Ri_o = \frac{g}{2To}\left[\frac{\left(\Theta_\infty - \Theta_o\right)\delta_\Theta\delta^2}{U_\infty^2\left(\delta_u^2 + \delta_v^2\right)}\right] \qquad (3.56)$$

This yields

$$\delta \le \left[\frac{2\ Ri_o(crit)U_\infty^2}{g/To\left(\Theta_\infty - \Theta_o\right)\delta_\Theta}\right]^{1/2} \left[\delta_u^2 + \delta_v^2\right]^{1/2} \qquad (3.57)$$

Under stable conditions we expect the turbulent scale to be limited by the ratio of the turbulent energy to Brunt-Vaisala frequency, i.e.

$$\Lambda \le q/N = q\ \delta\left[\frac{g}{T}\left(\Theta_\infty - \Theta_o\right)\delta_\Theta\right]^{-1/2} \qquad (3.58)$$

In this case Ri_B can be computed from Equation 3.18 with

$$\chi = \alpha \frac{C_1 \left[\frac{g}{T} \left(\theta_\infty - \theta_o \right) \delta_\theta \right]^{1/2}}{q \left(\ln \frac{z_s}{z_o} - 1 \right)} \tag{3.59}$$

Thus δ is computed as the minimum of Equation 3.52 or Equation 3.57 and Ri_B is the minimum of Equation 3.17 with δ replacing z_a or Equation 3.18 with Equation 3.59.

In summary, the surface boundary conditions to be used with the quasi-equilibrium formulation of section II in the tests to be discussed in Section V are:

$$C_{f_u} = \frac{1}{\left(\ln \frac{\xi_1}{z_o} - 1 \right)} \left[0.16 - \frac{f \left(v_g - v_1 \right) z_a}{q u_1} \right] f_1 \left(Ri_b \right) \tag{3.60}$$

$$C_{f_v} = \frac{1}{\left(\ln \frac{\xi_1}{z_o} - 1 \right)} \left[0.16 + \frac{f \left(u_g - u_1 \right) z_a}{q v_1} \right] f_1 \left(Ri_b \right) \tag{3.61}$$

$$C_\theta = \frac{0.22}{\left(\ln \frac{\xi_1}{z_o} - 1 \right)} f_2 \left(Ri_b \right) \tag{3.62}$$

$$\xi_1 = \min \left(z_a, z_s \right) \tag{3.63}$$

$$f_1 \left(Ri_b \right) = \max \left[\frac{1 - 2.35 \, Ri_b}{1 + 0.78 \, Ri_b} , \frac{0.5}{1 + 0.78 \, Ri_b} \right] \tag{3.64}$$

$$f_2\left(Ri_b\right) = \max\left[\frac{1 - 2.35\ Ri_b}{1 + 1.83\ Ri_b}\ ,\ \frac{0.5}{1 + 1.83\ Ri_b}\right] \tag{3.65}$$

with

$$Ri_b = \min\left[\frac{g}{To}\ \frac{\left(\theta_1 - \theta_o\right) z_a}{u_1^2 + v_1^2 + q^2}\ ,\ 10\right] \quad \text{but} \geq -0.21 \tag{3.66}$$

$$z_s = \min\left[\frac{0.012\left(u_1^2 + v_1^2 + q^2\right)}{\left(g/T_o\right)\left(\theta_1 - \theta_o\right)},\ 0.346\right] \tag{3.67}$$

The system is closed by

$$q^2 = \max\left[\ 5.2\ \left(c_{f_u} u_1^2 + c_{f_v} v_1^2 - \frac{g}{T_o} c_\theta \left(\theta_1 - \theta_2\right) z_a\right);\right. \tag{3.68}$$

$$\left. 4.16\left(c_{f_u} u_1^2 + c_{f_v} v_1^2\right)\right] \Big/ g_1 \qquad z_a,\ z_o,\ z_s \tag{3.69}$$

$$g_1 = \ln z_a/z_o \qquad z_a \leq z_s \tag{3.70}$$

$$= \ln \frac{z_s}{z_o} + \frac{z_a}{z_s} - 1 \qquad z_a \geq z_s \tag{3.71}$$

unless a separate equation is required for δ.

4. RESULTS FOR SOME TEST PROBLEMS

The best test of any sub-grid flux parameterization is in how well it allows the model within which it is used to agree with real world data. However, it is tough to carry out conclusive tests of this type for two reasons. First, it is difficult to separate out the effects of the flux parameterization from the effects of the remaining model characteristics and second, it is seldom possible to find sufficiently complete data that all the uncertainty involved in input conditions can be removed. We have chosen an easier type of test, which involves comparing the results of coarse grid, highly parameterized simulations, with high resolution, less parameterized simulations.

We use the results of high resolution simulations using our full second-order closure model of turbulent transport as a standard, and wish to show the extent to which our low resolution parameterized model proposed in Sections 2 and 3 will agree with these high resolution results.

All the results presented in this section come from 1-D simulations where only vertical gradients are considered. These are appropriate tests for sub-grid parameterization for a model like NORAPS where the horizontal grid resolution is likely to be approximately 100km. However, to support the results of our 1-D, high resolution, full second-order closure model we have also conducted some tests using a 2-D version of our full model. The advantage of the 2-D simulations is that they are made under conditions when we expect much of the turbulent transport to be carried by relatively large 2-D eddies, which can be resolved by the grid system used. Thus, the results show little sensitivity to the closure assumptions. These 2-D, large eddy

simulations then provide direct tests of the sub-grid, flux parameterization used in the high resolution simulations. The results presented in Appendix C show that the 1-D, high resolution results are quite close to the 2-D, LES results, even under the unstable conditions where simple, second-order closure results have been reported to fail to provide satisfactory entrainment results (Zeman and Lumley, 1976), Wyngaard, 1981). These 2-D results are somewhat of a digression from our main task of providing sub-grid parameterization appropriate for a mesoscale model, but we felt it was necessary to provide clear support for the accuracy of the 1-D full closure equations before using these results as a standard for our parameterization tests.

We have chosen 3 quite different meteorological regimes to test our proposed parameterization. The first is the unstable, relatively well mixed planetary boundary layer under conditions quite similar to those used in the 2-D simulations of Appendix C. The second regime is that where a constant cooling rate is applied which allows the PBL to approach an equilibrium stable layer. The third test is where we allow the surface heat flux to transition from unstable to stable and back to unstable on a cycle which simulates a typical diurnal variation. The full closure model was run with a sufficiently fine grid to make the solution independent of the grid. The Q.E. model was run with 4 different grid resolutions as given in Table 1.

Comparisons between the Q.E. results and the full closure results for these three tests are given in Figures 4.1 to 4.17. When the great simplification in the model is considered, the Q.E. results appear quite acceptable.

Results for an unstable PBL growing into a stable region similar to conditions of Appendix C are given in Figures 4.1 to 4.2. The Q.E. result shows a negative temperature gradient across the middle of the boundary layer which is not present in the results of the full closure model. This gradient is required to maintain the positive heat flux across the bulk of the layer. The diffusion terms in the full closure model allow the heat flow with little or no gradient across much of the layer. In spite of this difference the results are reasonably close. Results for the free convection simulation of

Figures. 4.4 and 4.5 are quite similar.

Results for the constant cooling rate case are shown in Figures 4.3 to 4.7. A nominal neutral PBL with U_g = 10 m/sec, z_o = 0.01 m, f = 10^{-4} sec^{-1} is simulated for 12 hours and then a surface cooling rate of 1.8 °C/hour is applied. The near surface Δz for each of these is indicated on the figure. Figure 4.3 shows that the Q.E. model tracks the surface friction velocity very well for all of the grids tested. The surface heat flux comparison does not show quite as much agreement. The larger the grid size, the more disagreement over the first 3 hours. However, this improvement with grid resolution is not consistent in the asymptotic, late/time results.

The vertical profile of u, v, and T are given in Figures 4.5 and 4.6 at one particular time 6 hours after the cooling began. Even the coarse grid Q.E. results are quite reasonable. The maximum turbulent velocity is shown in Figure 4.7. The full closure result is significantly higher than the Q.E. results principally because the maximum q is occurring at the surface and the Q.E. models use a turbulent velocity averaged over a significant fraction of the boundary layer.

Results for the diurnal day variation are shown in Figures 4.8 to 4.17. The largest discrepancies occur in the morning transition when there is a thin unstable layer eroding the surface inversion which has built up over the night. This causes a big difference between the course resolution and fine resolution Q.E. results over approximately 6 hours.

Other comparisons are shown in Section V and in Appendices C and D.

TABLE 1

Computational Grids - Q.E. Model

Constant Cooling - Uniform grid spacing

Grid	Δz	No. Points	z(1)
A	140	7	70
B	100	10	50
C	70	14	35
D	30	31	15

Diurnal Day and Unstable Boundary Layer

Uniform grid spacing

Grid	Δz	No. Points	z(1)
C	140	7	70

Nonuniform grid spacing

Grid	Δz(1)	No. Points	z(1)
A	140	31	70
B	60	39	30

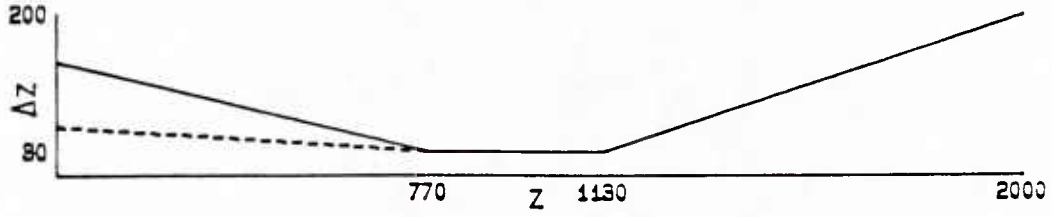

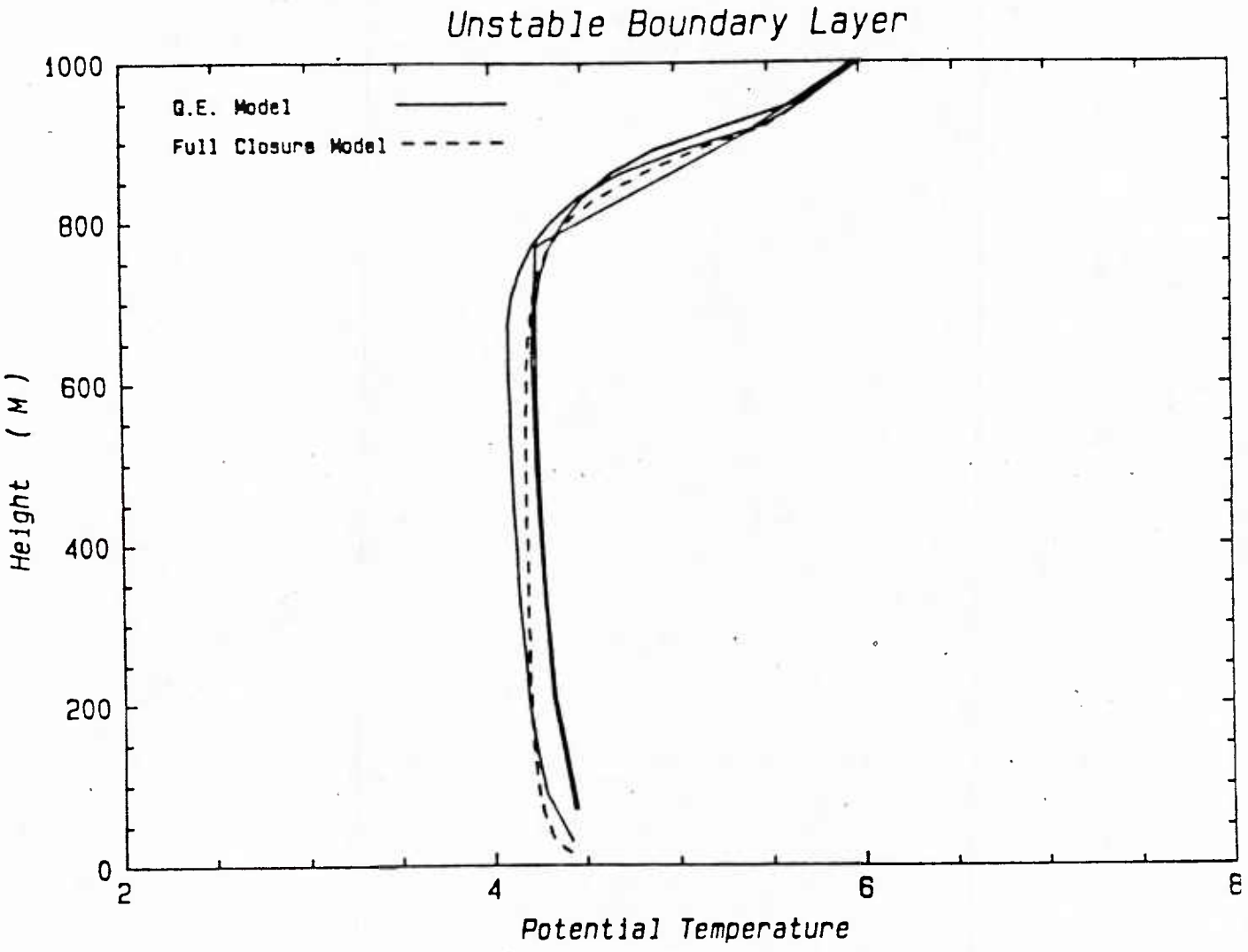

FIGURE 4.1: COMPARISON OF THE POTENTIAL TEMPERATURE DISTRIBUTION AS PREDICTED BY THE Q.E. MODELS OF TABLE 1 WITH THAT PREDICTED BY THE FULL CLOSURE MODEL FOR A QUASI-STEADY UNSTABLE FLOW.

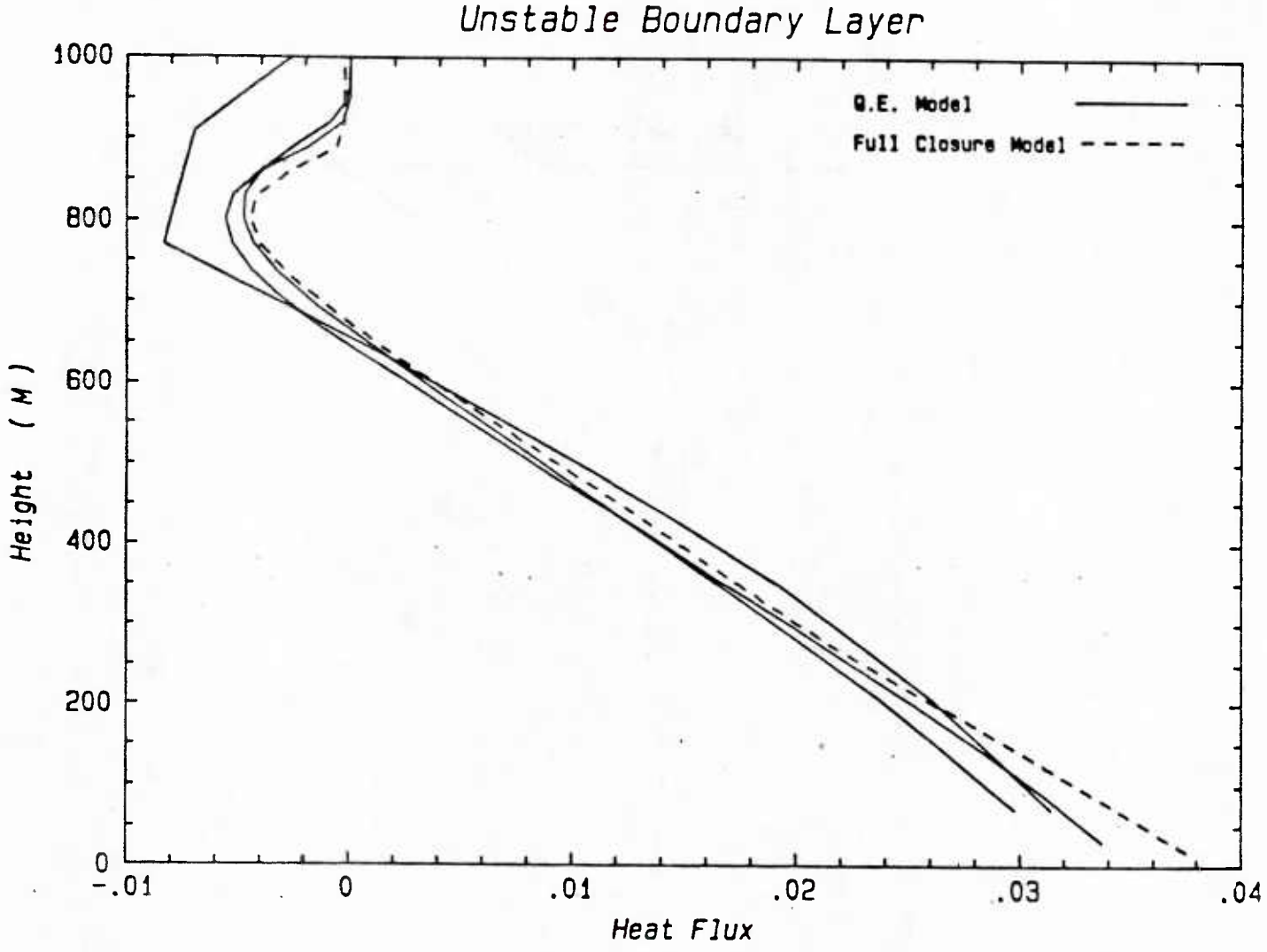

FIGURE 4.2: COMPARISON OF THE HEAT FLUX DISTRIBUTIONS WHICH GO WITH THE POTENTIAL TEMPERATURE DISTRIBUTIONS OF FIGURE 4.1

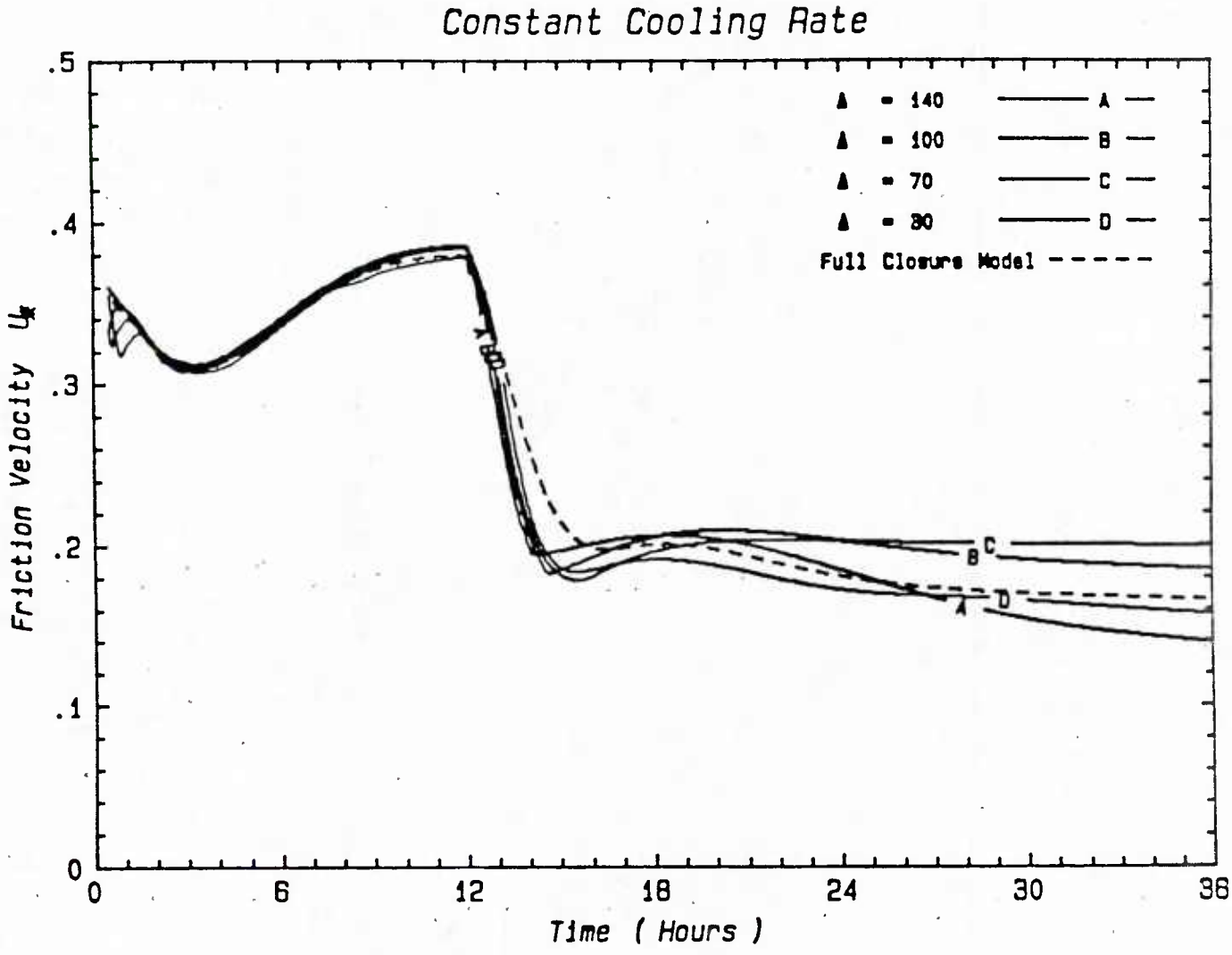

FIGURE 4.3: FRICTION VELOCITY AS A FUNCTION OF TIME AFTER A CONSTANT COOLING RATE OF 1.8°c/HOUR IS APPLIED TO THE SURFACE.

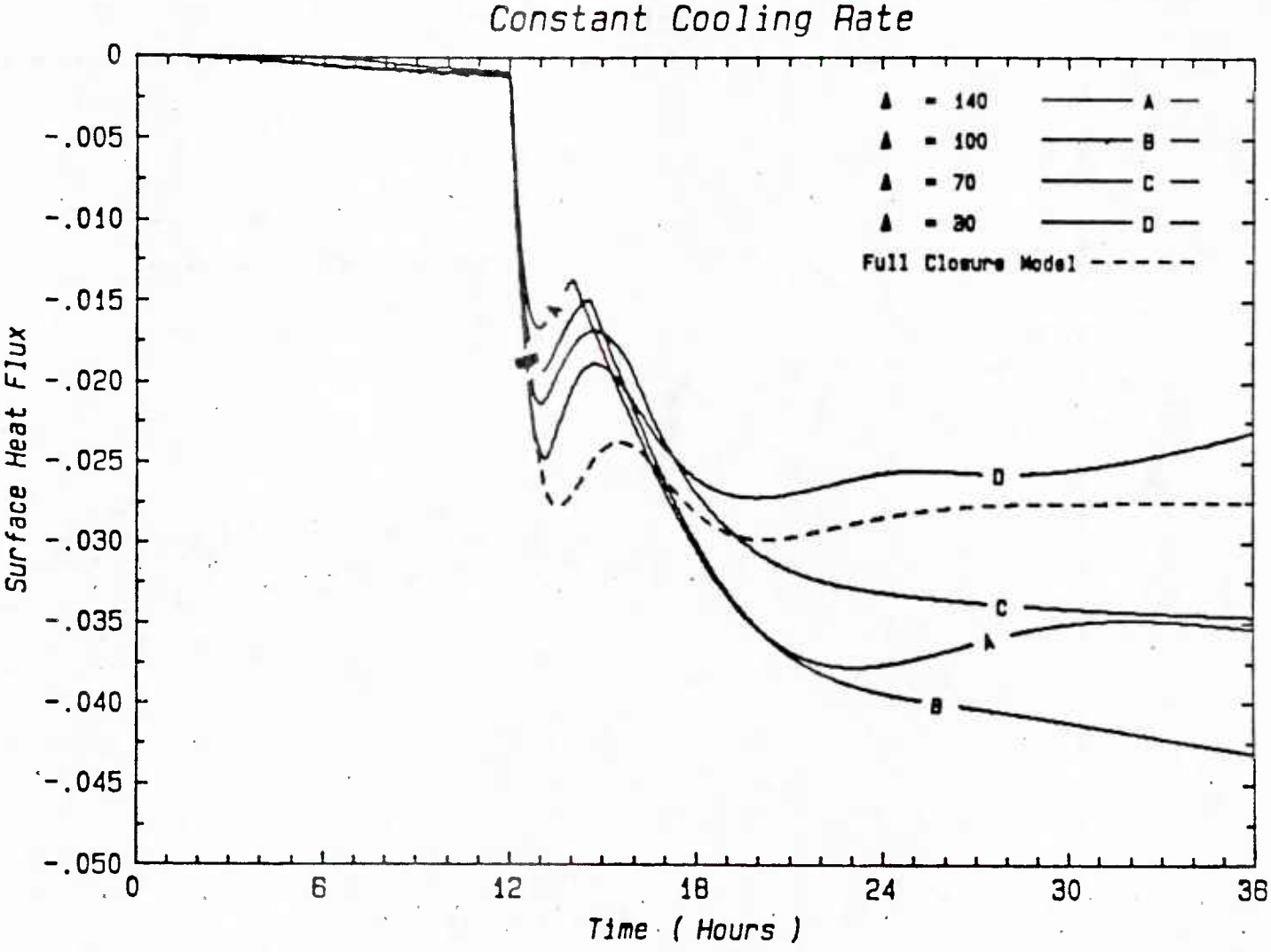

FIGURE 4.4: SURFACE HEAT FLUX AS A FUNCTION OF TIME AFTER A CONSTANT COOLING RATE OF 1.8°c/HOUR IS APPLIED TO THE SURFACE.

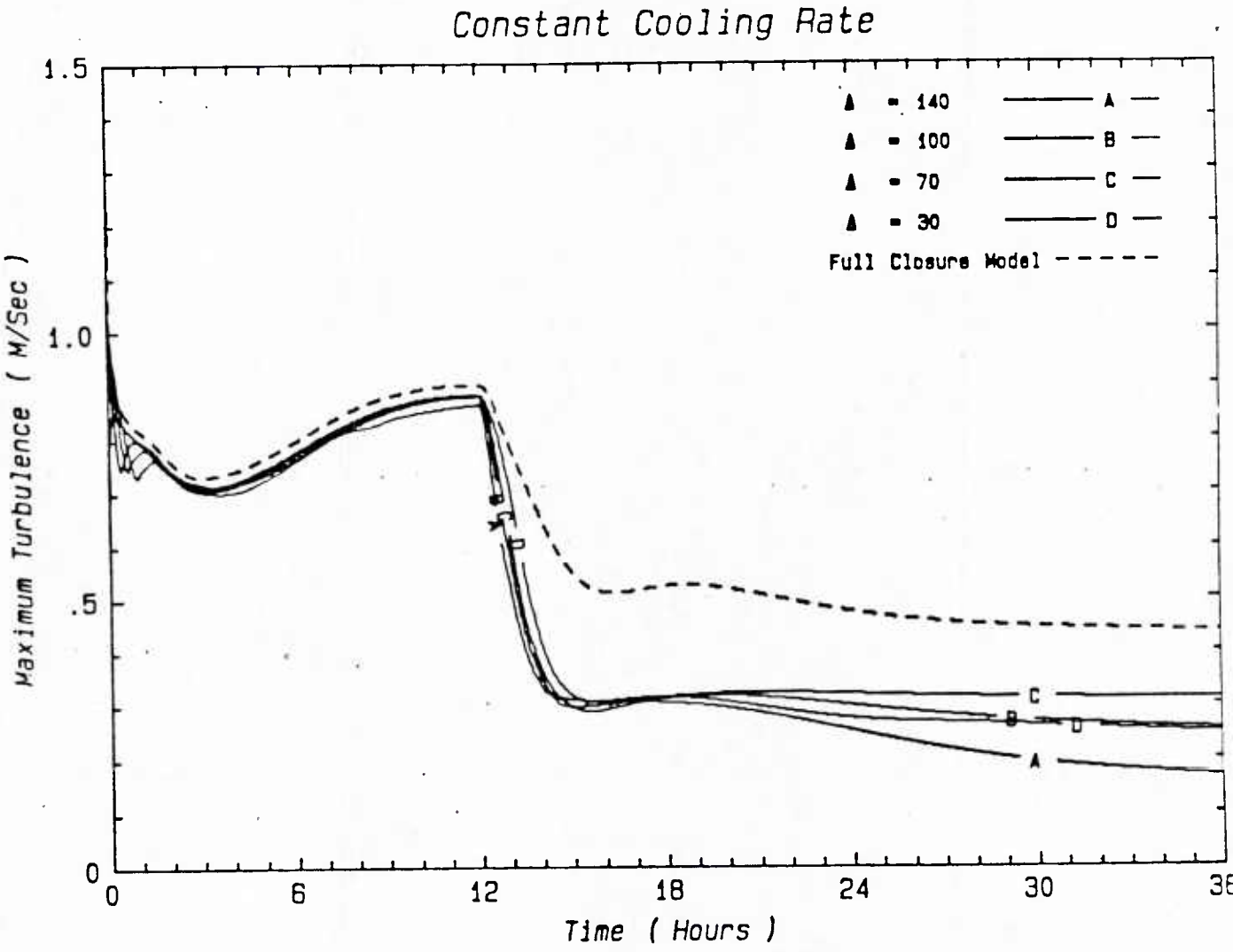

FIGURE 4.5: MAXIMUM TURBULENT VELOCITY FLUCTUATIONS AS A FUNCTION OF TIME AFTER A CONSTANT COOLING RATE OF 1.8°c/HOUR IS APPLIED TO THE SURFACE.

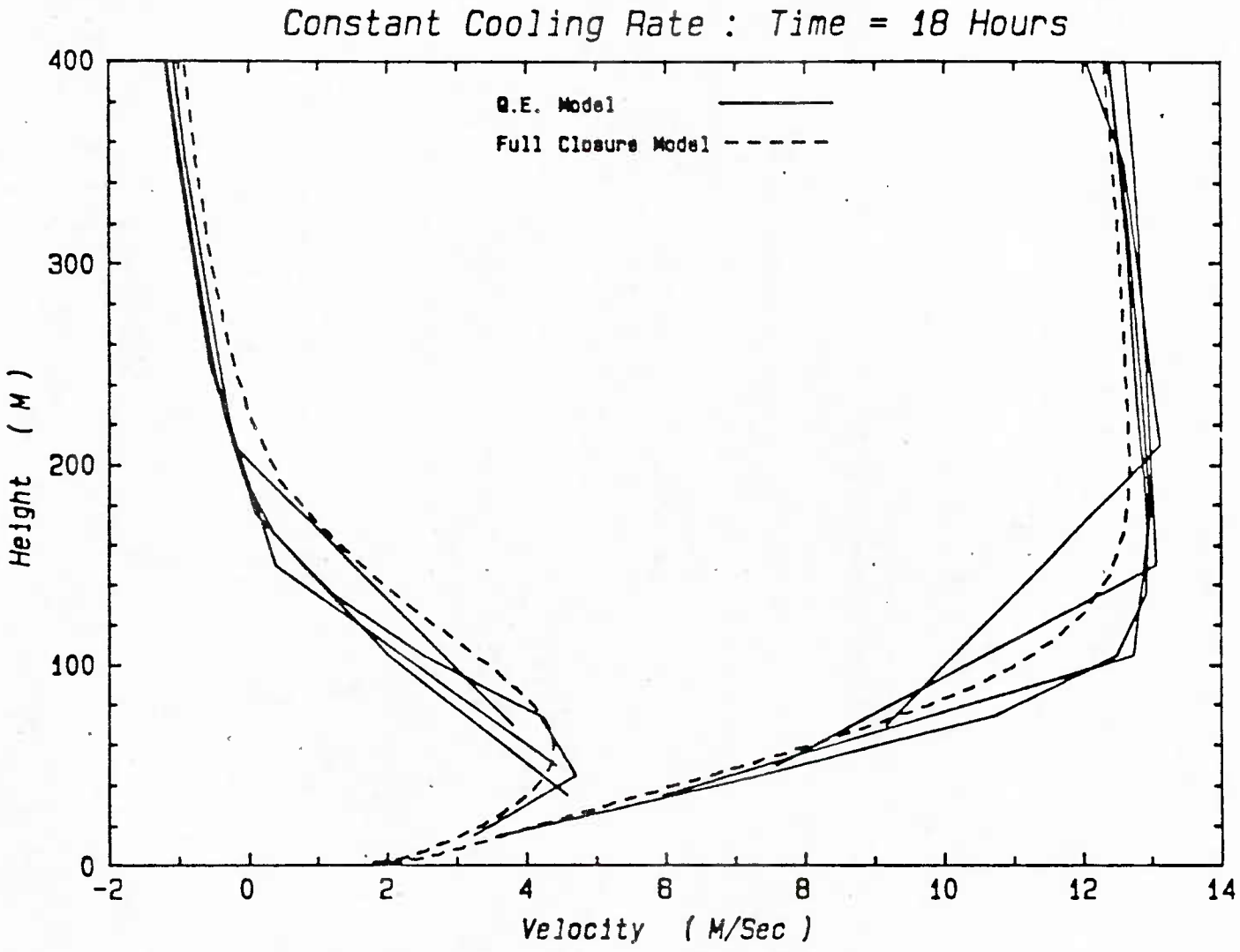

FIGURE 4.6: VELOCITY DISTRIBUTIONS OBTAINED 6 HOURS AFTER THE APPLICATION OF THE CONSTANT COOLING RATE.

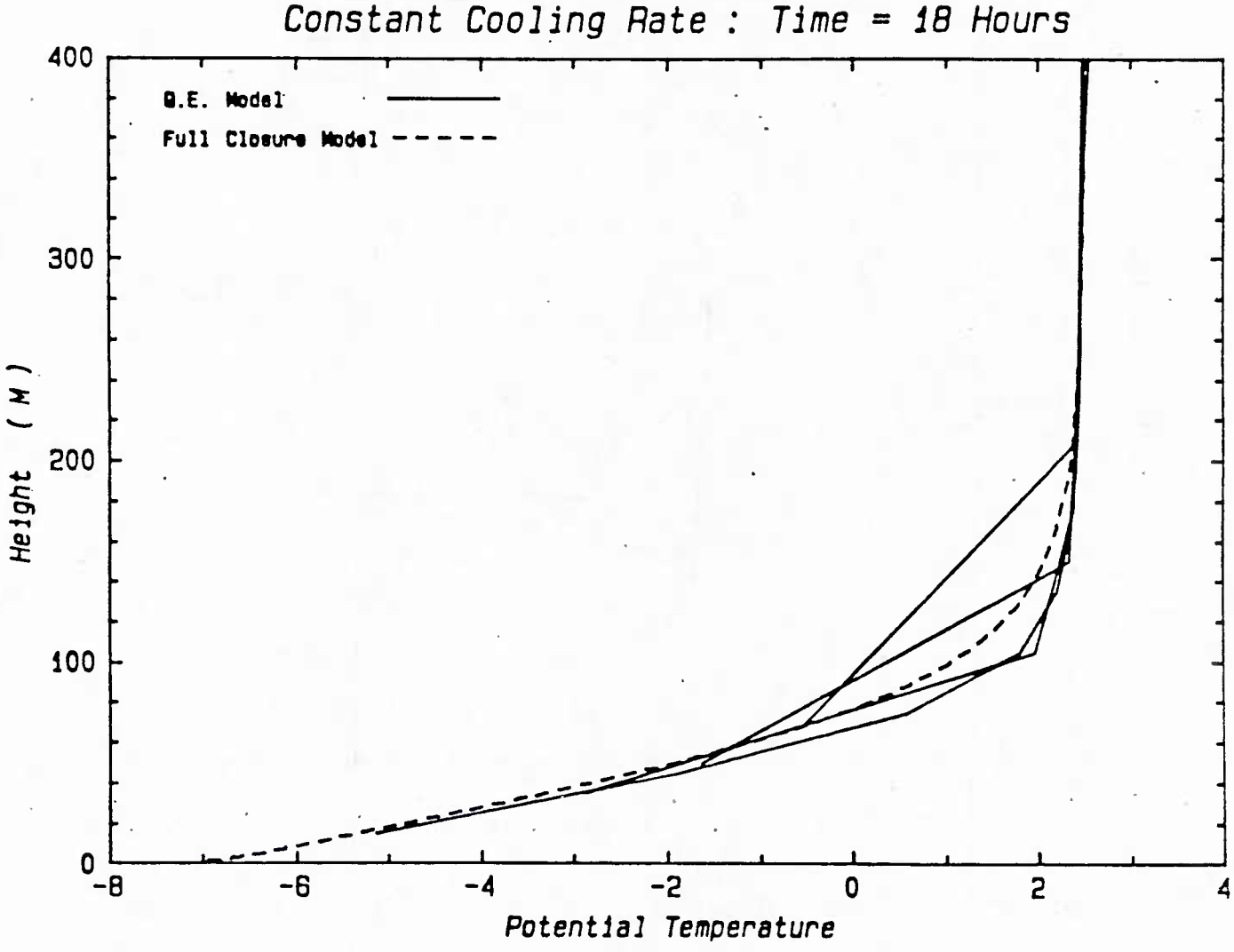

FIGURE 4.7: TEMPERATURE DISTRIBUTION OBTAINED 6 HOURS AFTER THE APPLICATION OF THE CONSTANT COOLING RATE.

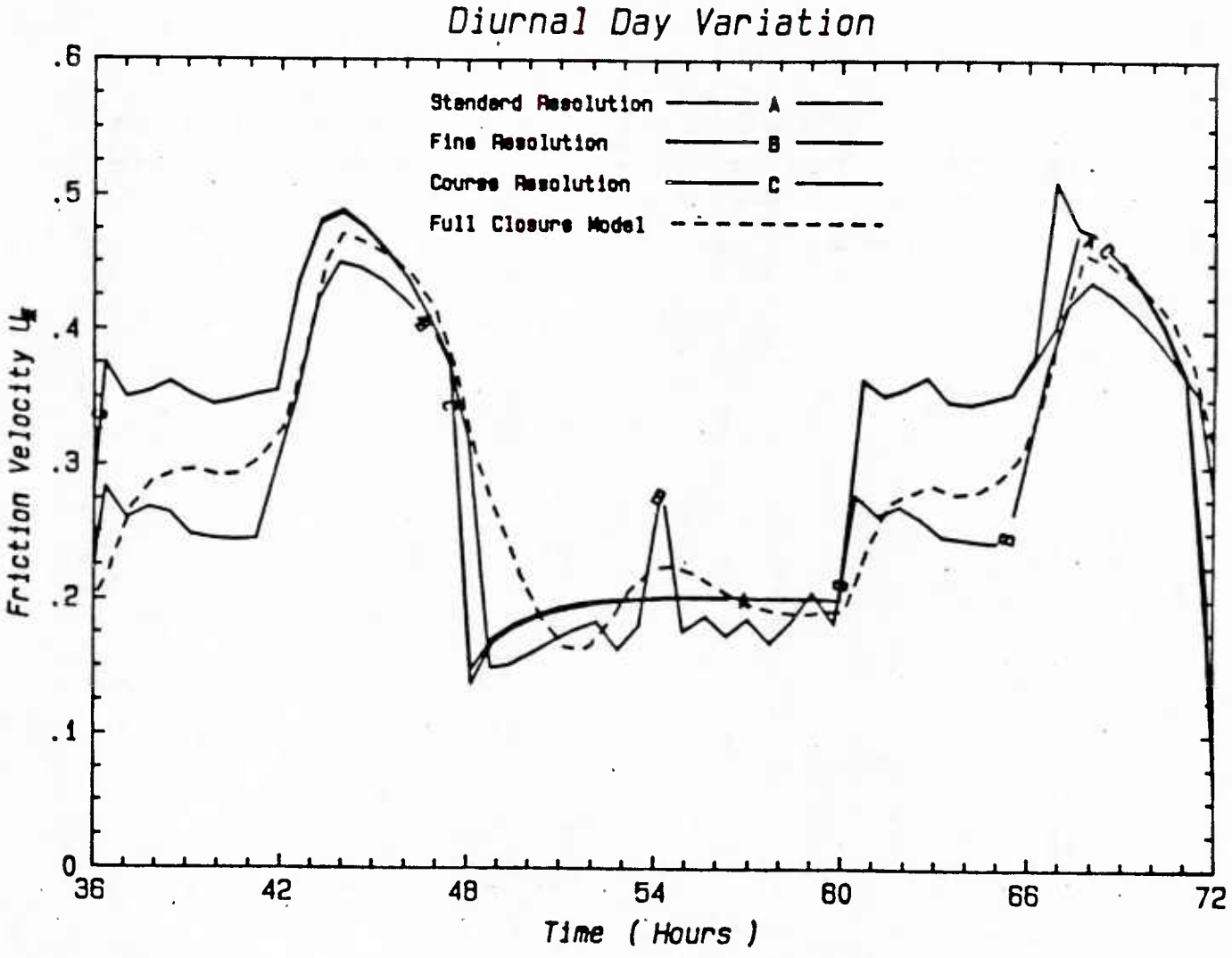

FIGURE 4.8: DIURNAL VARIATION OF THE SURFACE FRICTION VELOCITY.

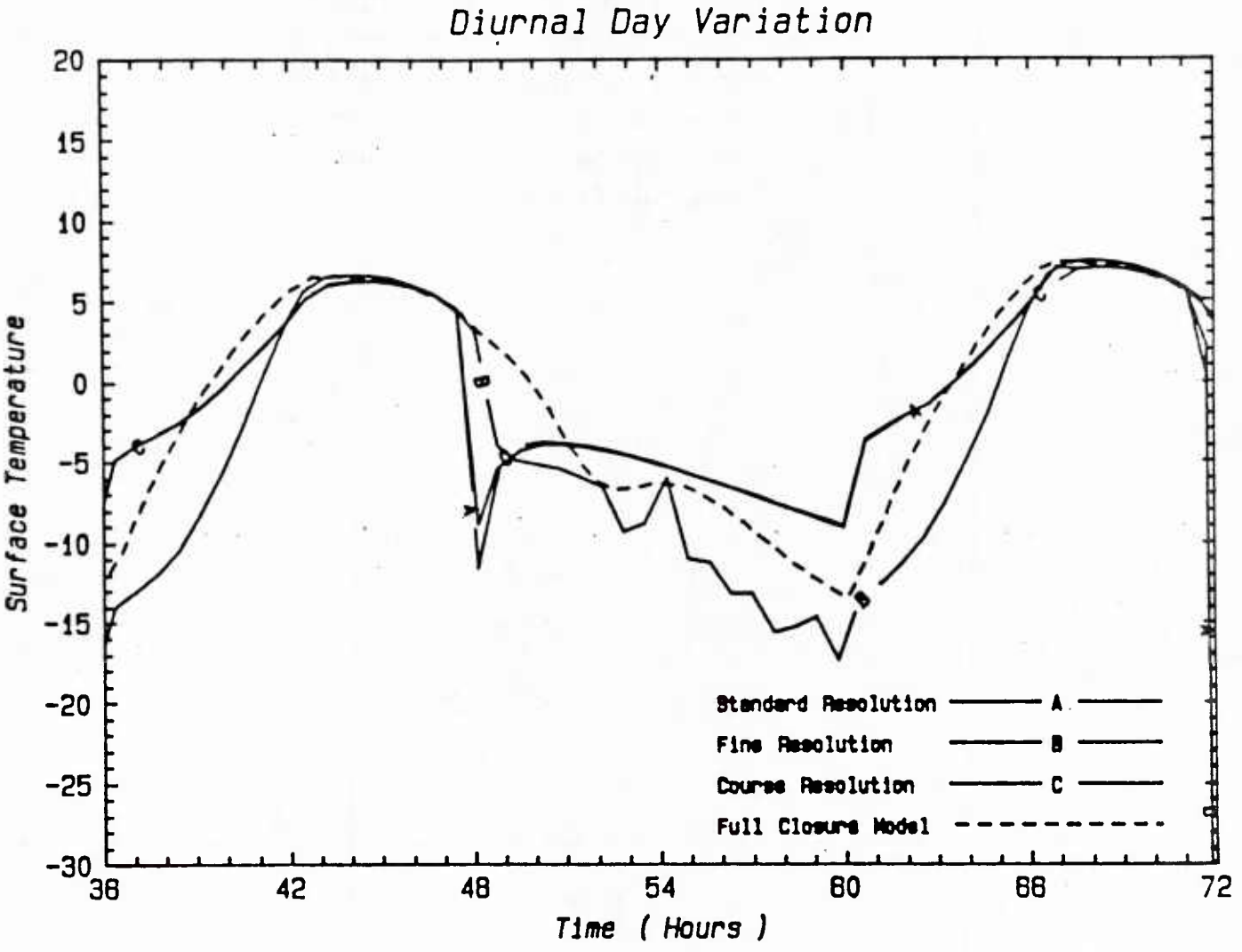

FIGURE 4.9: DIURNAL VARIATION OF THE SURFACE TEMPERATURE.

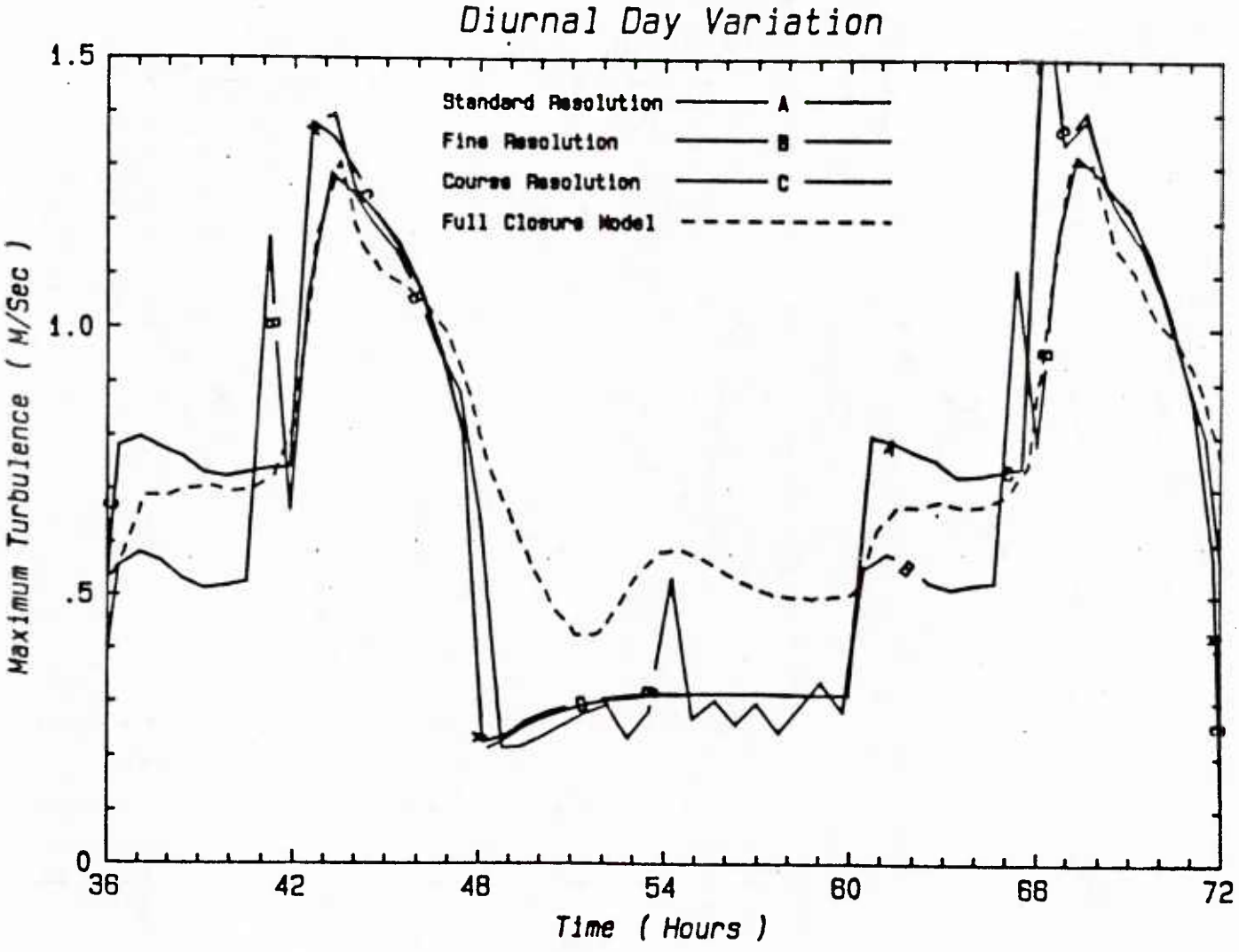

FIGURE 4.10: DIURNAL VARIATION OF THE MAXIMUM TURBULENT VELOCITY VARIATION.

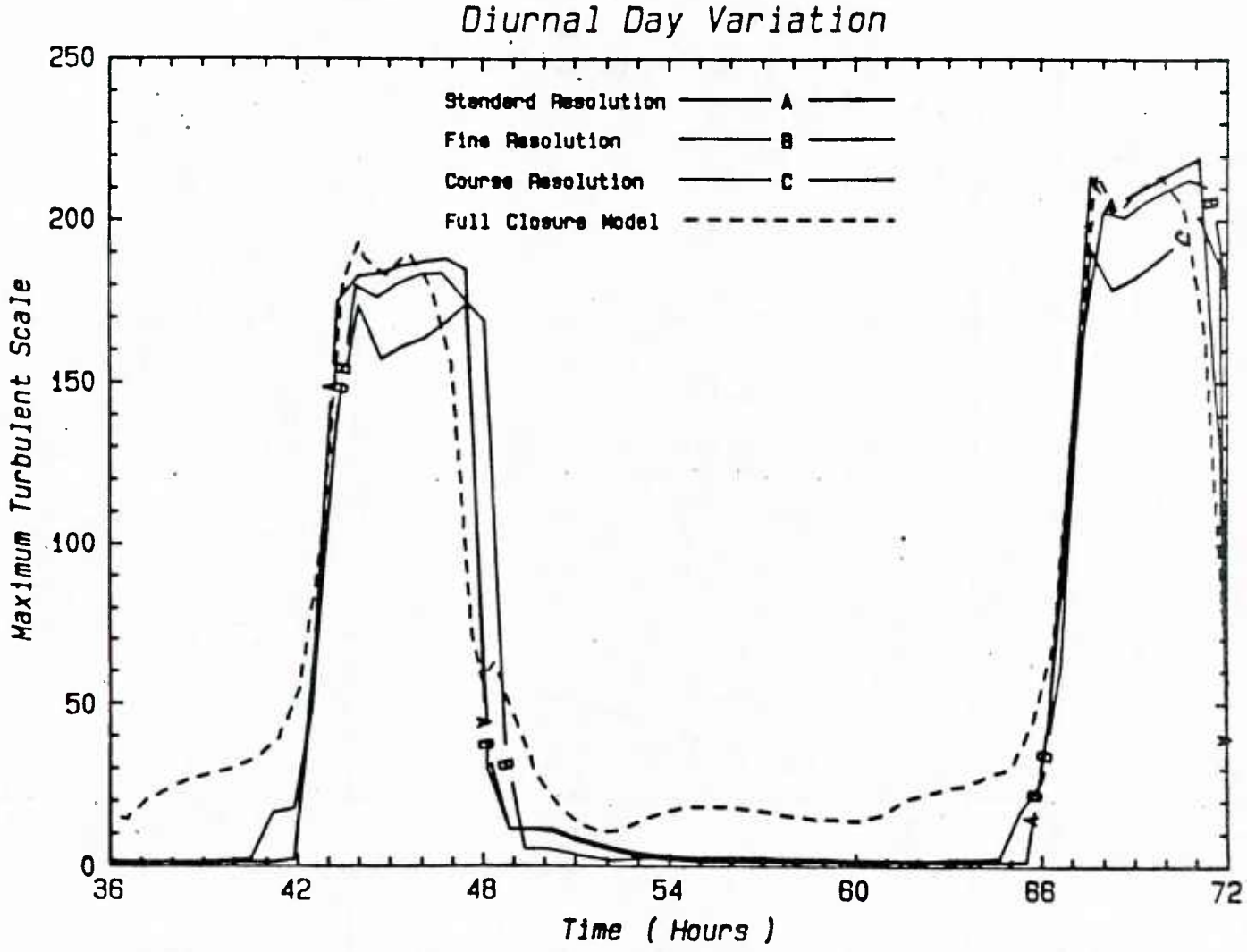

FIGURE 4.11: DIURNAL VARIATION OF THE MAXIMUM TURBULENT LENGTH SCALE.

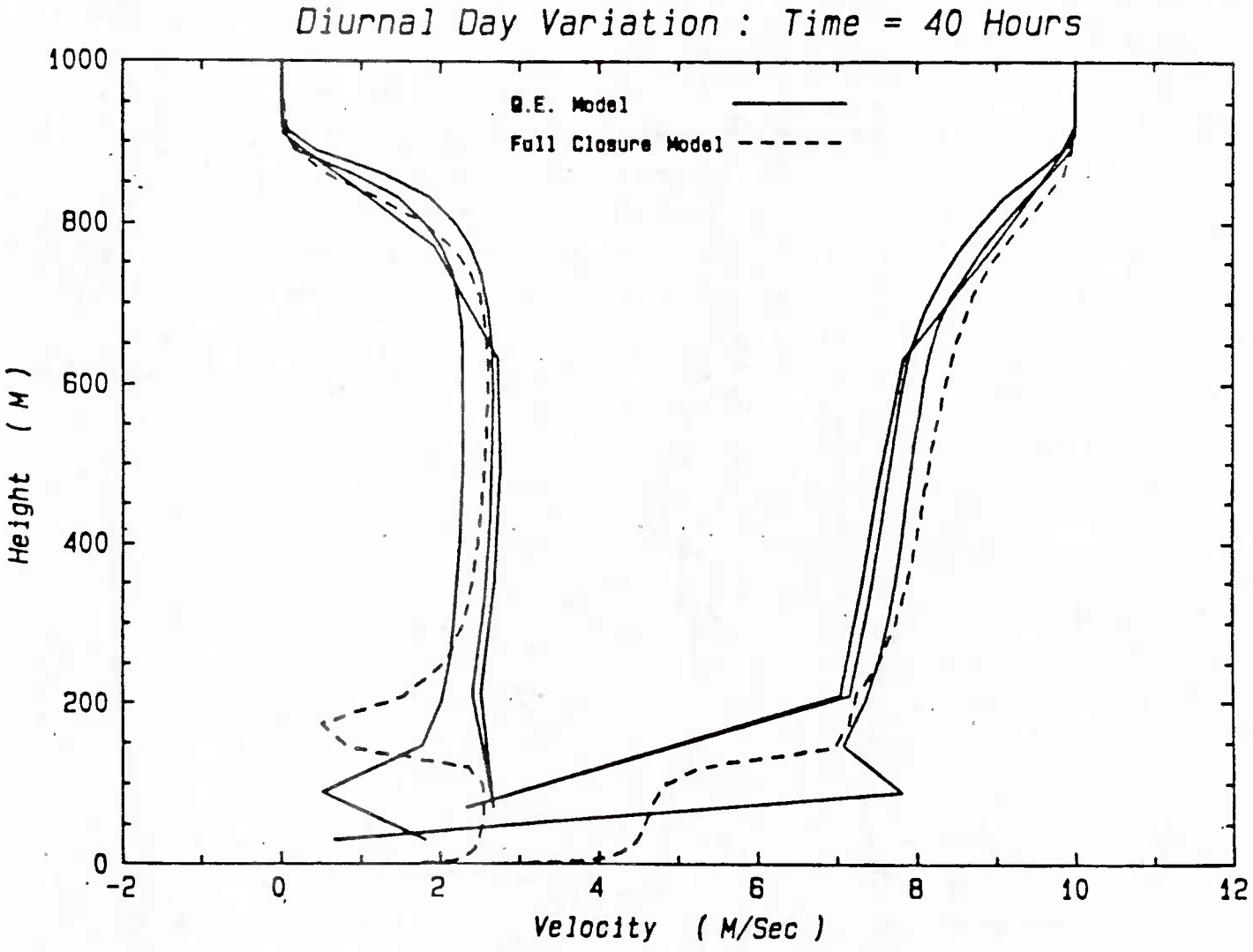

FIGURE 4.12: WIND VELOCITY DISTRIBUTIONS DURING THE MORNING TRANSITION.

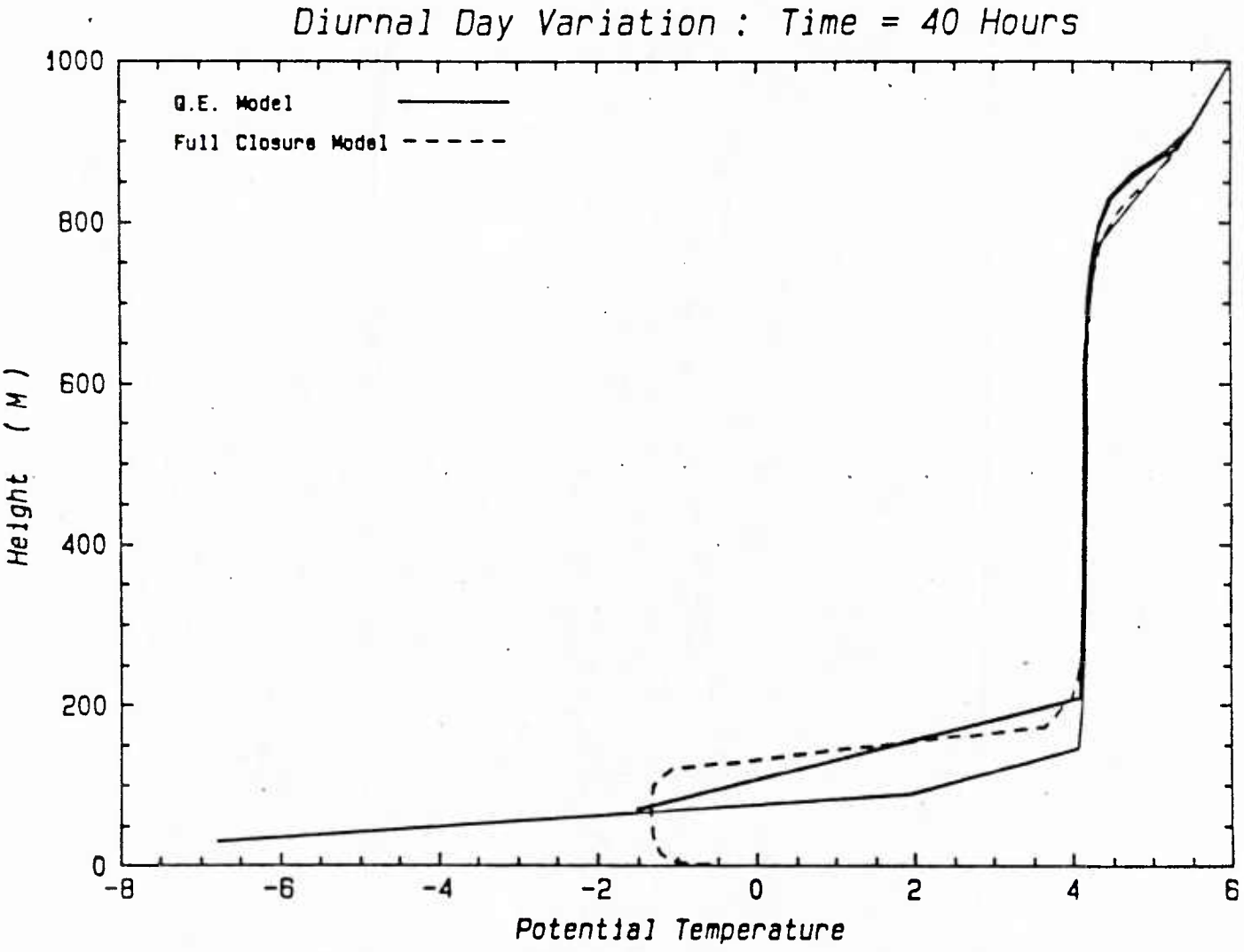

FIGURE 4.13: POTENTIAL TEMPERATURE DISTRIBUTION DURING THE MORNING TRANSITION.

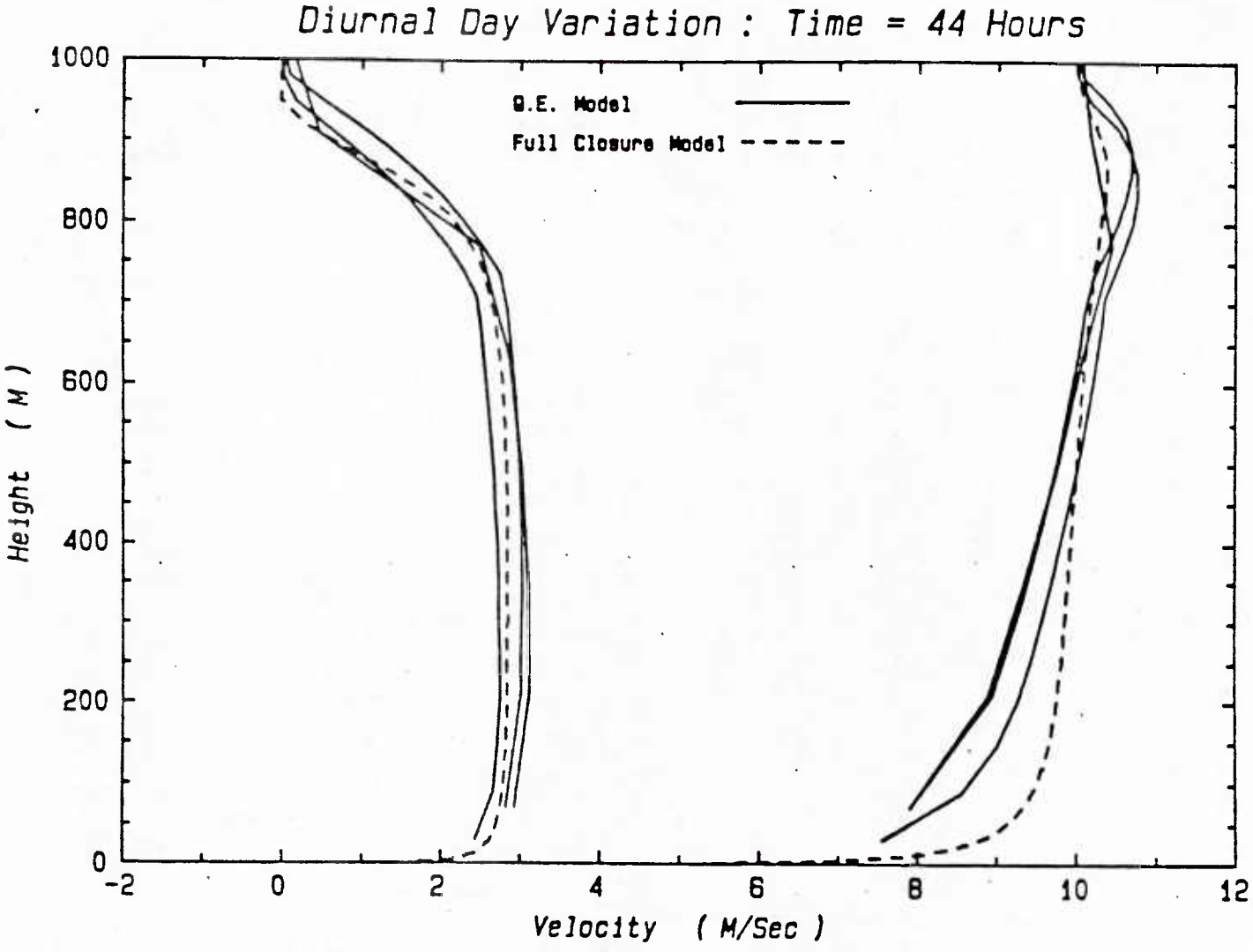

FIGURE 4.14: WIND VELOCITY DISTRIBUTIONS DURING AFTERNOON UNSTABLE CONDITIONS.

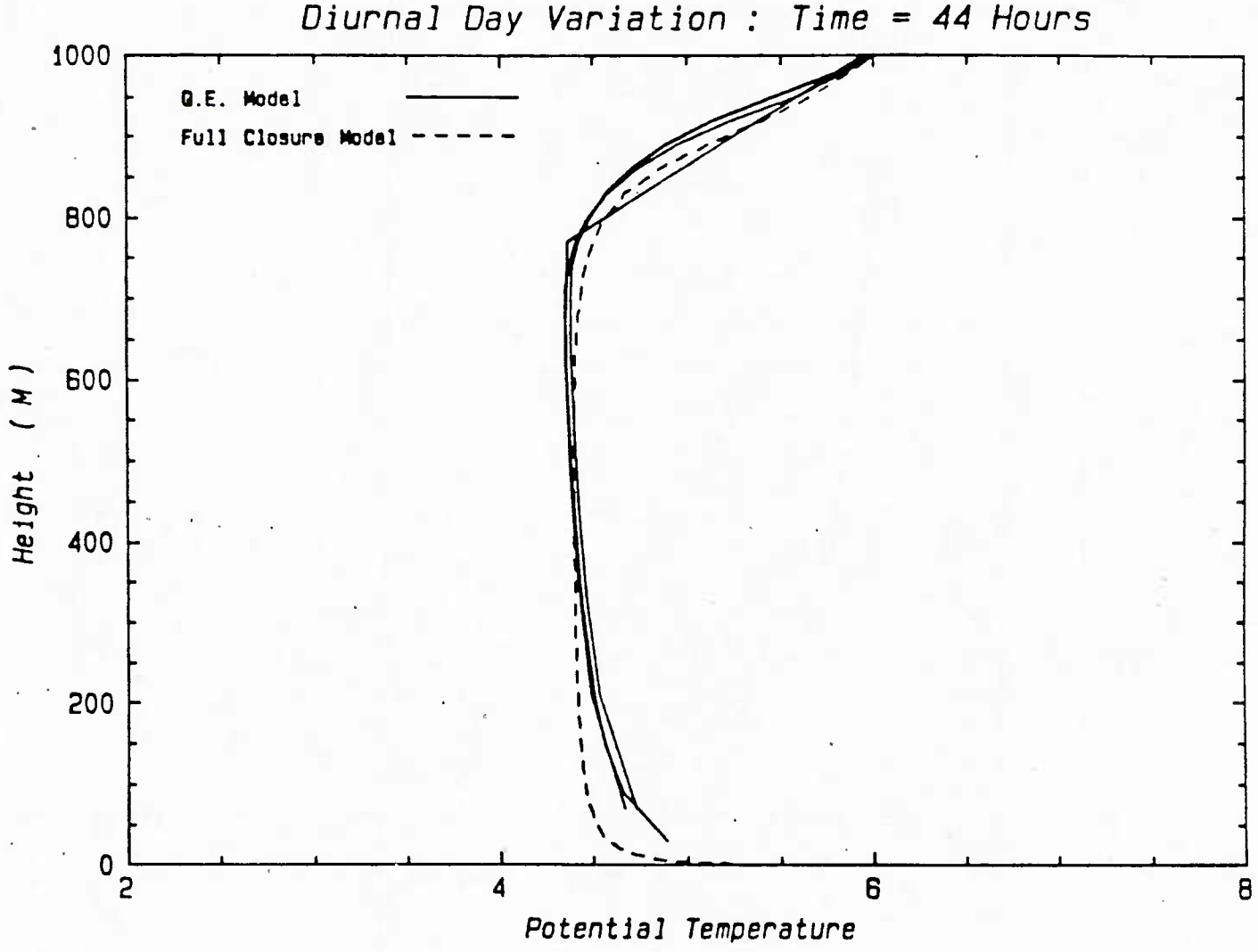

FIGURE 4.15: POTENTIAL TEMPERATURE DISTRIBUTION DURING AFTERNOON UNSTABLE CONDITIONS.

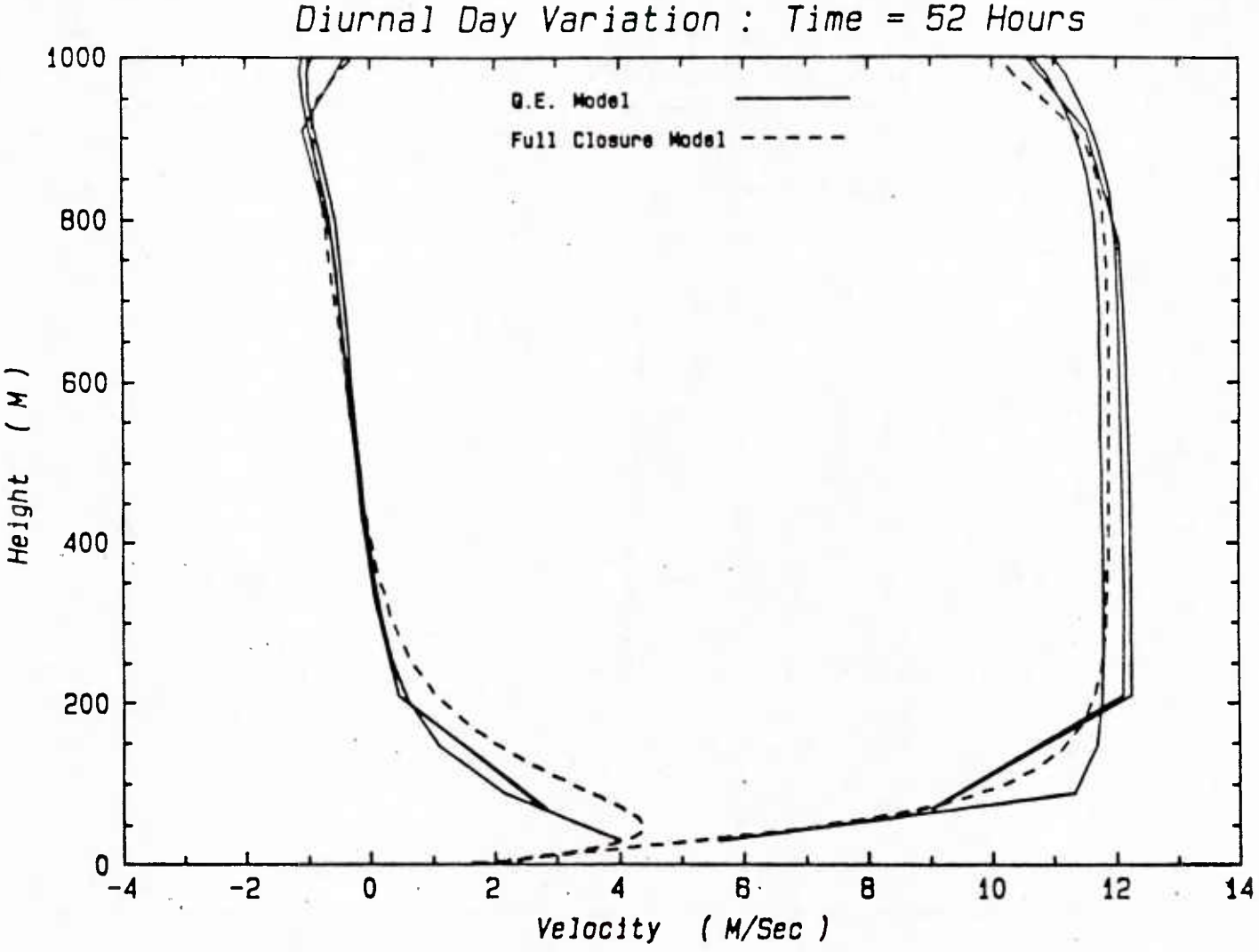

FIGURE 4.16: WIND VELOCITY DISTRIBUTIONS SHORTLY AFTER TRANSITION TO NOCTURNAL CONDITIONS.

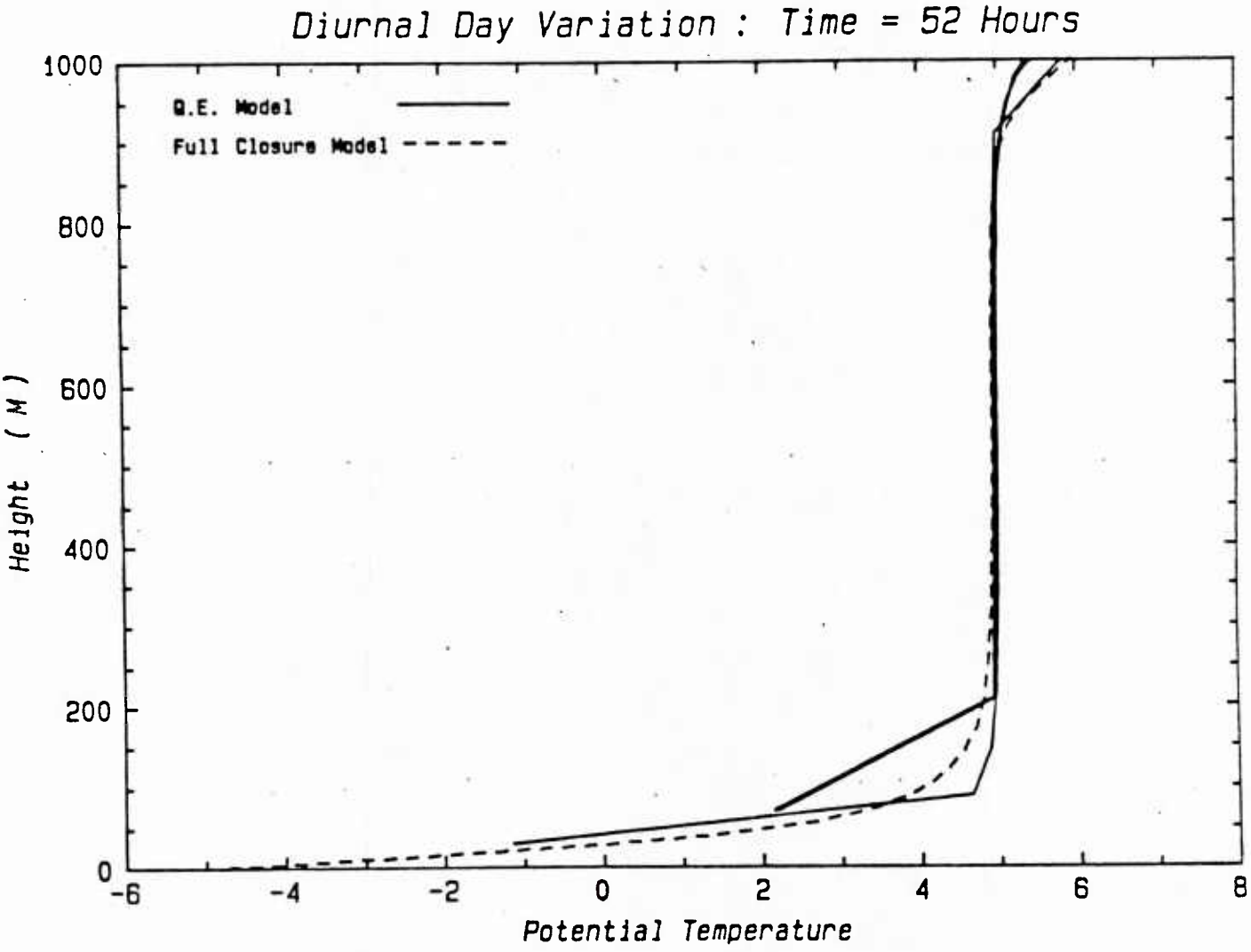

FIGURE 4.17: POTENTIAL TEMPERATURE DISTRIBUTIONS SHORTLY AFTER TRANSITION TO NOCTURNAL CONDITIONS.

5. INCORPORATION OF CUMULUS PARAMETERIZATION INTO THE TURBULENT FLUX RELATIONS

A large part of turbulent transport in the atmosphere involves cloud dynamics. Therefore, before any subgrid flux parameterization can have any general applicability for a mesoscale model it must represent these dynamics, at least, in some approximately valid manner. The cumulus analysis of Lewellen, Sykes and Oliver (1983) provides the basis for extending the parameterization of section 2 to include cumulus transport. As long as the turbulent kinetic energy equation, Equation 2.1, is written in terms of the virtual potential temperature, it remains unchanged in the presence of change of phase of the water in the atmosphere. The strong influence of the change of phase comes in the equations for $\bar{\theta}_v$ and $\overline{w'\theta'_v}$. In the absence of any radiation flux divergence it is

$$\theta_w = \theta_v - \beta\Gamma \int_{zo}^{z} \bar{r}\,dz \tag{5.1}$$

which is the conserved buoyancy quantity as shown in Equation 5.12 of L.S.O.

$$\frac{D\theta_w}{Dt} = - \frac{\partial \overline{w'\theta'_w}}{\partial z} = - \frac{\partial \overline{w'\theta'_v}}{\partial z} + \beta\Gamma\, \overline{r'w'} \tag{5.2}$$

If we assume that the vertical flux of θ_v needed for the T.K.E. equation may be given by a quasi-equilibrium version of Equation 5.9 of L.S.O. then it can be written as:

$$\overline{w'\theta'_v} = - q\Lambda S_H \left(\frac{\partial \bar{\theta}_v}{\partial z} - \beta\Gamma\bar{r} \right) \tag{5.3}$$

with

$$S_H = \frac{1/3}{1 + 8.6\ R} \tag{5.4}$$

$$R = g\,\frac{\Lambda^2}{q^2}\,\frac{\partial \theta_w}{\partial z} \tag{5.5}$$

Expressions for $\bar{r}$ and $\overline{r'w'}$ may be obtained from Equations 5.26 and 5.29

$$\bar{r} = 1/2\ \left[1 + \mathrm{Erf}\left(Q/\sqrt{2}\right)\right] \tag{5.6}$$

$$\overline{w'r'} = \left(\sigma_r/\sigma_\lambda\right)\left(a\ \overline{w'h'} - b\ \overline{w'\theta_v'}\right) \tag{5.7}$$

with

$$\sigma_r = \frac{1}{\sqrt{2}}\exp\left(-Q^2/2\right) \tag{5.8}$$

$$Q = \left(\bar{h} - h_s\right)/\sigma_\lambda \tag{5.9}$$

$$\sigma_\lambda^2 = a^2\,\overline{h'^2} - 2ab\,\overline{h'\theta_v'} + b^2\,\overline{\theta_v'^2} \tag{5.10}$$

$$a = 1 - \left[-0.61 + \left(\bar{\mu}^{-1} + 0.61\right)\bar{r}\right]\beta_T\, h_s \tag{5.11}$$

$$b = \left[1 + \left(\bar{\mu}^{-1} - 1\right)\ \bar{r}\ \right]\beta_T h_s/T_r \tag{5.12}$$

$$\bar{\mu} = 1 + \frac{R_v}{C_p}\ h_s\beta_T^2 \tag{5.13}$$

$$\beta_T = L/R_v T \tag{5.14}$$

The expressions for $\overline{w'h'}$, $\overline{h'h'}$, $\overline{h'\theta_v'}$, and $\overline{\theta_v'^2}$ analogous to Equation 5.3 are:

$$\overline{w'h'} = - q\Lambda S_H \frac{\partial \bar{h}}{\partial z} \tag{5.15}$$

$$\overline{\theta_v'^2} = \frac{S_H}{bs} \Lambda^2 \left(\frac{\partial \bar{\theta}_v}{\partial z} - \beta \Gamma \bar{r} \right)^2 \tag{5.16}$$

$$\overline{h'^2} = \frac{S_H}{bs} \Lambda^2 \left(\frac{\partial \bar{h}}{\partial z} \right)^2 \tag{5.17}$$

$$\overline{\theta_v' h'} = \frac{S_H}{bs} \Lambda^2 \left(\frac{\partial h}{\partial z} \right) \left(\frac{\partial \bar{\theta}_v}{\partial z} - \beta \Gamma \bar{r} \right) \tag{5.18}$$

Thus

$$\sigma_\lambda^2 = \frac{S_H}{bs} \Lambda^2 \left[a^2 \left(\frac{\partial h}{\partial z} \right)^2 - 2ab \left(\frac{\partial h}{\partial z} \right) \left(\frac{\partial \bar{\theta}_v}{\partial z} - \beta \Gamma \bar{r} \right) + b^2 \left(\frac{\partial \theta_v}{\partial z} - \beta \Gamma \bar{r} \right)^2 \right] \tag{5.19}$$

This set of equations provides a complete set of relations for two-phase turbulent flow. However, the character of the turbulence is likely to be quite different under conditionally unstable conditions then it is under either fully stable or unstable conditions. Equation 5.3 shows a given virtual potential temperature gradient may be stable in the absence of cloud and unstable in the presence of the cloud. Further, Equations 5.6, 5.9 and 5.10 show that $\bar{r}$ will be larger in the presence of strong turbulence. Thus, there is a natural feedback which will drive the flow to divide between regions of high turbulence and regions of little or no turbulence. It is necessary to make some adjustments in our transport modeling to account for this intermittency. We define intermittency, ω^2, as the volume fraction of the sub-grid ensemble space occupied by the turbulent regions. We argue in LSO that the principle effect this has on our transport modeling is to increase the characteristic velocity q in the modeled terms by ω^{-1} so that

they are based on the average turbulent velocity in the turbulent region rather than the average over the layer ensemble space. We must determine how this should affect Equations 5.2 to 5.18 and how this new variable ω should be determined.

Let us address the determination of ω first. Rather than attempt to generate an equation from either a conditional moment approach or probability distribution function approach (Kollman, 1984), we will tentatively rely on a simple time scale relationship to determine intermittency. Under stable conditions, it has been established both theoretically and observationally that the scale of 3-D turbulence should not exceed q/2N. Theoretically, this limit is based on the energy required for an eddy to turn over in the presence of stable stratification. Observationally, it agrees with the limits necessarily imposed on the scale to obtain agreement with the Monin-Obukhov similarity functions in the stable surface layer (Lewellen, 1981). If the turbulence is instead permitted to be intermittent then the scale can exceed the limit of q/2N. Thus, in regions where the scale is observed to exceed q/2N we can expect the intermittency to be proportional to $q/N\Lambda$, i.e.

$$\omega = Kq/N\Lambda \tag{5.20}$$

Thus, a consistent determination of Λ will through Equation 5.20 also provide a determination of ω. For purposes of preliminary tests we will stick with essentially the same Λ algorithms as given in 2.2 and 2.3 except the stability limit on Λ is applied with $\bar{N}$ based on the moist lapse rate, $\partial\bar{\theta}_v/\partial z - \beta\Gamma$. Thus, Λ will be equal to Λ^* in the central region of the boundary layer and determined by $[d\Lambda/dz] = 0.65$ at both the top and the bottom of the boundary layer. In the regions where $q/2\bar{N}$ would have yielded a smaller Λ the flow is intermittent as given by Equation 5.20. The biggest weakness of this approach to intermittency is that it builds on the ad-hoc nature of Λ. However, this is not as damaging as it might first appear since the combination $\omega\Lambda$ appears together in all the modeled terms except the diffusion term where the relevant combination is Λ/ω. Since there is theoretical justification for taking $\omega\Lambda$ as proportional to q/N in the stable regions in which we are interested most of the uncertainty is tied to the diffusion terms. Of course, since the net

effect of intermittency is to increase the effect of the diffusion terms it does make the modeling of this term more important.

With an algorithm for determining ω at our disposal we can address how the quasi-equilibrium expressions should be affected by ω. By following the rule that q in the modeled terms should be increased by ω^{-1}, the quasi-equilibrium expressions may be written as

$$\frac{D(q^2/2)}{Dt} = - \overline{u'w'} \frac{\partial \bar{u}}{\partial z} - \overline{v'w'} \frac{\partial v}{\partial z} + \frac{g}{T} \overline{w'\theta_v'} + \frac{v_c}{\omega} \frac{\partial}{\partial z} \left(q \Lambda \frac{\partial q^2/2}{\partial z} \right) - \frac{bq^3}{\omega \Lambda} \tag{5.21}$$

$$\overline{u'w'} = - \omega q \Lambda S_M \frac{\partial \bar{u}}{\partial z} \tag{5.22}$$

$$\overline{v'w'} = - \omega q \Lambda S_M \frac{\partial \bar{v}}{\partial z} \tag{5.23}$$

$$\overline{w'\theta'_v} = - \omega q \Lambda S_H \left(\frac{\partial \theta_v}{\partial z} - \beta \Gamma \bar{r} \right) \tag{5.24}$$

$$\overline{w'h'} = - \omega q \Lambda S_H \frac{\partial \bar{h}}{\partial z} \tag{5.25}$$

$$S_H = \frac{1/3}{1 + 8.6R} \quad , \quad S_m = S_H \left[0.75 + 3.1R \right] / \left[1 + 1.33R \right] \tag{5.26}$$

$$R = \min \left[\frac{g \Lambda^2}{T_o q^2} \left(\frac{\partial \theta_v}{\partial z} - \beta \Gamma \bar{r} \right) , 0.25 \right] \tag{5.27}$$

$$\omega = \min \left[1 , \frac{q}{2\Lambda} \left[\frac{g}{T_o} \left(\frac{\partial \theta_v}{\partial z} - \beta \Gamma \bar{r} \right) \right]^{-1/2} \right] \tag{5.28}$$

It is also desirable to adjust the cloud functions to account for the nonguassian distribution of the humidity and temperature fluctuations. Bougeault, 1981 has shown that skewness has a large influence on the $\bar{r}$ and σ_r functions, particularly for $Q \leq -1$. We can roughly compensate for this by allowing the guassian expressions given in Equation 5.6-5.10 to apply only in the turbulent part of the ensemble volume. The expressions then become:

$$\bar{r} = \frac{\omega^2}{2}\left[1 + \mathrm{Erf}\left(Q/\sqrt{2}\right)\right] \tag{5.29}$$

$$\sigma_r = \frac{\omega}{\sqrt{2}} \exp\left(-Q^2/2\right) \tag{5.30}$$

$$Q = \omega\left(\bar{h}-\bar{h}_s\right)/\sigma_\lambda \tag{5.31}$$

with σ_λ given by Equation 5.19.

If we wish the parameterization to include precipitating cumulus, it will also be necessary to add a term to the $\overline{w'h'}$ expression which represents this. We would expect this to be accomplished by combining a sedimentation rate which is a function of droplet size Gunn and Kinzer (1949) with a Marshall-Palmer droplet radius distribution as a function of liquid water content. The liquid water content can be obtained following the same analysis as led to $\bar{r}$, σ_r, and σ_λ. This is a refinement which can be added after it is demonstrated that the basic non-precipitating parameterization is valid.

As a test of our algorithm for determining intermittency, we have recomputed the convective boundary layer of Section 4 using Equations 5.20-5.27. Without including humidity we can compare with the intermittency observations of Deardorff, Willis and Stockton (1980) in the capping stable layer. The potential temperature profiles of Figure 5.1 and the heat flux profiles of Figure 5.2 are modified very little from those presented earlier for the Q.E. result of Section 4. The intermittency results in Figure 5.3 are in quite reasonable agreement with Deardorff, et.al.'s observation points for $K = 1$ in Equation 5.20. Although

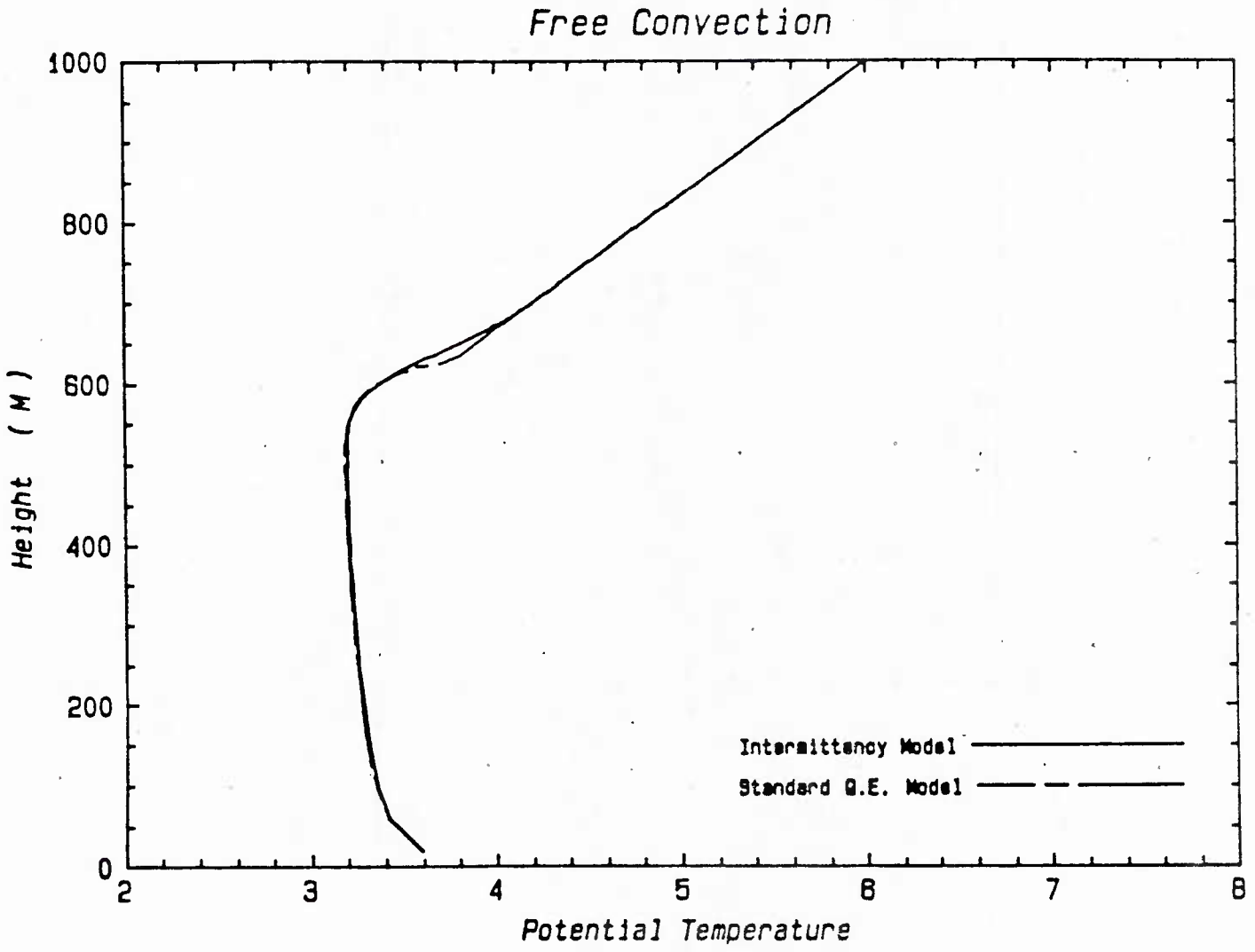

FIGURE 5.1: COMPARISON OF THE TEMPERATURE DISTRIBUTION PREDICTED FOR FREE CONVECTION BY THE INTERMITTENT MODEL WITH THAT FOR THE STANDARD Q. E. MODEL.

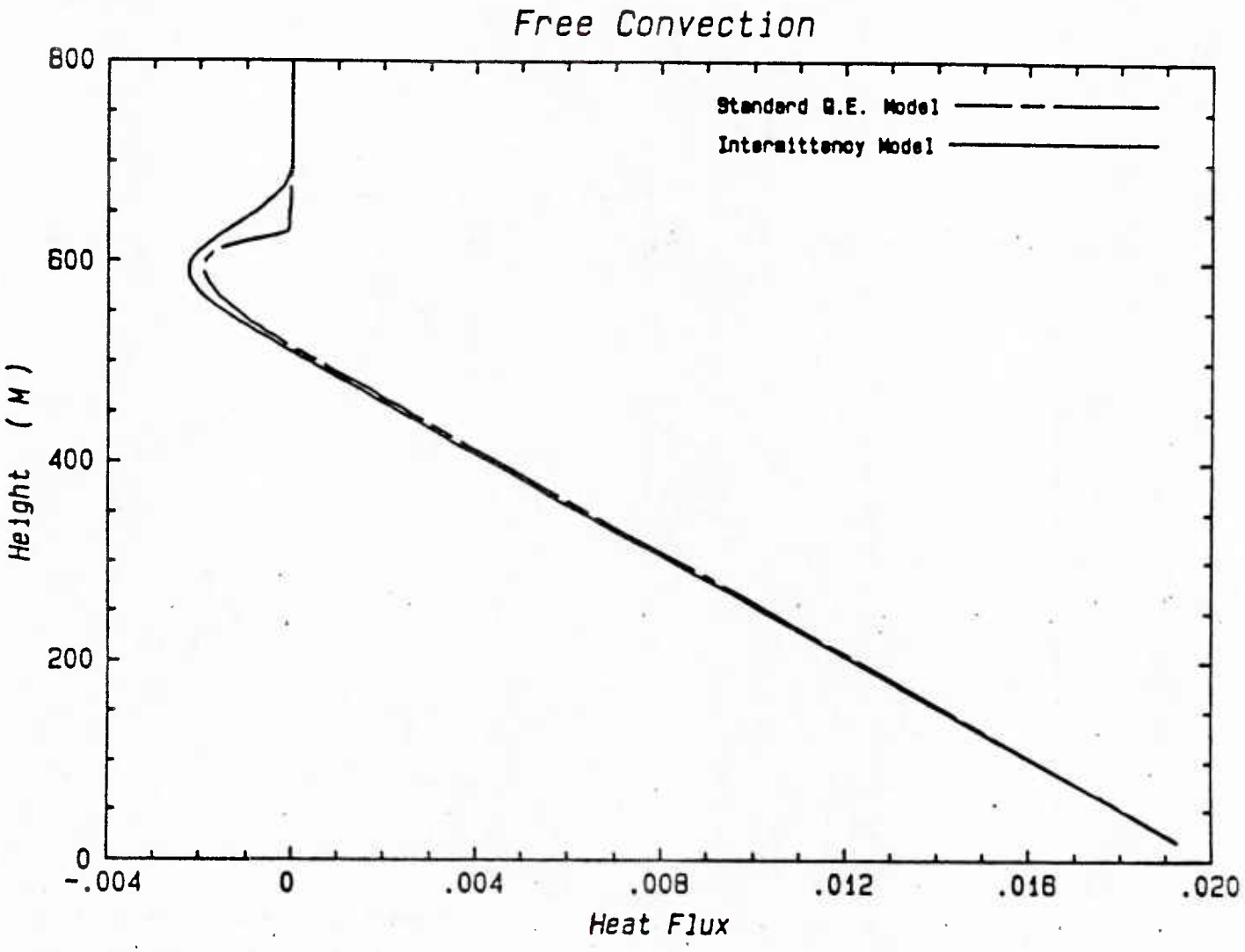

FIGURE 5.2: COMPARISONS OF THE HEAT FLUX DISTRIBUTIONS WHICH GO WITH THE TEMPERATURE DISTRIBUTIONS OF FIGURE 5.1.

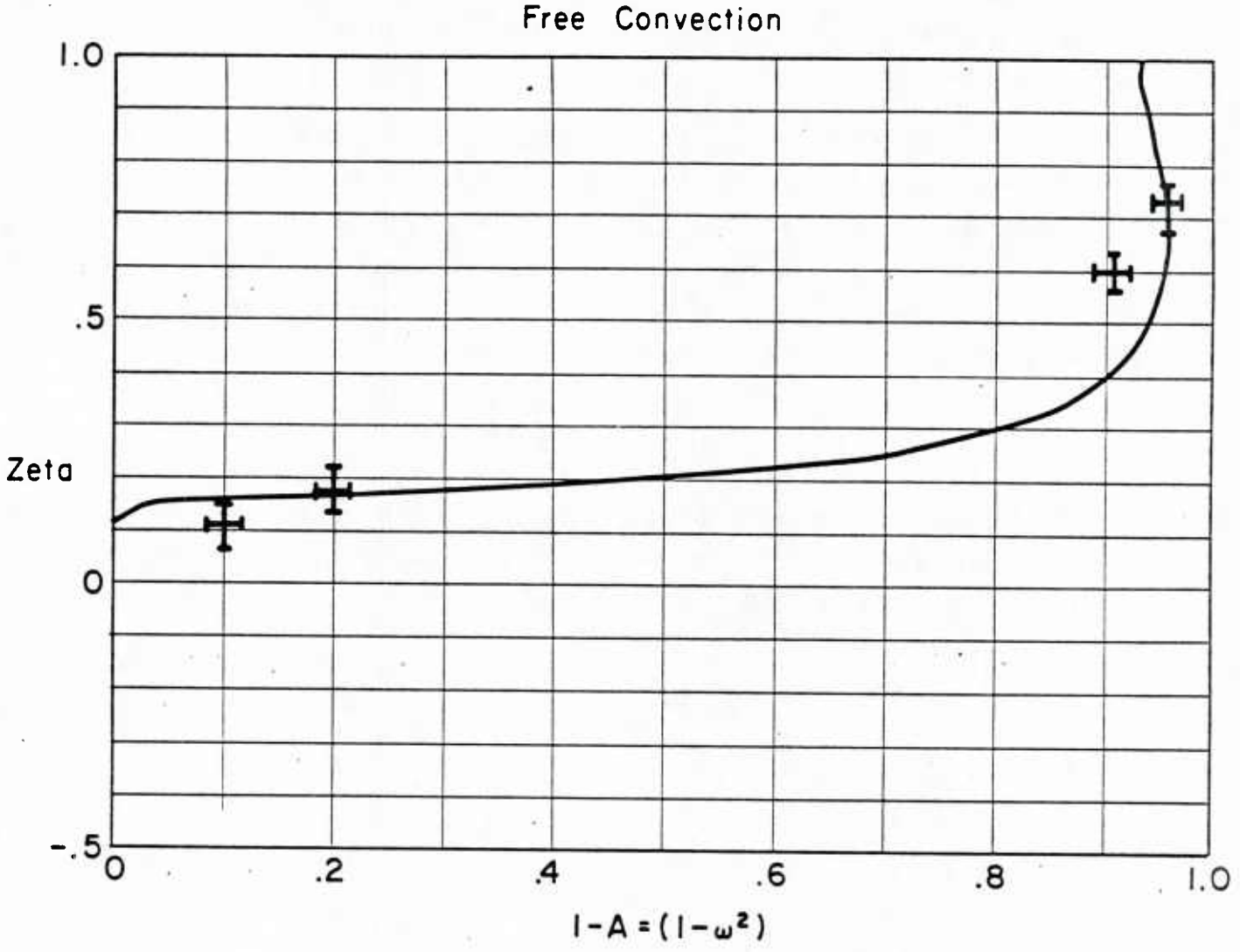

FIGURE 5.3: MODEL PREDICTIONS OF THE INTERMITTENCY WITHIN THE INTERFACIAL LAYER AT THE TOP OF A FREE CONVECTION LAYER AS COMPARED WITH THE DATA OF DEARDORFF, ET.AL (1980). ZETA IS THE DISTANCE FROM THE HEIGHT AT WHICH THE HEAT FLUX GOES TO ZERO NORMALIZED BY THE INTERFACIAL THICKNESS.

intermittency does not play a strong dynamical role in this flow, we take it as a very encouraging sign that our intermittency algorithm is compatible with the observations.

In checking this model for the conditions presented in LSO, it appears that neglecting terms like $\overline{w'w'r'}$ in the $\overline{w'\theta_v'}$ equation may not be acceptable, although this would seem appropriate for a quasi-equilibrium approximation. This type term can be included in a straightforward fashion if we accept the model proposed in Equation 5.44 of LSO. In this case it is only necessary to replace $\bar{r}$ in Equations 5.24, 5.27 & 5.28 with

$$\bar{r} + a_r \sigma_r / \omega$$

An appropriate value of a_r, will need to be determined by numerical experimentation. A value of unity leads to qualitative consistency for the example considered in LSO.

6. CONCLUDING REMARKS

We have presented recommendations for a subgrid flux parameterization scheme appropriate for mesoscale meteorological models. Initial tests of this scheme, as compared with results from a full second-order closure, 1-D model indicate reasonable results when model grid resolution is adequate to determine the height of the unstable boundary layer. When resolution is not adequate for this it will be desirable to include a prognostic equation for the boundary layer thickness or incorporate parameterization for an elevated subgrid shear layer.

Our scheme incorporates cumulus parameterization as an integral part of the quasi-equilibrium formulation. Our tests suggest that intermittency, a fundamental feature of cumulus cloud environments, may be represented in the model in a relatively simple fashion. These initial results indicate that inclusion of the effects of cumulus dynamics into the quasi-equilibrium approximation of turbulent transport should be feasible. We recommend further testing.

REFERENCES

Deardorff, J. W., 1972: "Parameterization of the Planetary Boundary Layer for use in general circulation models." Monthly Weather Review, Vol. 100, pp. 93-106.

Deardorff, J. W., Willis, G. E., and B. H. Stockton, 1980: "Laboratory Studies of the Entrainment Zone of a Convectively Mixed Layer." J. of Fluid Mechanics, Vol. 100, pp. 42-64.

Gunn, R. and G. D. Kinzer, 1949: "The Terminal Velocity of Fall for Water Drops in Stagnant Air." J. Meteor., 6 452-461.

Kollman, W., 1984: "Prediction of the Intermittency Factor for Turbulent Shear Flows." AIAA J., Vol. 22 pp. 486-492.

Lewellen, W. S., 1977: "Influence of Body Forces on Turbulent Near a Surface." J. App. Math. and Phys., (ZAMP) 28, 825-834.

Lewellen, W. S., 1981: "Modeling the Lowest 1KM of the Atmosphere." Agardograph 267.

Lewellen, W. S. and Teske, M. E., (1973) Prediction of the Monin-Obukhov Similarity Formations from an Invariant Model of Turbulence. J. Atmos. Sciences, 30, 1340-1345.

Lewellen, W. S., Sykes, R. I., and Oliver, D. A. (1983) Further Developments of the A.R.A.P. Model for the Atmospheric Marine Environment. A.R.A.P. Report 488.

Mellor, G. L. and Yamada, T (1974) A Hierarchy of Turbulence Closure Models for Planetary Boundary Layers. J. Atmos. Sci. 31, 1791-1806.

Randall, D. A. (1976) The Interaction of the Planetary Boundary Layer with large-scale circulations, Ph.D thesis U.S.L.A. 247pp.

Wyngaard, J. C. and R. A. Brost, (1984). Top-Down and Bottom-Up Diffusion of a Scalar in the Convective Boundary Layer, Journal of Atmospheric Sciences, Vol. 41, pp. 102-112.

Zeman, O. and Lumley, J. L. (1976) Modeling Buoyancy-driven Mixed Layers. J. Atmos. Sci. 33, 1974-1988.

APPENDIX A

PARAMETERIZATION OF SUBGRID-SCALE FLUXES AND ESTIMATION OF DISPERSION

by

W.S. Lewellen

Aeronautical Research Associates of Princeton, Inc.
50 Washington Road, P.O. box 2229
Princeton, N.J. 08540

ABSTRACT

The parameterization of subgrid scale turbulent fluxes of momentum, energy, and mass in mesoscale meteorological models is discussed. Theoretical analyses and available observational data are used to describe our current understanding of the interdependence between turbulent diffusion and the resolved scale distributions of wind, temperature, and species. Emphasis is placed on the dependence of subgrid parameterization on the simulation resolution in ensemble space as well as in physical space and time. Specific recommendations are presented for the particular problem of dispersion from point sources.(*)

*Presented at the AMS workshop on Urban Boundary Layers, October, 1983, Baltimore, MD

1. INTRODUCTION

The turbulent fluxes of mass, momentum and energy are at least partially composed of motions that are too small to ever hope to be resolved in urban or mesoscale models. These turbulent fluxes control the interaction of the atmosphere with the surface and the dispersal of anything released within the atmosphere. Such mesoscale phenomena as the sea-breeze circulation, mountain-valley circulations, and the moisture build-up in the boundary layer necessary to drive convective clouds are all dominated by turbulent interactions with the surface. As long as the turbulent motions in these interactions cannot be resolved in the simulation, the parameterization of subgrid scale fluxes will play an important role in determining the accuracy of the simulation of any of these phenomena. This is perhaps most evident in the simulations of the dispersal of passive tracers in the atmosphere where almost all the motions responsible for dispersion are unable to be resolved in the meteorological model of the region of interest.

In addition to the question of what scale of motion can be resolved by a feasible grid system, there is the question of how much of the motion we wish to resolve. Flow in the atmospheric boundary layer inherently contains a turbulent stochastic component. Even if one were able to accurately numerically simulate all of the scales of motion in time and space for one particular realization, this would not provide a precise prediction of the motion in time and space for any other particular realization. In general, what we would like to simulate is the ensemble mean flow distribution in time and space. We would also like to gain some information about the variability of particular realizations from this mean. Numerical simulations either involve ensemble averaging of the equations or averaging of the simulations realized. For nonhomogeneous, nonstationary problems the choice of scales to average over before the numerical simulation is an important part of the problem. The larger the scales over which the equations are averaged the more uncertainty introduced by the closure approximations, but the smaller the scales the larger the computational requirements and the more averaging which must be done after the simulation to provide proper interpretation of the

results. The implications of the choice of the ensemble averaging scale on subgrid parameterizations are discussed in the next section.

The rest of the paper reviews some subgrid parameterization schemes and speculates on how they may be improved. Particular attention is given to dispersion from point sources because this is a problem where accurate parameterization of the unresolved turbulence is essential, and because this is an area where we have carried our speculations further.

2. THE INFLUENCE OF THE SCALE OF ENSEMBLE AVERAGING ON SUBGRID FLUX PARAMETERIZATION

The ensemble of flows of interest are all the possible flows which satisfy the prescribed input data. In ideal problems this input data may be sufficient to relatively tightly constrain this ensemble of flows, but in attempts to simulate local meteorological flows which occur at a specific time and place the input data is unlikely to provide tight constraints. Such simulations must be able to deal with relatively large variances from the resulting ensemble mean solution. This may be accomplished either by ensemble averaging over the equations prior to performing the numerical simulations or by performing an average over a number of different simulations which fall within the uncertainty of the prescribed input conditions. A different subgrid scale flux parameterization needs to be used for these two approaches. In practice, the distinction between the two approaches is usually made in terms of the scales of motion. In so-called large eddy simulations, some ensemble averaging is done at small scales, while higher-order closure approaches which deal with ensemble averaged equations over much larger scales may still resolve some of the dominant eddies in the flow.

The standard ensemble average velocity may be defined as

$$\langle \underline{u}(\underline{x},t) \rangle = \int_{\Omega} \underline{u}(\underline{x},t) p(\alpha) d\alpha \qquad \text{(A-2.1)}$$

where Ω is the set of all velocity fields which satisfy the prescribed input conditions and $p(\alpha)$ is the probability density function of any particular velocity field indicated by α. We wish to divide up this domain ensemble into a set of sub ensembles so that $\Omega=\sum_i \Omega_i$. Each Ω_i is the set of all velocity fields which satisfy the prescribed input conditions and are similar at scales of motion greater than some scale ℓ_e. A sub ensemble average

$$\langle \underline{u}(\underline{x},t)\rangle_i = \int_{\Omega_i} \underline{u}(\underline{x},t)p(\alpha)d\alpha \qquad \text{(A-2.2)}$$

is then equivalent to a particular large eddy simulation of the velocity.

In order to make this concept more explicit, consider the velocity field $\underline{u}(\underline{x},t)$ existing in a space domain V_o during a time interval T_o. As long as the Reynolds number based on a characteristic velocity and a characteristic length in the domain is large, $\underline{u}$ at any $\underline{x}$ and t can assume a wide variety of values with the probability of any individual continuous field indicated by α specified by the probability density function $p(\alpha)$. From this variety of possibilities let us choose one particular continuous field. Having chosen this unique field we average, or filter, it over an arbitrarily chosen scale, ℓ_e to eliminate all fine scale motions of a scale less than ℓ_e. It should then be possible to chose other neighboring fields that when similarly filtered vary at most by an ε from that chosen first. All such fields are included in the set Ω_1. As long as the Reynolds number based on ℓ_e and the characteristic velocity in Ω_1 is large, their will also be a large number of individual distributions which fall within Ω_1. The process can be repeated to form a Ω_2 set, etc. The number of possible Ω_i sets is also large as long as ℓ_e is significantly less than the dominant shear layer thickness in the computational domain.

The choice of ℓ_e determines the break between resolved and unresolved motions. Since a given grid cannot resolve a motion which is of a characteristic length less than about 3 times that of the grid, this sets a lower bound on ℓ_e. The upper bound is the characteristic length of the domain

of simulation. The lower bound is appropriate for Large Eddy Simulations (LES) where the goal is to resolve as much of the motion as possible. The upper bound is appropriate when the goal is to resolve only the mean motion in the time and space domain.

3. A HIERARCHY OF SUBGRID CLOSURE ASSUMPTIONS

The ensemble averaged equations are precisely defined for any ensemble as the Reynolds averaged Navier-Stokes equations

$$\frac{\partial \bar{u}_j}{\partial x_j} = 0 \tag{A-3.1}$$

$$\frac{\partial \bar{u}_i}{\partial t} + \frac{\partial}{\partial x_j}(\bar{u}_i \bar{u}_j + \overline{u_i' u_j'}) = -\frac{\partial \bar{p}}{\rho \partial x_i} + \nu \frac{\partial^2 \bar{u}_i}{\partial x_j^2} + \beta g_i (\bar{\theta} - \bar{\theta}_0) \tag{A-3.2}$$

$$\frac{\partial \overline{u_i' u_j'}}{\partial t} + \frac{\partial}{\partial x_k}(\bar{u}_k \overline{u_i' u_j'}) = -\overline{u_i' u_k} \frac{\partial \bar{u}_j}{\partial x_k} - \overline{u_j' u_k} \frac{\partial \bar{u}_i}{\partial x_k} \tag{A-3.3}$$

$$- \frac{\partial}{\partial x_k}(\overline{u_k' u_i' u_j'}) - \frac{\overline{u_i'} \frac{\partial p'}{\partial x_j}}{\rho} - \frac{\overline{u_j'} \frac{\partial p}{\partial x_i}}{\rho} + \nu \frac{\partial^2 \overline{u_i' u_j'}}{\partial x_k^2} - 2\nu \overline{\frac{\partial u_i'}{\partial x_k} \frac{\partial u_j'}{\partial x_k}}$$

$$+ \beta(g_i \overline{u_j' \theta'} + g_j \overline{u_i' \theta'})$$

The equations are well-defined but not closed. Some assumptions relating higher-order correlations must be made to close the system.

The assumptions made to close the ensemble averaged equations control what parameterizations are appropriate for subgrid turbulent fluxes. It should perhaps be noted that when Equation 3.2 is used for LES by choosing ℓ_e smaller than the scale of the large eddies, there is no inclusion of Leonard stress

terms (Leonard, 1974) as there is when the LES equations are derived by spatially filtering the equations of motion. The $\bar{u}_i$ obtained from the ensemble average over the scale of ℓ_e is thus somewhat different than the $\bar{u}_i$ obtained by spatially filtering over a scale of ℓ_e. However, this difference is generally masked by approximations in the Reynolds stress closure.

The simplest closure with some general applicability is Smagorinsky's (1963) model which replaces Equation 3.3 with the approximation

$$\overline{u_i' u_j'} = -2(c_s\Delta)^2 \left[S_{nm}S_{nm}\right]^{1/2} S_{ij} + \frac{1}{3}\delta_{ij}\overline{u_k' u_k'} \qquad \text{(A-3.4)}$$

where

$$S_{ij} = \frac{1}{2}\left(\frac{\partial \bar{u}_i}{\partial x_j} + \frac{\partial \bar{u}_j}{\partial x_i}\right) \qquad \text{(A-3.5)}$$

and the isotropic part of the Reynolds stress is absorbed within the mean pressure.

The length scale Δ should be an order one fraction of ℓ_e. If ℓ_e, and consequently Δ, are chosen as small compared to the large eddies expected in the field, then the resulting simulation provides a single realization of the large eddies in the flow. In this case the desired domain ensemble average is obtained by averaging the results over a suitable number of these sub-ensemble flows or large eddy simulations. These individual realizations may be obtained by varying the input conditions within the constraints of the specified accuracy of the input conditions. On the other hand, if ℓ_e is chosen larger than the large eddies expected in the field, and Δ is appropriately chosen, then the simulation will approximate that of the ensemble average flow over the domain without any further averaging of the simulation results. Of course, at the level of closure of Equation 3.4 one should expect the first LES procedure to provide a much more accurate simulation in return for the much larger computational effort required to accomplish it.

If Δ is chosen to be larger than the mesh grid but still sufficiently small that the eddies to be represented by (3.4) are well within the inertial subrange of the turbulent spectra, then the domain ensemble average over LES sub-ensembles should agree with the domain ensemble results for smaller Δ, although the individual sub-ensemble flows may be quite different as a function of x and t. If the initial input for the two simulations are identical then the two simulations should initially differ only in their small scale eddy motions but this should spread to differences in the larger eddies as simulation time evolves. The higher resolution results should be superior if the assumptions on which (3.4) are based are not completely valid. The high resolution results will also provide a superior simulation when the resolution of the input conditions is higher than the low resolution LES. If Δ is chosen sufficiently small that the eddies to be represented by (3.4) are well within the inertial subrange of the turbulent spectra then it is possible to derive a theoretical value for c_s. However, researchers using this approach have found it more satisfactory to use a value which is significantly less than this theoretical value (c_s = 0.065) (Schumann, 1975). Equation (3.4) appears to provide reasonable results when $\overline{u_i' u_j'} \ll \bar{u}_i \bar{u}_j$. This imposes a stringent requirement on grid lengths close to a surface. In order to overcome this LES simulations have either made modifications to (3.4) close to surface or applied boundary conditions which incorporated turbulent surface layer relationships.

Close to a surface when $\overline{u_i' u_j'}$ becomes of the same order as $\overline{u_i u_j}$, the assumptions on which Equation 3.4 are based are violated, and it is desirable to transition to a form appropriate for ensemble averaging over a scale which is larger than the grid size used to resolve the mean flow close to the wall. The common mixing length model which is valid for the mean Reynolds stresses in the near-wall region is similar to Equation 3.4 but with Δ replaced by a mixing length proportional to the distance from the surface. The transition formula suggested by Schumann (1975) is

$$\overline{u_i' u_j'} = -2(c_s\Delta)^2 \left[2\left(S_{nm} - \langle S_{nm}\rangle\right)\left(S_{nm} - \langle S_{nm}\rangle\right)\right]^{1/2} \qquad \text{(A-3.6)}$$

$$\left(S_{ij} - \langle S_{ij}\rangle\right) - 2\nu_T^* \langle S_{ij}\rangle + \delta_{ij}\,\overline{u_k' u_k'}/3$$

where ν_T^* comes from the mixing length formula near the wall and is not allowed to exceed some upper bound depending upon the grid mesh. The angular brackets denote a transverse spatial average which due to the symmetry of his problem is roughly equivalent to an ensemble average. Close to the wall, $S_{ij}-\langle S_{ij}\rangle$ $\langle S_{ij}\rangle$ is appreciably less than one on average and the first term on the R.H.S. of (3.6) is much less than the last term, while far from the wall $\langle S_{ij}\rangle \to 0$ and Equation 3.6 approaches Equation 3.4.

When Equation 3.4 is viewed as an approximation to Equation 3.3 it becomes apparent that the non local dependence involved in the advection and diffusions terms has been omitted, the influence of stratification has been ignored and it has been assumed that the unresolved turbulence is isotropic. Under these conditions the dissipation term appearing in (3.3) may be approximated as

$$\varepsilon = c_\varepsilon(\overline{u_k'u_k'})^{3/2}\ \delta_{ij}/\Delta \qquad \text{(A-3.7)}$$

and the equation for $\overline{u_i'u_i'}=q^2$ from Equation 3.3 is consistent with Equation 3.4. More faithful representations of Equation 3.3 should permit ℓ_e to be increased, with resultant computational savings, without significant sacrifices in accuracy. Of course, the computational savings are only realized, if the additional computations required for Equation 3.3 do not exceed the savings accrued by relaxed space, time, and ensemble resolution requirements.

Second-order closure models for Equation 3.3 appropriate for variable density flows have been investigated by a number of researchers. Recent reviews have been given by Lewellen (1981), Zeman (1981), and Mellor and Yamada (1982). A model of Equation 3.3 which has proved satisfactory for a number of applications is

$$\frac{\partial\overline{u_i'u_j'}}{\partial t} + \frac{\partial\bar{u}_k\,\overline{u_i'u_j'}}{\partial x_k} = -\overline{u_i'u_k'}\frac{\partial\bar{u}_j}{\partial x_k} - \overline{u_j'u_k'}\frac{\partial\bar{u}_i}{\partial x_k} + \beta g_i\overline{u_j'\theta'} \qquad \text{(A-3.8)}$$

$$+ 0.3\frac{\partial}{\partial x_k}\left(q\Lambda\frac{\partial\overline{u_i'u_j'}}{\partial x_k}\right) - \frac{q}{\Lambda}\left(\overline{u_i'u_j'} - \delta_{ij}\frac{q^2}{3}\right) - \delta_{ij}\frac{q^3}{12\Lambda}$$

Compatible equations for $\overline{u_i'\theta'}$, $\overline{\theta'^2}$ and Λ which may be found in Lewellen (1981) are required to close the set at this level for the general case. Along with different forms of the modeled terms in Equation 3.8, a number of approximations intermediate to Equations 3.4 or 3.8 have been tried in the literature. A somewhat more general formula than (3.4) is to carry an equation similar to the contraction of Equation 3.8 for the unresolved turbulent kinetic energy $q^2/2$ and then to model $\overline{u_i u_j}$ as.

$$\overline{u_i'u_j'} = -q\ell\, S_{ij} + \delta_{ij}\, \overline{u_k'u_k'}\,/3 \qquad \text{(A-3.9)}$$

This turbulent-kinetic-energy-transport model for closure has been quite popular for simulations which have ensemble averaged over all scales of motion, and used by some LES models, e.g. Schumann (1975), and Deardorff (1980).

The next level of approximation is to allow for anisotropic behavior of ν_T. This can be obtained by combining the full equation for $\overline{u_i'u_j'}$ from Equation 3.8 with an algebraic approximation to Equation 3.8 for the relationship between the individual components of $\overline{u_i'u_j'}$. This "algebraic Reynolds stress" model carries more flavor of second-order closure than using Equation 3.9 alone. We have called this a quasi-equilibrium approximation to Equation 3.3 in our use of it to compute the diurnal variation in the planetary boundary layer (Lewellen, et.al., 1974). Mellor and Yamada (1974) term it their level 2 1/2 approximation to second-order closure.

When the boundary layer assumption is valid, i.e., when gradients in only one direction are important in the production terms of Equation 3.8, the "algebraic Reynolds stress" can be written compactly similar to the form given by Yamada and Mellor (1975) as

$$\overline{u_i w} = -q\Lambda\, S_m \frac{\partial \bar{u}_i}{\partial z} \qquad \text{(A-3.10)}$$

$$\overline{w\theta} = -q\Lambda\, S_H \frac{\partial\bar{\theta}}{\partial z} \qquad \text{(A-3.11)}$$

with

$$S_m = \frac{\left(\frac{\overline{ww}}{q^2}\right) + \left(4/3\right)\Lambda g\beta\overline{w\theta}\,/q^3}{1 + \left(4/3\right)\Lambda^2 g\beta\frac{\partial\bar{\theta}}{\partial z}\,/q^2} \qquad \text{(A-3.12)}$$

$$S_H = \frac{(4/3)\ \overline{ww}\,/q^2}{1 + 5.9\Lambda^2 g\beta\frac{\partial\bar{\theta}}{\partial z}\,/q^2} \qquad \text{(A-3.13)}$$

where

$$\frac{\overline{w^2}}{q^2} = \frac{1}{3} + \left(2\ \overline{uw}\ \frac{\partial\bar{u}}{\partial z} + 2\overline{vw}\ \frac{\partial\bar{v}}{\partial z} + 4\beta g\overline{w\theta}\right)\Lambda\,/3\ q^3 \qquad \text{(A-3.14)}$$

This formulation provides for the important influence of buoyancy on the eddy viscosities in Equations 3.10 and 3.11, and has been used by Yamada (1979, 1983) in a number of 3-D simulations of atmospheric boundary layers.

The horizontal wind variances needed for dispersal estimates may be obtained the same way, but a better estimate is obtained by considering Equation 3.8 to refer only to the fully 3-D small scale turbulence. Estimates of the ratio of the horizontal length scale of the turbulence to the vertical length scale can then be used to adjust the horizontal wind variance so that:

$$\overline{u'^2} = \left\{\frac{q^2}{3} + \frac{2\Lambda^2}{3}\left[S_m\left(2\left(\frac{\partial\bar{u}}{\partial z}\right)^2 - \left(\frac{\partial\bar{v}}{\partial z}\right)^2\right) + \beta g S_H\ \frac{\partial\bar{\theta}}{\partial z}\right]\right\}\left(\frac{\Lambda_H}{\Lambda_v}\right)^{2/3} \qquad \text{(A-3.15)}$$

$$\overline{v'^2} = \left\{\frac{q^2}{3} + \frac{2\Lambda^2}{3}\left[S_m\left(-\left(\frac{\partial\bar{u}}{\partial z}\right)^2\right) + 2\left(\frac{\partial\bar{v}}{\partial z}\right)^2\right) + \beta g S_H\ \frac{\partial\bar{\theta}}{\partial z}\right]\right\}\left(\frac{\Lambda_H}{\Lambda_v}\right)^{2/3} \qquad \text{(A-3.16)}$$

It is important to note that this 1-D version of quasi-equilibrium is appropriate for boundary layer problems with $\ell_e >> \delta$ where the simulation corresponds to the domain ensemble average. If this closure were used for a LES with $\ell_e < \delta$ then the 1-D approximation used in the algebraic reduction would be violated by the inherent 3-D character of the large eddies in the boundary layer. On the other hand, a fully 3-D algebraic Reynolds stress formulation is not much simpler than dealing directly with Equation 3.8.

The only computation attempted for a fully 3-D, unsteady Reynolds stress model has been that of Deardorff (1972a) of flow in the planetary boundary layer. He used ℓ_e of the same order as the grid mesh to perform a LES. In his numerical simulations which imposed a logarithmic law-of-the-wall at the surface rather than attempt to resolve the surface layer, the added sophistication of using a modeled Equation 3.3 did not provide significantly different results from that obtained using the simpler Equation 3.4. We would not conclude, as some have, from this single experiment that higher-order closure is not useful in any LES. The extent to which Equation 3.3 can be closed to faithfully represent more of the turbulent spectrum, will eventually determine the extent to which second order modeling can make LES more practical.

We believe the marriage of LES and second-order closure (SOC) should provide benefits unattainable by either at the present time. The relaxation of the grid resolution problems at the higher frequency end of the spectrum of motions should allow the LES to concentrate on the eddies which dominate turbulent transfer in a more efficient manner. Conversely, permitting the SOC model to directly resolve the largest eddies should provide a generality to SOC which has so far eluded research modelers. The 2-D LES of Lewellen, Teske and Sheng (1980) for roll vortices in the planetary boundary layer and by Sykes and Lewellen (1982) of Kelvin-Helmholtz wave breaking in a shear layer have been a step in this direction. These simulations had a stronger than desired dependence on ℓ_e, since the SOC model was not general enough to precisely represent the effect of large 2-D eddies and any large 3-D eddies could not be represented by the 2-D simulation, but judicious choices of ℓ_e

permitted very reasonable simulations of the two phenomena.

In most regional scale models it will be necessary to set ℓ_e as of the order of 1 km or larger since any finer mesh than a few hundred meters in the horizontal appears to impose prohibitively large computational requirements. This means that the boundary-level eddies must be ensemble averaged over and the straightforward application of (3.4) is only appropriate at most for parameterizing the horizontal fluxes of momentum. The vertical flux of momentum will be controlled by the next to last term in Equation 3.6. In this case the most sensitive parameter in the formulation is the bounds placed on $\overline{\nu_T^*}$ in the outer part of the boundary layer. The most popular formulation for this is O'Brien's (1970) which prescribes a cubic polynomial fit to ν_T^* by matching value and slope to surface layer relationships, at some assumed top of the surface layer and fixing the value at the top of the boundary layer. This formulation depends explicitly on a separate dynamic prediction of the boundary layer height. A number of other formulations for ν_T^* have been reviewed by Blackadar (1979).

We believe a reasonable compromise for ℓ_e of order 10 km is to carry a dynamic equation for q^2 obtained from modeling Equation 3.3. A proper model of this equation on this scale should recognize the disparate nature of the largely 2-D mesoscale eddies from the 3-D eddies equal to or smaller than the boundary layer scale. A 1-D algebraic Reynolds stress model may then be used for the vertical fluxes of momentum, energy, and mass while an approximation similar to Equation 3.9 is used for the horizontal fluxes. The determination of the vertical distribution of the length scale for the 1-D algebraic Reynolds stress model will require an estimate of the boundary layer thickness. This requirement is compatible with the recommendation that integral equations for momentum, thermal, and turbulent kinetic energy boundary layer thickness be used in connection with the surface boundary conditions discussed in the next section.

4. SURFACE BOUNDARY CONDITION CONSIDERATIONS

Strong gradients occur in most of the meteorological variables in the immediate vicinity of the surface. The surface boundary conditions which are most appropriate for any numerical simulation then depend critically on the vertical grid resolution next to the surface. The straightforward use of no-slip conditions and no flow thru the solid boundary are generally not possible due to inadequate resolution next to the surface. It is possible to show that one should have $\Delta z << z_o$ before no-slip conditions are appropriate at $z=z_o$. Since this is not feasible, one must either asymptotically match to the surface layer conditions at some greater height where $\Delta z << z$ is feasible or integrate across the surface layer to obtain appropriate boundary conditions.

A reasonable choice is to define the values of turbulent fluxes at the lowest point in terms of a transport coefficient, i.e.

$$\overline{u'w'} = -c_f |\bar{u}|\bar{u} \tag{A-4.1}$$

$$\overline{w'\theta'} = -c_\theta u_* \left(\theta_1 - \theta_s\right) \tag{A-4.2}$$

where specification of c_f and c_θ is part of the subgrid parameterization. When the lower grid point falls within the surface layer these coefficients may be obtained by integrating over the Monin-Obukhov functions (Paulson, 1970).

$$c_f = \left[\frac{k}{\ell n\ z/z_0 - \Psi_1}\right]^2 \tag{A-4.3}$$

$$c_\theta = \frac{k}{\left[0.74 \ell n\ z/z_0 - \Psi_2\right]} \tag{A-4.4}$$

where

$$\Psi_1 = 2\ell n\left[\frac{1}{2}(1 + x)\right] + \ell n\left[\frac{1}{2}(1 + x^2)\right] - 2\tan^{-1}x + \pi/2$$

with

$$x = (1 - 15\, z/L)^{1/4}$$

and

$$\Psi_2 = 2\ell n\left(\frac{1}{2}\left[1 + \left(1-9\frac{z}{L}\right)^{1/2}\right]\right)$$

for

$$z/L \leq 0$$

and

$\Psi_1 = \Psi_2 = -4.7\ z/L$ for $z/L \geq 0$. $\left[\text{Note } L = -c_f\bar{u}^{\,2}T_0/kgc_\theta(\theta_1 - \theta_s)\right]$

This procedure breaks down when either the turbulence within the surface layer is not completely controlled locally within the surface layer, or the bottom grid point falls outside the surface layer. Deardorff (1972a) has provided algorithms to circumvent both these limitations. The first is accomplished by replacing u_* by $0.7w_*$ when this fraction of the characteristic convective velocity exceeds u_*. Since w_* depends on the boundary layer thickness this provides the non-local determination of the turbulent interaction. The second limitation is overcome by assuming shape functions of δ/L for the velocity and temperature profiles over the outer 97.5% of the boundary layer. This allows him to generalize the surface layer c_f and c_θ relationships to be a function of δ/z_0, the ratio of the boundary layer thickness to the surface roughness, and

$$Ri_b = \frac{g\delta(\theta_a - \theta_s)}{\theta_a u_m^2}$$

a bulk Richardson number. These relationships may then be applied even when z_1

greatly exceeds the surface layer thickness. The overall boundary-layer thickness is estimated from an integral of the temperature equation with upper bounds applied under certain neutral and stable conditions. Deardorff intended his PBL parameterization for global weather models but it has also been used for some limited area models.

We believe Deardorff's scheme for parameterizing c_f and c_θ can be improved by replacing Equations 4.1 and 4.2 with

$$\overline{u'w'} = -c_{f_u}\, q\, u \qquad \text{(A-4.5)}$$

$$\overline{v'w} = -c_{f_v} qv \qquad \text{(A-4.6)}$$

$$\overline{w'\theta'} = -c_\theta q(\theta_1 - \theta_s) \qquad \text{(A-4.7)}$$

where q is obtained from the dynamic equation for the turbulent kinetic energy. The coefficients defined in Equations 4.5 to 4.7 may be parameterized in terms of 4 different boundary layer thicknesses. Two velocity displacement thicknesses, δ_u and δ_v, the thermal thickness, δ_θ, and the turbulent kinetic energy thickness $\delta_q 2$, may be determined by integrating the momentum, temperature, and turbulent kinetic energy equations. We plan to investigate such a scheme in our work for the Naval Environmental Prediction Research Facility.

We expect the appearance of q in the surface coefficient definition to directly provide the more global dependence of the coefficients required under unstable conditions and hope that the use of the 4 integral constraints will permit more of the influence of unsteady and various horizontal pressure gradient effects to be included in the parameterization than is possible when only the thermal boundary layer thickness is used.

5. DISPERSION FROM POINT SOURCES

A subgrid scale problem of considerable importance is that of dispersion from a point source of a passive tracer. When the plume is small relative to a few grid widths of the meteorological simulation its dispersion is completely controlled by the subgrid turbulence. Due to the importance of turbulent parameterization for this phenomenon and because we have recently made what we believe to be significant progress in this area, we will discuss this in some detail. A subgrid plume from a point source may be modeled as a gaussian plume with the spread of the plume obtained from a dynamic equation derived by averaging over the dynamic equation for the turbulent species flux (Lewellen, 1981). With the mean wind and turbulence quantities considered homogeneous within the subgrid volume this yields

$$\frac{D^2(\sigma_r^2)}{Dt^2} = 2\overline{u_i' u_j'}\,\delta_{ij} - \frac{Aq}{\Lambda}\frac{D\sigma_r^2}{Dt} \qquad \text{(A-5.1)}$$

where σ_r^2 is the spread of the plume perpendicular to its mean trajectory.

Equation 5.1 provides the basis for using pertinent information about the wind fluctuations, the normal components of the Reynolds stress, and the length scale of the turbulence, to directly determine the spread of a subgrid plume rather than depend on empirical functions of downwind distance for different stability classes. It is important to note that Equation 5.1 provides an estimate of the ensemble plume spread. For relatively large values of $\bar{\Lambda}/q$, the time scale of the turbulence, a large part of this spread will be in ensemble space which manifests itself as a meandering plume, i.e., an uncertainty in position of a much narrower plume in physical space. The magnitude of this uncertainty in concentration may be analyzed by dealing directly with the concentration variance equation. When this is also assumed to have a guassian distribution the integrated variance equation can be written simply as (Lewellen and Sykes, 1983)

$$\frac{D}{Dt}\left\langle \overline{c'^2} + \bar{c}^2 \right\rangle = -\left\langle \overline{c'^2}/\tau_c \right\rangle \qquad \text{(A-5.2)}$$

where τ_c is the time scale of the dissipation of $\overline{c'^2}$ and $\langle\ \rangle$ denotes integration over the cross section of the plume. The Guassian distribution has been shown to be a reasonable approximation for homogeneous turbulence by Sykes, Lewellen and Parker (1983) and the predictions obtained from (5.2) have been demonstrated to be compatible with the data on concentration variances from a point source in a wind tunnel boundary layer taken by Fackrell and Robins (1982). Both the data and the analyses show that $\sigma_c/\bar{c}$, the ratio of the standard deviation of the concentration fluctuations to the mean value, can often exceed 1 even on the centerline of the plume as shown in Figure A.1 and can be much larger in the edges of the plume.

The calculation of the concentration variance by Equation 5.2, or similar equation, provides information that cannot be readily obtained from releasing random particles into even a completely known flow unless sufficient particles are tracked to provide some resolution in ensemble space as well as physical space.

6. THE USE OF A VARIANCE CALCULATION AS A MEASURE OF PREDICTABILITY

An estimate of the ensemble variance of the velocity field provides important complementary information to the estimate of the mean. It provides a measure of the predictability of the velocity and is essential to providing simulations of dispersion of a passive tracer in the flow. Uncertainty in the initial conditions of a particular simulation may be used to specify initial values for the velocity variance as a function of space. In a SOC simulation the evolution of this velocity variance field may be tracked as the mean field is tracked. Subsequent ratios of $(\sigma_u/\bar{u})$, as a function of x and t provide a measure of how well the velocity field is specified for the particular input constraints. Initially σ_u is determined completely by the uncertainty in the initial conditions. However, at subsequent times both the internal production terms of Equation 3.3 and uncertainties in the boundary conditions will contribute to σ_u. Even if it were possible to very closely define the initial conditions and boundary conditions so that $\sigma_u \approx 0$ both initially and on the boundaries, the production terms in Equation 3.3 would still impose a variance on the field which may be expected to grow with time until some type

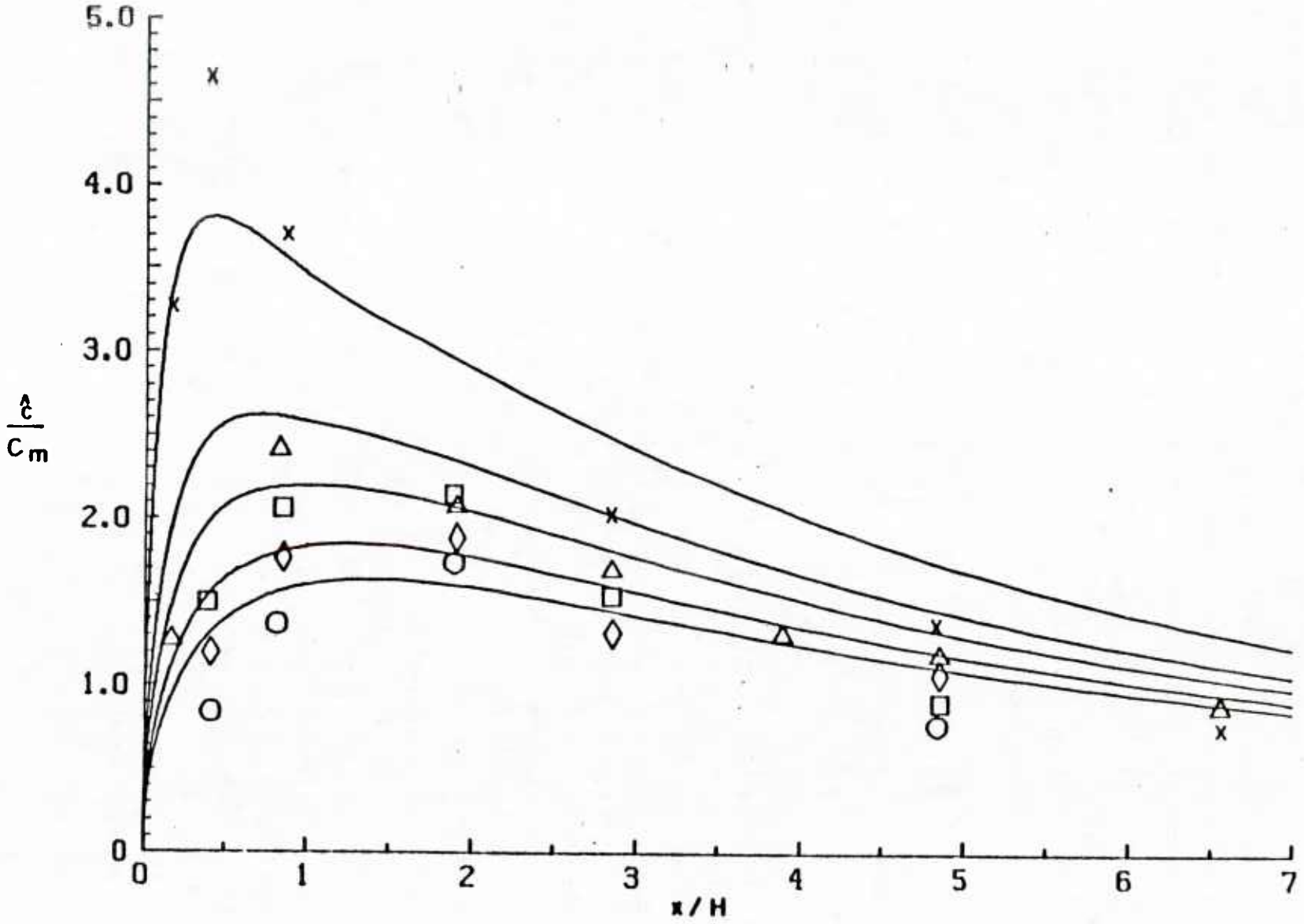

FIGURE A.1: Comparison of model predictionsby Sykes, et.al. (1983) with the observations of Fackrell and Robins (1982) for the centerline ratio of the standard deviation of concentration fluctuations to the mean value of concentration for an elevated source of various diameters within a laboratory turbulent boundary layer as a function of normalized downstream distance. x represents observed data for source diameter of 3mm; Δ, 9mm; □, 15 mm; ◇, 25 mm; 0, 35mm

equilibrium between production and dissipation is reached. Added precision in specifying the initial conditions will only reduce the variability in the field at times earlier than this equilibrium time. The faithful modeling of Equation 3.3 should thus provide a useful means of investigating the impact of various modeling improvements on predictability as a function of time.

When ℓ_e is set at less than the characteristic scale of the domain so that individual eddies are simulated, the effect of uncertainties in input conditions must be determined by sensitivity runs. The variability introduced by an inverse cascading of energy from high frequency motions to low frequency, what Leslie and Quarini (1978) refer to as subgrid backscatter, will be more difficult to assess. It might be possible to assess this by investigating the sensitivity of the LES to random perturbations in the LES field which are consistent with the variance computed for the sub ℓ_e motions.

The velocity variance determines the dispersion of a passive tracer in the flow. It is generally recognized that the high frequency velocity motions are responsible for the diffusion of a tracer as a puff of tracer material is transported by the low frequency velocity motions. What is not so well recognized is that intermediate range motions may either diffuse the puff or introduce an uncertainty in the transport of the puff. All of the variance serves to spread the puff in ensemble space but only the motions of a scale less than the scale of the puff serve to diffuse the instantaneous puff. The rest of the ensemble spread manifests itself as a meander of the plume.

The contributions of these meanders to the diffusions of a time-averaged puff are determined by the relative time scale of the meanders and the sampling time. A mesoscale gap in the wind energy spectrum (van der Hoven, 1957) is often evoked as justification for a distinct division between mean, transporting winds, and fluctuating, diffusing winds. This gap is generally not as pronounced as theoreticians would desire. The wind energy spectrum from the 100m level of a tower at the Kincaid power plant site in Illinois is given in Figure A.2 for 2-3 week periods in 1980 as taken from Lewellen, Sykes, and Parker (1983). Some interaction boundaries have been sketched on the spectrum to indicate what part of the spectrum may be expected to contribute to

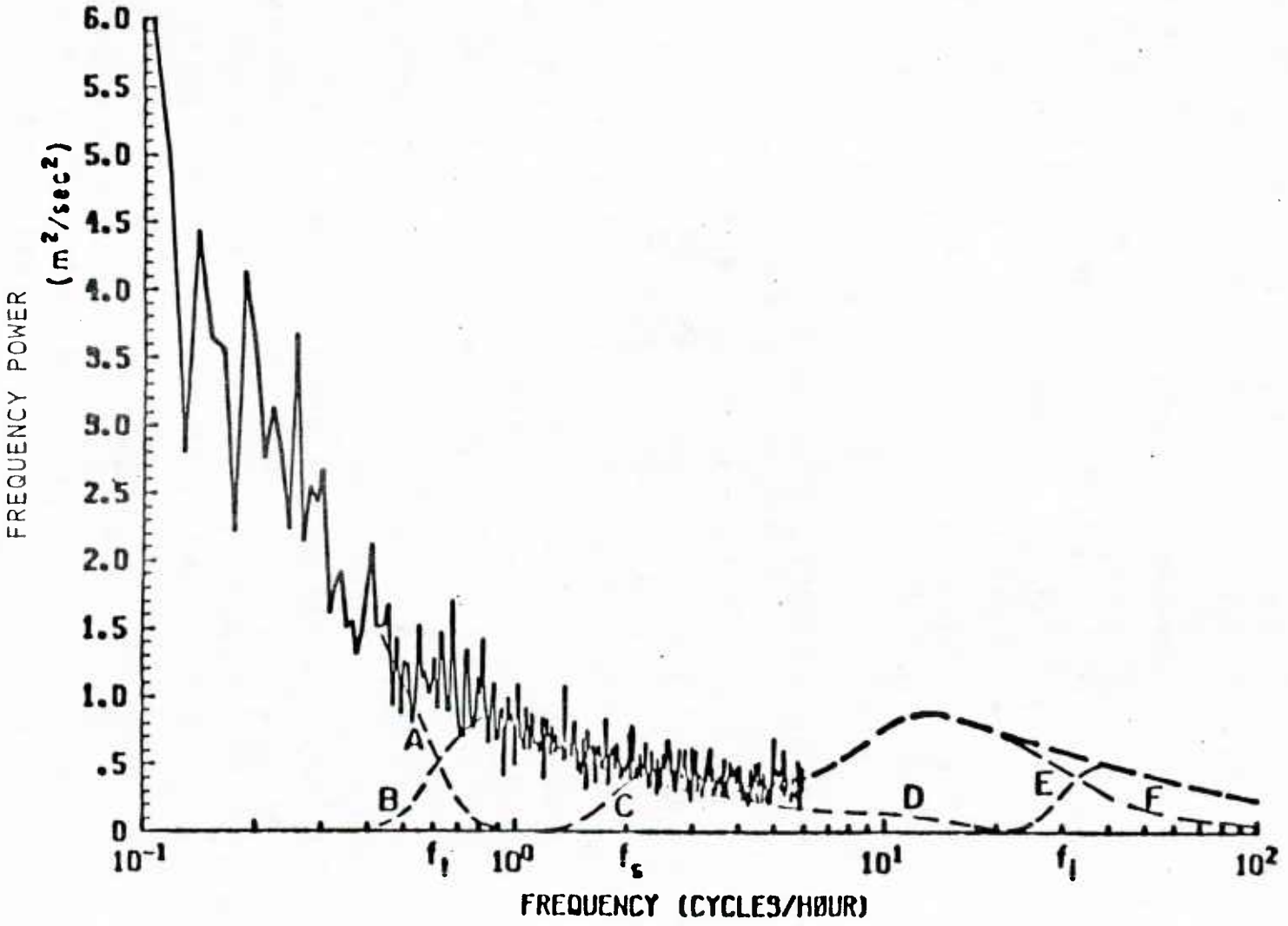

FIGURE A.2: Spectrum of the horizontal wind fluctuations at the Kincaid site (from Lewellen et.al. 1983) with the dashed lines, A, B, C, D, E, and F indicating the boundaries of different interactions between the plume and the atmospheric motions. These interactions are discussed in the text.

different effects.

Line A is intended to represent the bound of motions included in the mean transport of the plume. The motions at frequencies less than this bound must be adequately resolved so that the transport of a plume element may be tracked. There must be a consistency between the time for which the plume is tracked and the spatial resolution of the wind motion. In Figure A.2 the transition between transport and turbulence has been arbitrarily place at f_t=0.5 cycle/hour. This would permit a 4 m/s mean wind to transport the plume approximately 30 km before spatial correlation between the transporting wind at the tower and at the plume is lost. The shape of line A is symbolic of the fact that there is not a discontinuous break at this bound, but rather than there is a transition range of frequencies over which the ability to include the wind energy into the mean transport is lost.

Line B represents the lower frequency bound of the energy which can be included as a part of the turbulence. B should complement A in such a way as to assure that there is no source or sink of wind kinetic energy in this transition from mean transport winds to turbulent winds.

At the high frequency end of the spectrum, line E represents the lower bound of motions which contribute directly to the diffusion of the instantaneous plume. Line F represents the upper bound on motions which contribute to the total ensemble variance of the concentration. Higher frequencies contribute to the dissipation of the variance rather than its production. The larger the spatial spread of the instantaneous plume, the lower the frequency which can contribute either to the diffusion of this instantaneous plume or the dissipation of the concentration variance. Thus, lines E and F will move to the left to lower frequencies as the plume spreads downstream. The turbulent kinetic energy between B and E is responsible for the meander of the instantaneous plume. If the plume is tracked sufficiently far downwind of the stack then E may move to the left of B. If the additional spatial information is available so that the A-B boundary still correctly represents the transition from transport to turbulence, then when E crosses to the left of B it means that part of the resolvable transport motion is now

contributing to the "diffusion" of the instantaneous plume.

The meander of the plume driven by the energy between boundaries B and E can contribute to either the time-averaged diffusion of the plume or to the uncertainty in the position of the time-averaged plume. The location of these boundaries C and D on Figure A.2 are determined by the sampling time period. The position of C and D sketched is arbitrarily set at a sampling frequency of twice per hour. Line C represents the bound on energy affecting the concentration level of the time-averaged sample. Motions represented by energy to the left of boundary C move the time-averaged plume around as a coherent entity rather than contributing to its diffusion. Boundary D represents the boundary between the motions which contribute to the time-averaged variance of the concentration and that which contribute to the time-averaged diffusion. Energy to the right of D contributes only to the time-averaged diffusion of the plume. We expect the contribution of energy in frequencies greater than f_s to the time-averaged variance to fall off as (f_s/f) approximately; this determines the shape of D. The shape C is harder to set but is determined by the enhanced diffusion resulting from the interaction of the small scale inner plume turbulence with the distortions of the plume forced by the large scale motion. As sampling time is reduced lines C and D approach lines E and F, respectively.

Our purpose here is not to try to precisely define the shape of all the boundaries on Figure A.2, but to argue that such boundaries exist and qualitatively note the type of influence the energy bounded by the different lines has on the plume. This breakdown of the interactions of different scales of motion illustrates that a level of uncertainty is an inherent part of plume dispersion which can not be eliminated even by a perfect model. However, improved models should be able to provide an estimate of the variance along with their predictions of the mean concentration distribution.

7. RELATED SUBGRID PARAMETERIZATION PROBLEMS

1) Subgrid Scale Sources

Not only is it necessary to model the subgrid transport of mass, momentum, and energy, but it is also often necessary to model subgrid sources (or sinks) of one or more of these quantities. Relatively less work has been devoted to this subject than to the modeling of the turbulent transport terms although in urban models the influence is likely to be nearly as important. Subgrid surface sources generally have been incorporated into the effective roughness of the surface. This is appropriate as long as: (1) the height of the source is well below the first vertical grid point above the surface, and (2) the sources are relatively uniformly distributed between the horizontal grid points. When this is not the case a more accurate formulation should improve the simulation, particularly if the detailed influence of these sources are of interest. Pielke (1981) has proposed that subgrid scale terrain forcing can be neglected in mesoscale models if the subgrid scale terrain height variance is small compared with the grid resolvable terrain variance and has investigated the Spectra of terrain height variance over parts of Virginia (Pielke and Kennedy, 1980) and Colorado (Young and Pielke, 1983) to see what limits on mesoscale resolution this imposes as long as subgrid terrain is neglected. The conclusion is that this limits the maximum allowable horizontal grid spacing to 100m in Colorado and 1 km in Virginia. Subgrid terrain forcing is probably even more important than that implied by the ration of the integrated subgrid terrain height variance to the integral of the resolved terrain variance due to the role of subgrid terrain changes in separating the boundary layer flow. However, even this conservative estimate indicates that such forcing can not be neglected in hydrostatic mesoscale simulations which have a lower bound on the horizontal grid spacing of approximately 5 km. This problem clearly warrants more attention than it has received.

2) Unresolved Shear Layers Away from the Surface

Another subgrid phenomena which merits work in mesoscale models is that of dealing with local regions of high gradients which cannot be resolved by the grid mesh. It might be argued that the grid should be set so that all shear layers of importance to the phenomena under investigation could be resolved, but this is not likely to always be feasible. Thus, subgrid flux parameterization may be improved if it can be formulated in such a way as to permit thin shear layers to exist within the subgrid space without being wiped out. The top of the surface mixed layer or the remnants of what was once the top of the mixed layer often falls into the category of a shear layer which needs such parameterization. A potential technique for this might be to compute the subgrid Richardson number in the vertical direction and limit it to not exceed a critical value of approximately 1/4, i.e., require that

$$Ri = \frac{g}{To} \frac{\Delta T \Delta z}{\left[(\Delta u)^2 + q^2 \right]} < 1/4 \qquad \text{(A-7.1)}$$

The rationale for imposing this limit is the recognition that if Ri is significantly bigger than this, turbulence cannot be supported within the layer. Conversely, if Ri is significantly less than this value the layer is likely to be unstable and grow in thickness. Thus a simple, rough parameterization of a turbulent shear layer may be accomplished by setting Ri=1/4. If the computed value exceeds 1/4 then a subgrid shear layer with a Ri=1/4 may be placed within the grid. The shear layer would be joined by slopes of $\Delta T_-/\Delta z_-$, $\Delta u_-/\Delta z_-$ on the lower side and $\Delta T_+/\Delta z_+$, $\Delta ud_+/\Delta z_+$, on the upper side. The subgrid location of the shear layer could only be determined if other considerations are introduced. Compatibility with the computed boundary layer thickness could provide such a constraint in the case of the shear layer at the top of the boundary layer.

3) Cumulus Parameterization

Cloud dynamics play a strong part in the interaction of the surface with the atmosphere. Cumulus clouds present a particular problem to mesoscale simulations because ℓ_e is sufficiently large that individual clouds can not be

resolved and the dynamical role of clouds must be included in the subgrid parameterization. When the clouds are fairly uniformly distributed over the ℓ_e domain then the principal import of the clouds is the influence of the latent heat release on the temperature equation and the subsequent effect of this on the buoyant generation of vertical motions. An added complication is introduced when the cloud instability begins to control the turbulent motion. This natural instability of the cloud motion tends to concentrate the vertical motions and causes the turbulence to be distributed very intermittently in time and space. The usual turbulence closure approximations assume some uniformity of the turbulence within the ensemble domain. Strong intermittency can seriously invalidate these approximations. Thus a serious attempt to incorporate cumulus dynamics into a general representation of subgrid turbulent fluxes, rather than rely on ad hoc parameterization of the influence of cumulus convection such as those given by Kuo (1974) and Arakawa and Schubert (1974), must find a reasonable closure approximation for intermittent turbulence. We have speculated (Lewellen, et.al., 1983) that this may crudely be accomplished by allowing the turbulent time scale to be proportional to an intermittency variable. This permits a more rapid redistribution and dissipation of turbulent energy. It remains to be seen how well we can accomplish the critical step of determining an appropriate equation for the intermittency variable.

8. CONCLUDING REMARKS

We wish to emphasize the importance of correctly interpreting variability within ensemble space when attempting to simulate mesoscale temporal and spatial distributions of meteorological variables. The appropriate choices for subgrid flux parameterization depend strongly on the domain in ensemble space a modeler wishes the simulation to represent. The subgrid flux parameterization is easier when the ensemble domain is tightly constrained, but more averaging of particular realizations is required to provide a correct interpretation of the simulation results. We have attempted to provide some guideline for flux parameterization in general and have recommended a specific framework which we will be testing for the Naval Environmental Prediction

Research Facility. We have also made specific recommendations for the particular problem of dispersion from point sources.

References

Arakawa, A., and W.H. Schubert, 1974: "Interaction of a Cumulus cloud ensemble with the large-scale environment, Part I," J. Atmos. Sci., 31, pp. 674-701.

Blackadar, A.K., 1979: "High-resolution models of the planetary boundary layers," Advances in Envir. Sci. and Eng., 1, pp. 50-85.

Deardorff, J.W., 1972a: "Numerical investigation of neutral and unstable planetary boundary layers," J. Atmos. Sci., 29, pp. 91-115.

Deardorff, J.W., 1972b: "Parameterization of the planetary boundary layer for use in general circulation models," Monthly Weather Review, 100, pp. 93-106.

Fackrell, J.E., and A.G. Robins, 1982a: "Concentration fluctuation and fluxes in plumes from point sources in a turbulent boundary layer," J. Fluid Mech., 117, pp. 1-26.

Kuo, H.L., 1974: "Further studies of the parameterization of the influence of Cumulus convection on large-scale flow," J. Atmos. Sci., 31, pp. 1232-1240.

Leonard, A., 1974: "On the energy cascade in large-eddy simulations of turbulent fluid flows," Advances in Geophysics 18A, pp. 237-248.

Leslie, D.C., and G.L. Quarini, 1979: "The application of turbulence theory to the formulation of subgrid modeling procedures," J. of Fluid Mech., 91, pp. 65-91.

Lewellen, W.S., 1981: "Modeling the lowest 1 Km of the atmosphere," AGARD-AG-267. Available from NTIS.

Lewellen, W.S., and R.I. Sykes as a measure of natural uncertainty in observed concentration samples," Proc. AMS 6th Symp. Turbulence and Diffusion, Boston, MA.

Lewellen, W.S., R.I. Sykes, and D.A. Oliver, 1983: "Further developments of the A.R.A.P. model for the atmospheric marine environment," A.R.A.P. Report No. 488.

Lewellen, W.S., R.I. Sykes, and S.F. Parker, 1983: "Analysis of plume variability based on select periods of the Kincaid data set," ARAP Report 495, May 1983.

Lewellen, W.S., M.E. Teske, and C. duP. Donaldson, 1974: "Turbulence model of diurnal variations in the planetary boundary layer," Proc. of the 1974 Heat Trans. and Fluid Mech. Inst., (edited by L.R. Davies and R.E. Wilson), Stanford Univ. Press, Stanford, CA, pp. 301-319.

Lewellen, W.S., M.E. Teske, and Y.P. Sheng, 1980: "Micrometeorological applications of a second-order closure model of turbulent transport," Turbulent Shear Flows 2, Selected papers from the Second Int'l. Symp. on Turbulent Shear Flows, Imperial College London, July 2-4, 1979, Springer-Verlag, (New York), pp. 366-378.

Mellor, G.L., and T. Yamada, 1974: "A hierarchy of turbulence closure models for planetary boundary layers," J. Atmos. Sci., 31, pp. 1791-1806.

Mellor, G.L., and T. Yamada, 1982 "Development of a turbulence closure model for geophysical fluid problems," Reviews of Geophysics and Space Physics, 20, pp. 851-875.

O'Brien, J.J., 1970: "A note of the vertical structure of eddy exchange coefficients in the planetary boundary layer," J. Atmos. Sci., 27, pp. 1213-1215.

Paulson, C.A. 1970: "The mathematical representation of wind speed and temperature profiles in the unstable atmospheric surface layer," J. Appl. Meteorology, 9, pp. 857-861.

Pielke, R.A., 1981: "Mesoscale numerical modeling," Adv. Geophys., 23, pp. 185-344.

Pielke, R.A., and E. Kennedy, 1980: "Mesoscale terrain features," Report No. UVA-ENV SCI-MESO-1980-1, University of Virginia. (Avail. from R.A. Pielke, Dept. of Atmospheric Science, Colorado State Univ., Fort Collins, Colorado 80523.)

Schumann, U., 1975: "Subgrid scale model for finite difference simulations of turbulent flow in plane channels and annuli," J. Comp. Phys., 18, pp. 376-404.

Smagorinsky, J.S., 1963: "General circulation experiments with the primitive equations, I: The basic experiment," Monthly Weather Review, 91, pp. 99-

Sykes, R.I., and W.S. Lewellen, 1982: "A numerical study of breaking Kelvin-Helmholtz billows using a Reynolds-stress turbulence closure model," J. Atmos. Sci., 39, pp. 1506-1520.

Sykes, R.I, W.S. Lewellen, and S.F. Parker, 1984: "A turbulent transport model for concentration fluctuations and fluxes," J. Fluid Mech., 139, pp. 193-218.

Van der Hoven, I., 1957: "Power spectrum of horizontal wind speed in the frequency range from 0.0007 to 900 cycles per hour," J. Meteor., 14, pp. 160-164.

Yamada, T., 1979: "An application of a three-dimensional simplified second-moment closure model to study atmospheric effects of a large cooling-pond," J. Atmospheric Environment, pp. 693-704.

Yamada, T., 1983: "Numerical simulation of winds and turbulence in the California geysers area," Proc. AMS, 6th Symp. Turbulence and Diffusion.,

Yamada, T., and G.L. Mellor, 1975: "A simulation of the wangara atmospheric boundary layer data," J. Atmos. Sci., 32, pp. 2309-2329.

Young, G.S., and R.A. Pielke, 1983: "Application of terrain height variance spectra to mesoscale modeling," submitted to JAS.

Zeman, O., 1981: "Progress in the modeling of planetary boundary layers," Annual Review of Fluid Mech., 13, pp. 253-272.

APPENDIX B

PARAMETERIZATION OF THE SURFACE LAYER UNDER CONDITIONS APPROACHING FREE CONVECTION

Monin-Obukhov surface similarity contains a singularity under free convection conditions. We wish to explore the parameterization of the surface layer under conditions approaching this singularity. It is often assumed under these conditions that $\sigma_w \sim w_* z^{1/3}$ and $\sigma_H \sim w_*$. Indeed, available data taken in the surface layer appears to support this limit reasonably well. However, this data is generally taken at moderately large values of z to be sure that (-z/L) is very large. This simple form cannot hold at sufficiently small z because σ_H must be reduced to zero in some neighborhood of z_o. Thus, we expect some inner region of the free convection surface layer to be dominated by a cascading process induced by the unsteady shear stress produced by the horizontal fluctuations interacting with the surface roughness elements. We will provide an estimate of the height of this inner layer and discuss the implications of this layer for the parameterization of surface boundary conditions.

ANALYSIS

In order to provide a quantitative estimate of this inner layer thickness, let us approximate the time-averaged, small-scale, turbulent kinetic energy equation, vertically integrated over this layer as:

$$c_f q u_1^2 + \frac{g}{T_o} \overline{\theta' w'_o}\, \delta_i - 0.2\, q^3 \ln \frac{\delta_i}{z_o} = 0 \qquad (B.1)$$

The first term represents the shear production of high frequency energy resulting from the relatively low frequency horizontal velocity fluctuations interacting with the surface. The second term represents the buoyant production term due to the heat flux through this layer. The final term represents the dissipation of high frequency energy in this region were the dissipation length scale is assumed to be inversely proportional to the distance from the surface. The coefficient 0.2 comes from the ratio of the two coefficients b/α in the standard A.R.A.P. model.

We have defined the inner layer as that region within which the shear production exceeds the buoyant production. Let us arbitrarily define δ as precisely the height where the first 2 terms of Equation 1 become equal. Above this height, the first term will remain essentially constant while the second term continues to grow linearly. From both laboratory (Willis & Deardorff, 1974) and field observations (Panofsky, et.al., 1977), the u_1^2 scaling is given by

$$u_1^2 = 0.6 \left(\frac{g}{T_o} \overline{\theta' w'_o}\, h \right)^{2/3} \qquad (B.2)$$

thus

$$\delta_i = 0.6 \quad c_f a \left(\frac{\delta_i}{h}\right)^{1/3} \quad h \tag{B.3}$$

with

$$q = a \left(\frac{g}{T_o} \overline{\theta' w'_o} \delta_i\right)^{1/3} \tag{B.4}$$

and

$$a^3 = 2 \Big/ \left(0.2 \ln \frac{\delta_i}{z_o}\right) \tag{B.5}$$

Equations (3) and (5) give

$$\delta_i = 1.47 \left(c_f\right)^{3/2} \left(\ln \frac{\delta}{z_o}\right)^{-1/2} \quad h \tag{B.6}$$

Under neutral surface layer conditions c_f as defined by

$$c_f = \frac{-\overline{u'w'_o}}{qu} \tag{B.7}$$

would be given by

$$c_f = 0.16/\ln \left(\delta_i/z_o\right) \tag{B.8}$$

When Equation 8 is increased by 50% to allow for some instability in this layer, and used for c_f in Equation 6, the final result is

$$\delta_i \left(\ln \delta_i/z_o\right)^2 = 0.17 \; h \tag{B.9}$$

When h is approximately 1km and z_o is approximately 0.01m, Equation 9 will give $\delta_i = 4.6$m. Over water where the unstable mixed layer may be as small as 100m and z_o as small as 10^{-4}m, the inner surface layer thickness will

be as small as ≈ 0.3m.

When z_o is greater than approximately 0.1, a significant part of this inner layer is likely to be occupied by the canopy layer which extends out past $10z_c$ and the horizontal velocity fluctuations will play an even more active role in the interaction between the surface and the atmosphere.

Deardorff (1972) in his parameterization of the planetary boundary layer recognized that free convection conditions can not extend all the way to the surface. His reasonable fix for this condition was to not allow c_u to exceed $2\, c_{u_N}$ or c_θ to exceed $3.33\, c_{\theta_N}$ where he defined c_u and c_θ as:

$$c_u = \left|\overline{u'w'}_o\right|^{1/2} u_m \tag{B.10}$$

$$c_\theta = \frac{-\overline{w'\theta'}_o}{\left|\overline{u'w'}_o\right|^{1/2} (\theta_m - \theta_s)} \tag{B.11}$$

and c_{u_N} and c_{θ_N} are the neutral values of these transport coefficients.

The accuracy of c_u is not very critical in this limit where the mean wind is approaching zero but the heat flux cannot be allowed to go to zero also. Deardorff imposes a lower bound of

$$\overline{w'\theta'}\ \text{free convection} = 0.0019 \left(\theta_s - \theta_m\right)^{4/3}\ \text{m.dg/sec} \tag{B.12}$$

Our inner layer analysis presented here suggest that the lower bound on

$$\overline{w'\theta'}_{f.c.} = c_{f_\theta} q_w \left(\theta_s - \theta_m\right) \tag{B.13}$$

is given by

$$\overline{w'\theta'}^{2/3}_{f.c.} = c_{f_\theta} a \left(\frac{g}{T_o}\delta_i\right)^{1/3} \left(\theta_s - \theta_m\right) \tag{B.14}$$

so that

$$\overline{w'\theta'}_{f.c.} = c_{f_\theta} \left(\theta_s - \theta_m \right)^{3/2} \left(\frac{g}{T_o} \frac{10\ \delta_i}{\ln \delta_i / z_o} \right)^{1/2} \qquad (B.15)$$

Consistent with Equation 9, we estimate that c_{f_θ} should be approximately 1.5 times that appropriate for a neutral surface layer of thickness δ_i, i.e.,

$$c_{f_\theta} = 0.33 \Big/ \left(\ln \delta_i / z_o \right) \qquad (B.16)$$

thus

$$\overline{w'\theta'}_{f.c.} = \frac{0.6}{\left(\ln \frac{\delta_i}{z_o} \right)^2} \left[\frac{g}{T_o} \delta_i \right]^{1/2} \left(\theta_s - \theta_m \right)^{3/2} \qquad (B.17)$$

For typical values of $g/T_o = 1/30$, $z_i = 1\text{km}$, and $z_o = 0.01\text{m}$, this gives

$$\overline{w'\theta'}_{f.c.} = 0.006 \left(\theta_s - \theta_m \right)^{3/2} \qquad (B.18)$$

which is approximately three times that given by Equation 12 when $\theta_s - \theta_m = 1°$. For $z_o = 0.1\text{m}$ and $\theta_s - \theta_m = 10$ the ratio would be approximately 10. Thus, for large temperature differences and rough surfaces Equation 12 can underestimate the free convection heat flux by as much as an order of magnitude.

Louis (1979, 1982) provides a PBL parameterization which approaches the free convection limit with heat flux given by

$$\overline{w'\theta'}_{f.c.} = 0.2 \left[\frac{g}{T_o} z_o \right]^{1/2} \left(\theta_s - \theta_m \right)^{3/2} \qquad (B.19)$$

This is the same temperature dependence as given in Equation 17 and although Equation 19 is independent of h and a quite different dependence on z_o, it leads to an expression approximately 40% less than Equation 18 for the same conditions as specified for that equation. If z_o is decreased from 10^{-2}m to 10^{-4}m the coefficient in Equation 18 would be reduced by approximately a factor of 4 while Equation 19 would lead to a factor of 10 reduction.

CONCLUSIONS

The free convection surface layer conditions of $\sigma_w \sim z^{1/3}$ will not extend to the surface at z_o. When the Monin-Obukhov is negative and close to zero the convective inner layer described here will extend from $z \approx 20\ z_o$ out to $z = \delta_{c.i.}$, where $\delta_{c.i.}$ is given by Equation 9. This layer will not occur when $-L > \delta_{c.i.}$.

REFERENCES

Deardorff, J. W., 1972: "Parameterization of the Planetary Boundary Layer for use in General Circulation Models", Monthly Weather Review, vol. 100, pp. 93-106.

Louis, J. F., 1979: "A Parametric Model of Vertical Eddy Fluxes in the Atmosphere". Boundary-Layer Meteorology 17, 187-202.

Louis, J. F., Tiedtke, M. and J. F. Geleyn, 1982: "A Short History of the Operational PBL-Parameterization at ECMWFd". In a report on a workshop on Planetary Boundary Layer Parameterization at the European Centre for Medium Range Weather Forecasts.

Panofsky, H. A., Tennekes, H., Lenschow, D. H. and Wyngaard, J. C., 1977: "The Characteristics of Turbulent Velocity Components in the Surface Layer under Convective Conditions". Boundary-Layer Meteorology, vol. 11, pp. 355-361.

Willis, G. E. and Deardorff, J. W., 1974: "A Laboratory Model of the Unstable Planetary Boundary Layer". J. Atmos. Science, vol. 31, 1297-1307.

APPENDIX C

TWO-DIMENSIONAL TURBULENT SIMULATIONS

The justification for two-dimensional studies comes from atmospheric observations, and this allows us to make calculations of the large eddies explicitly and obtain results which are less sensitive to closure assumptions. We have utilized two different models for these studies; one is the A.R.A.P. closure model as reported by Teske and Lewellen (1979), and the second is the mixing-length parameterization model of Mason and Sykes (1982). Both models were previously used to study boundary-layer turbulence profiles and employed artifices which reduced the reliability of the entrainment predictions. Teske and Lewellen prescribed numerical damping at a short distance above the inversion, while Mason and Sykes included an artificial cooling term to obtain a steady mean state at the expense of a specific relation between the heat flux and mean temperature profiles. In the studies reported here, we consider a growing boundary layer beneath a deep, stably-stratified layer so that internal gravity waves are generated and transport momentum and energy in the vertical. An absorbing layer is placed at the upper levels to prevent reflection there.

The need to consider a growing boundary layer forces a compromise on the length of the numerical integration time; we wish to integrate for a long time so that initial conditions are not influencing the results, but we do not want the boundary layer to grow so deep as to make the computational mesh inappropriate. These requirements led us to choose the following parameters for our runs: geostrophic wind speed, $U_g = 10 ms^{-1}$; initial boundary layer

depth, z_i = 500m; initial surface heat flow, H_o = 0.1 $^oKms^{-1}$; overlying stable temperature gradient, $\Gamma = 6x10^{-3}\ ^oKm^{-1}$. The latter is a relatively strong gradient, but these parameters produce a boundary layer which grows from 500m to about 900m in 4 hours, and has a Monin-Obukhov length, L, growing from 100m to about 300m, which is in the correct range to obtain longitudinal roll convection. We estimate that critical conditions are detectable in the rolls for about 1 - 1-1/2 hours, and also that average statistics need to be taken over a period of about 1 hour to be reliable; these experiments force us to integrate for at least 3 hours.

Initial conditions for the model runs were obtained from a one-dimensional, steady-state solution using the artificial cooling of Mason and Sykes (1982). A two-dimensional perturbation was superimposed to initiate the convective rolls, and the surface temperature was fixed at the initial value. An unfortunate result of this procedure was that the two models, mixing length and second-order closure, produce different steady-state profiles from the same external parameters, and therefore it was very difficult to obtain a very precise comparison between the models. The steady-state initialization is important because imbalances in the wind field produce inertial oscillations via the Coriolis term which have an 18 hour period, and would consequently affect the entire run.

The initial conditions were obtained with l_o = 40m for the mixing length model, and Λ^* = 65m for the second-order closure model. Runs were made using these scales, and also using doubled values, i.e., 80m and 130m, to investigate sensitivity to closure. All runs were made using a domain oriented such that the longitudinal areas of the rolls lie 10^o to the left (facing downwind) of the geostrophic flow direction. This direction was found to produce the maximum momentum transport by Mason and Sykes, and is consistent with field observations.

Figures C.1 and C. 2 show a sequence of realizations of the flow field from the two models. Vertical velocity component, w, and temperature contours are shown. The SOC model, with Λ^* = 65m, produces rolls with less energy than the 40m mixing length model. The inversion structure and internal gravity

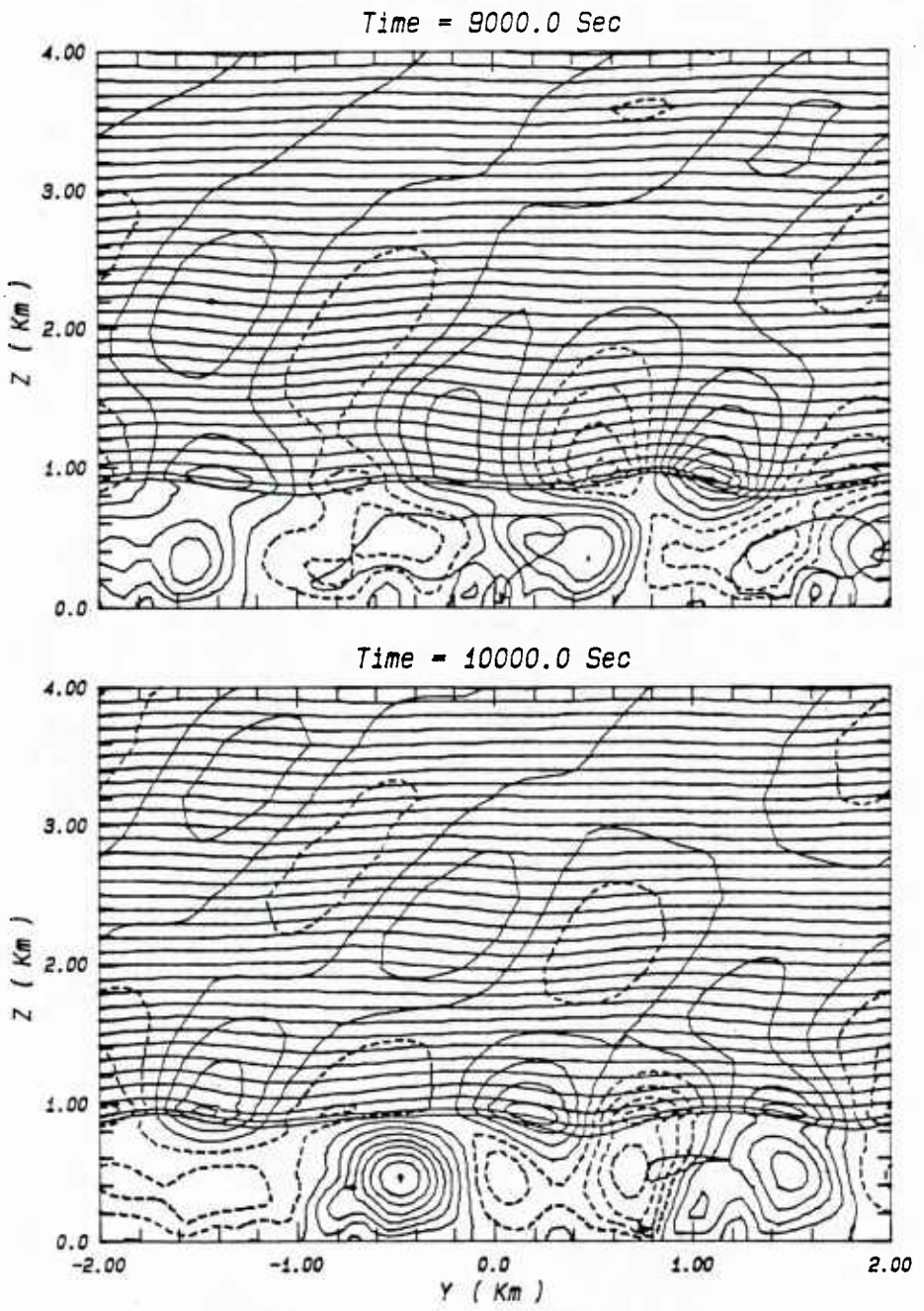

Variable	Units	Increment
Vertical Velocity	M/Sec	0.25
Temperature	°C	0.60

FIGURE C.1: FLOW FIELDS FROM THE TWO-DIMENSIONAL CLOSURE MODEL WITH $\Lambda_* = 65$m. HEAVY CONTOURS ARE VERTICAL VELOCITY. FAINT CONTOURS ARE ISOTHERMS.

2-D Roll Calculations - Mixing Length Model

Run Number = 0011

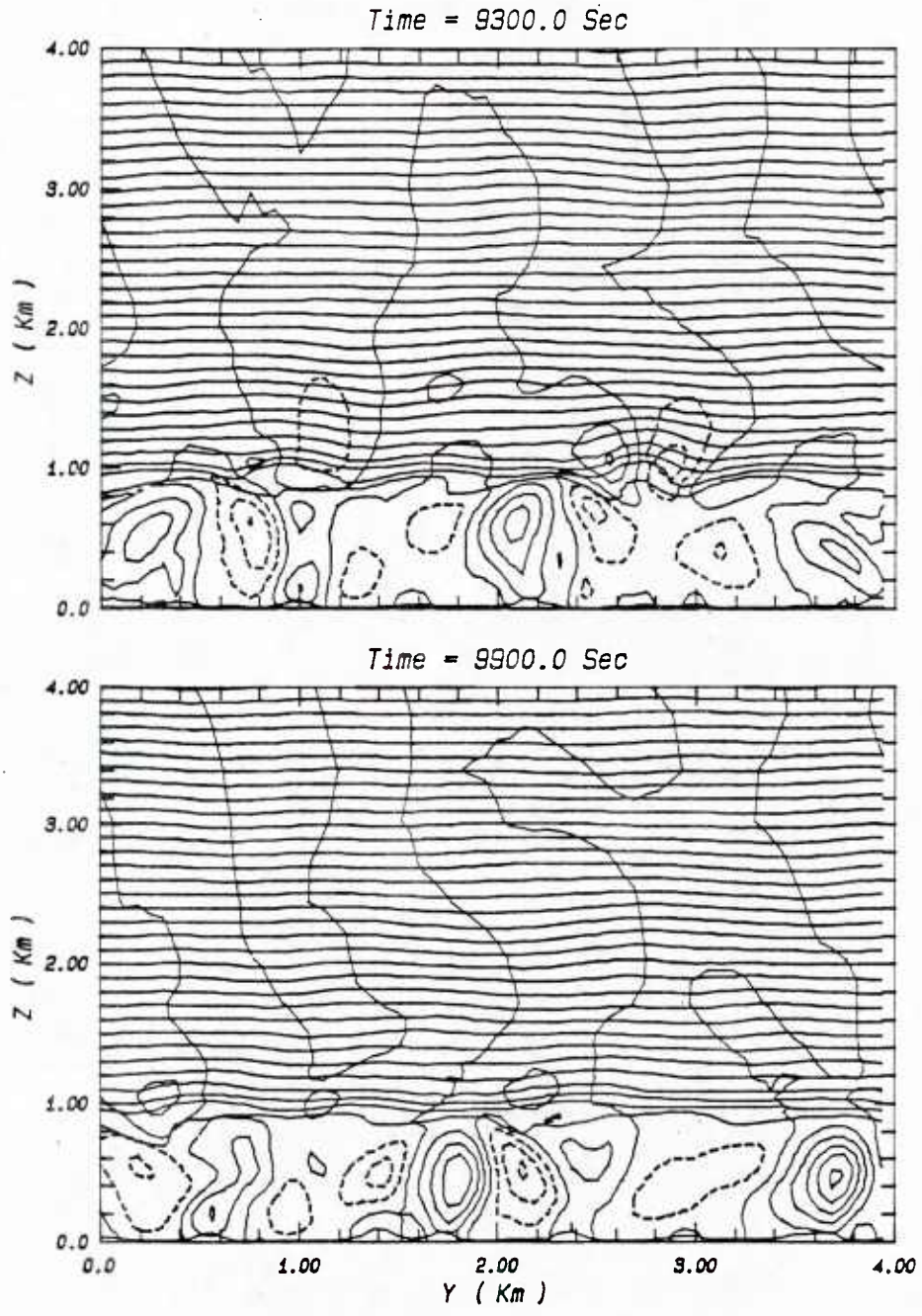

Variable	Units	Increment
Vertical Velocity	M/Sec	0.50
Temperature	°C	0.60

FIGURE C.2: FLOW FIELDS FROM THE MIXING LENGTH MODEL WITH l_o = 40m.

wave field is much better resolved in SOC, and seems to show a transient generation of wave trains by inversion distortions with a lifetime of about 30 mins. These features are produced by a large amplitude roll, and move along the inversion with the roll. A wave train is set up, propagating energy upward, until the roll decays and the source of energy is reduced. The wave train then detaches from the boundary-layer, and moves upward with the appropriate group velocity.

The mixing length run looks different, firstly because the domain is viewed from the opposite side, so that the direction of horizontal propagation is reversed, and secondly because the rolls are more intense, producing smaller scale disturbances in the stable layer. In fact, the model resolution around the inversion appears inadequate for this run.

Figure C.3 shows a sequence of realizations from the larger parameterized scale runs, i.e., $\Lambda^* = 130$m, and a mixing length of 80m. The mixing length model results are now much closer to the $\Lambda^* = 65$m pictures, while the SOC results show very much weaker rolls and wave activity.

The time and space-average heat fluxes from both SOC runs together with the one-dimensional solutions of the same flows are shown in Figure C.4, and the mean temperature profiles in Figure C.5. There is an encouraging agreement between the three SOC results, although the partition between resolved and parameterized fluxes changes dramatically. We should mention that profiles of other quantities such as turbulence energy levels or momentum flow would look very different for the various models, because these quantities contain the effects of internal gravity waves. The waves would be sensitive to domain orientation also, as shown by Mason and Sykes. However, the waves do not transport heat flux, and therefore the entrainment fluxes can be predicted equal by the different models.

A similar feature can be seen in the two mixing length runs, with resolved flux being replaced by parameterized flux as the scale is increased (Figure C.6). The magnitude is also similar to the SOC results. These results cannot be readily compared directly with the SOC profiles; because

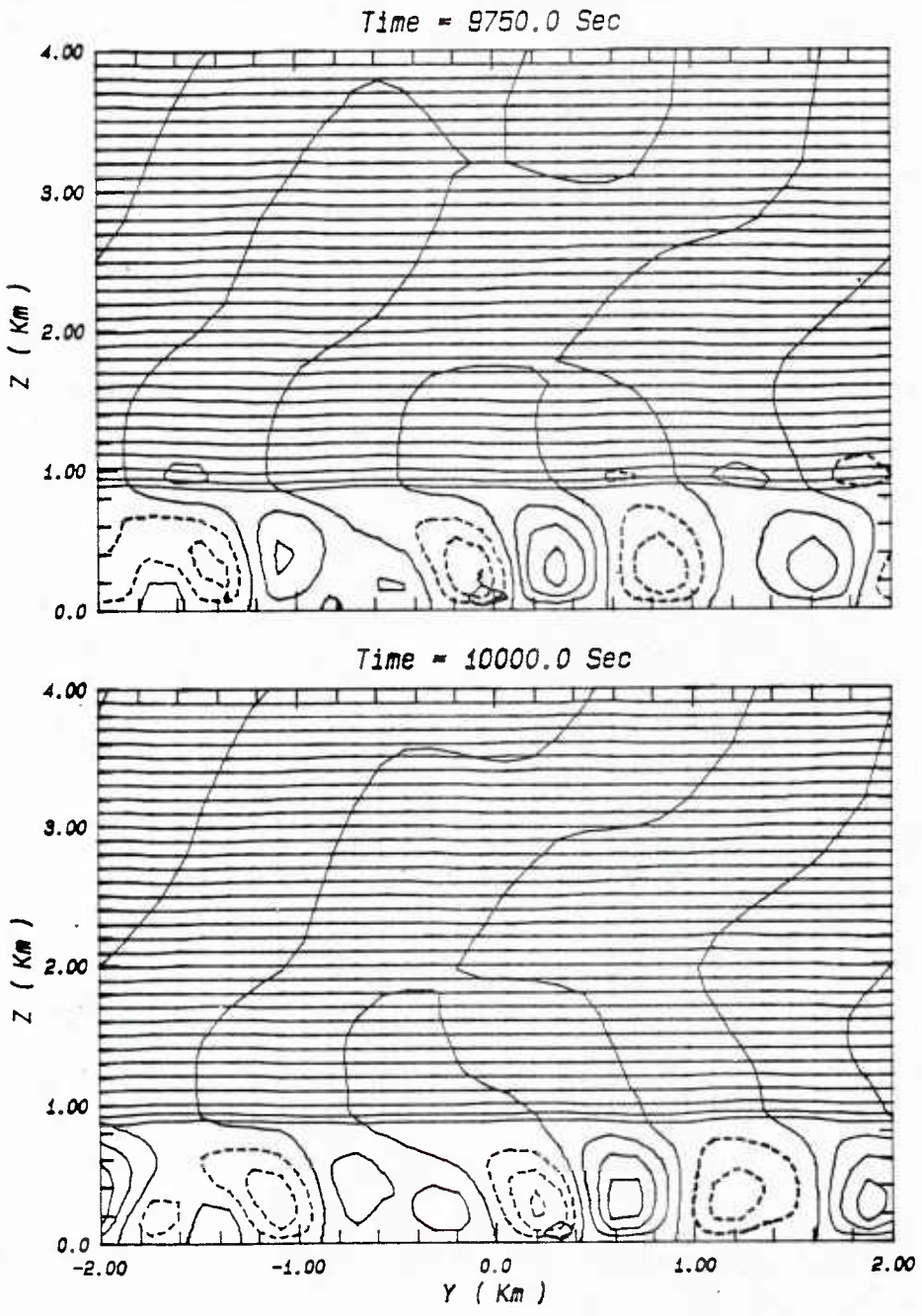

Variable	Units	Increment
Vertical Velocity	M/Sec	0.25
Temperature	°C	0.60

FIGURE C.3: CLOSURE MODEL WITH Λ_* = 130m.

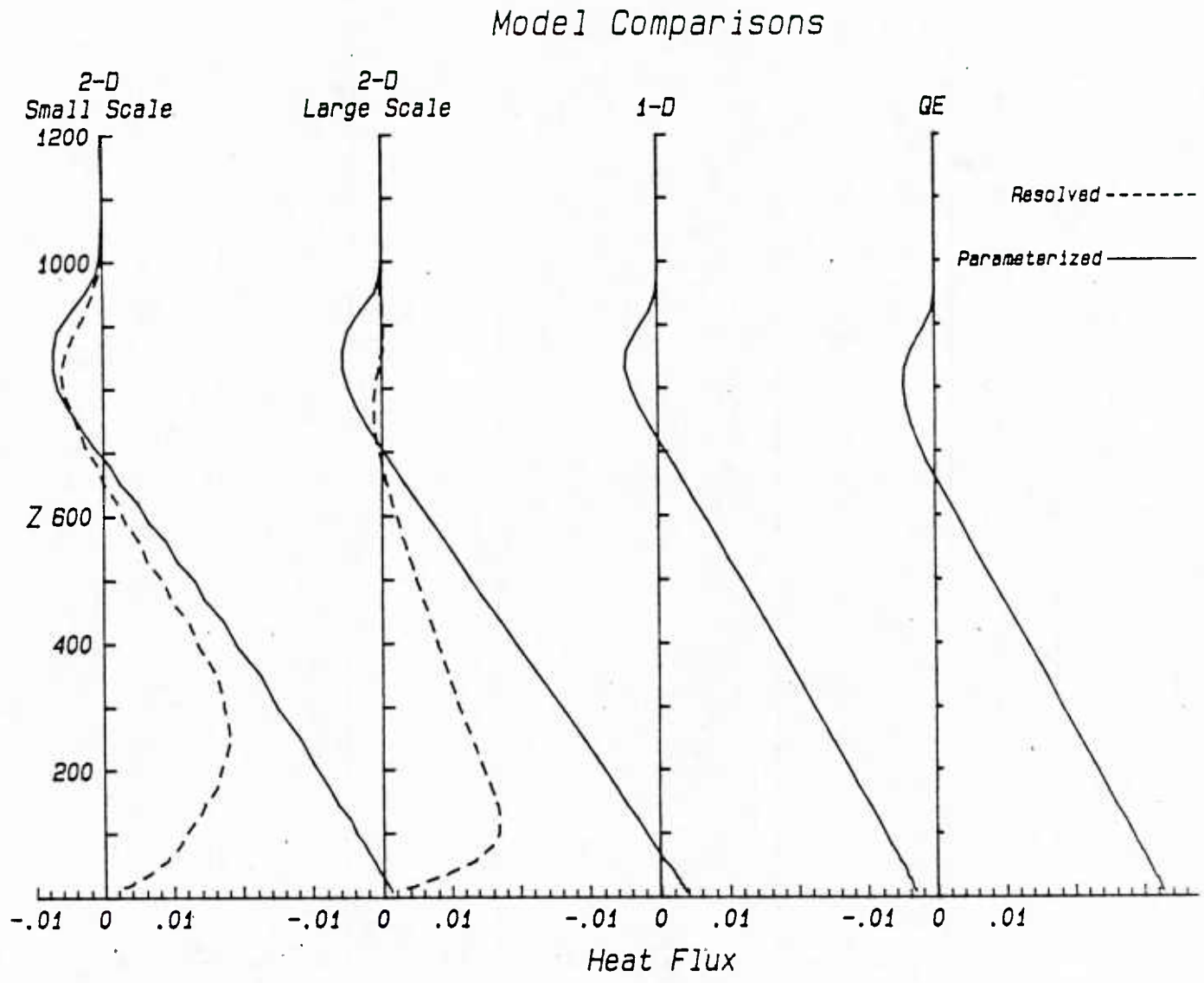

FIGURE C.4: HEAT FLUX PROFILES AVERAGED FROM t = 9000s to t = 12000s FROM THE DIFFERENT MODELS.

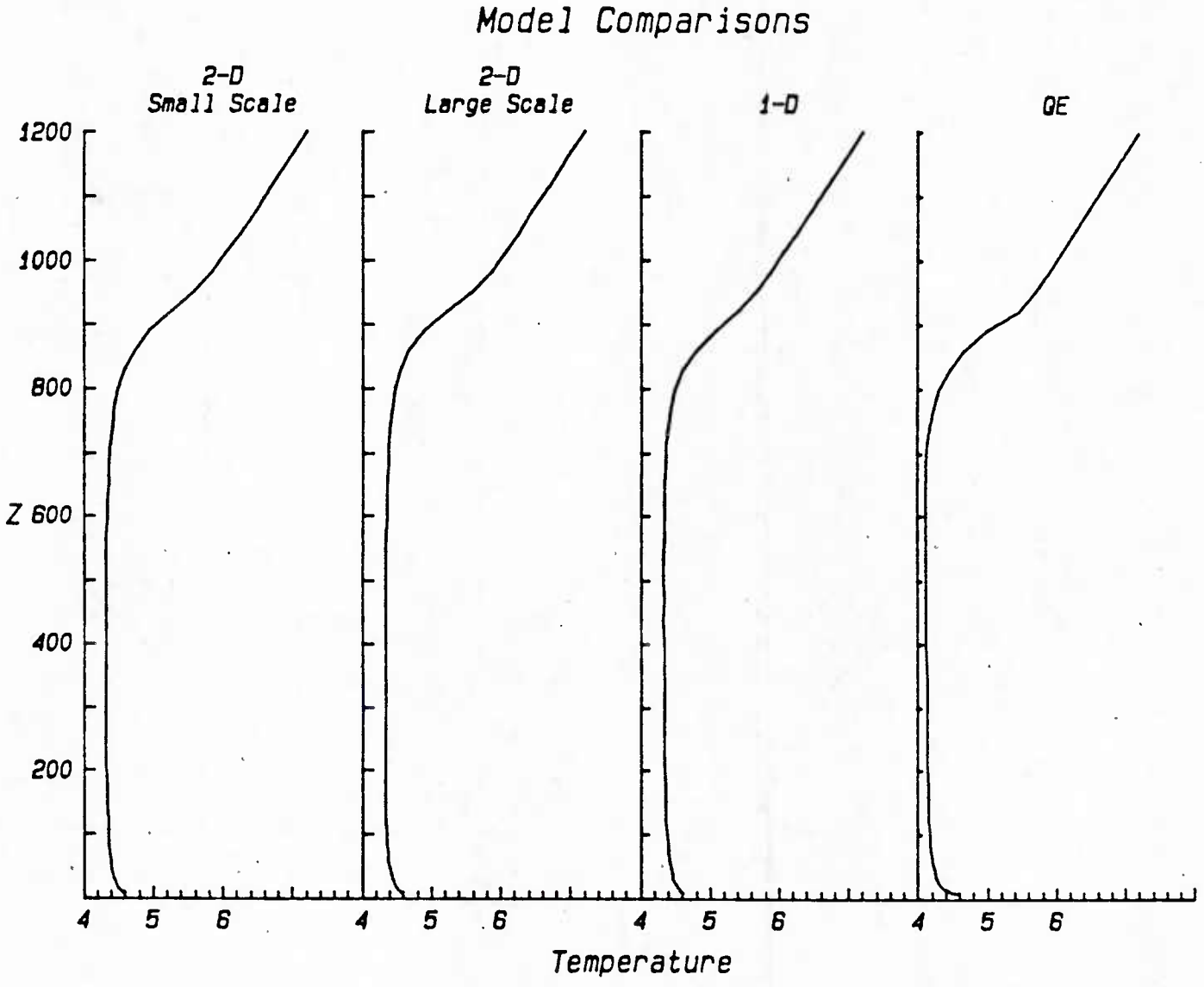

FIGURE C.5: AS FIGURE C.4, BUT FOR TEMPERATURE PROFILES

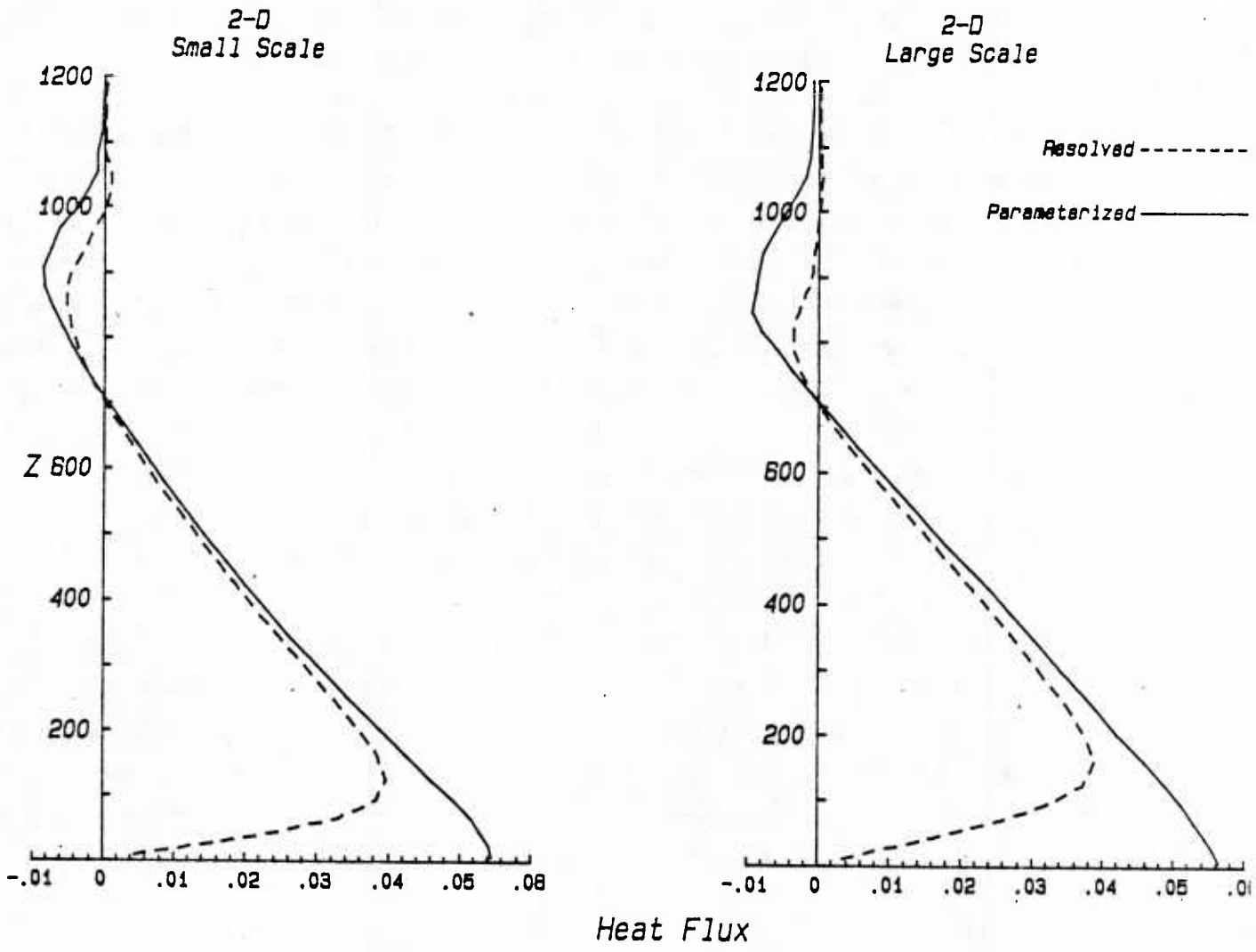

FIGURE C.6: HEAT FLUX PROFILES FROM t = 9000s TO t = 12000s FROM THE TWO MIXING LENGTH RUNS.

the surface temperature is higher, giving a larger surface heat flux. This is the problem with initial conditions which was referred to earlier.

In addition to providing independent calculations of the turbulent flow profiles, the two-dimensional studies also provide valuable insight into the dynamical mechanisms, since the large eddies are computed explicitly. We can see from the realizations of the flow field from the SOC model that there are significant vertical displacements of the inversion produced by the large eddies. However, the inversion does not suffer any large-scale overturning or breakdown, so there is no entrainment or detrainment due to large eddies engulfing stable air or exchanging mixed layer air for stable air. This seems to leave two mechanisms for entrainment; small scale processes at the inversion mixing stable air downward, or large eddies providing the mixing but in some way not involving overturning. The simplest mechanism we can postulate is that the large eddy carries fluid up to the inversion, where it gains some heat from the parameterized mixing processes, then the fluid parcels continue in the circulation and are brought down into the boundary-layer. Sample fluid particle trajectories from the 80m mixing length run are shown in Figure C.7; particles which originate near the surface at the base of an updraft and are carried up to the inversion, are invariably carried back down again. This tends to confirm the simple picture of entrainment.

There is, however, a problem in reconciling this simple conceptual model with the observation that the entrainment fluxes can be almost entirely carried by the large eddies, i.e., the small-scale mixing is not necessary. We must therefore seek an inviscid entrainment mechanism. It is appropriate to recall here that we are dealing with a boundary-layer which is growing due to a rising mixed-layer temperature via the surface heat flux. We can consider the simple "encroachment" concept of Carson and Smith (1974), which says that overlying fluid becomes part of the mixed layer as the temperature of the latter rises above that of fluid at the base of the inversion. This is effectively a "no motion" concept, and does not predict any downward heat flux; stable air simply becomes part of the mixed layer. This cannot explain

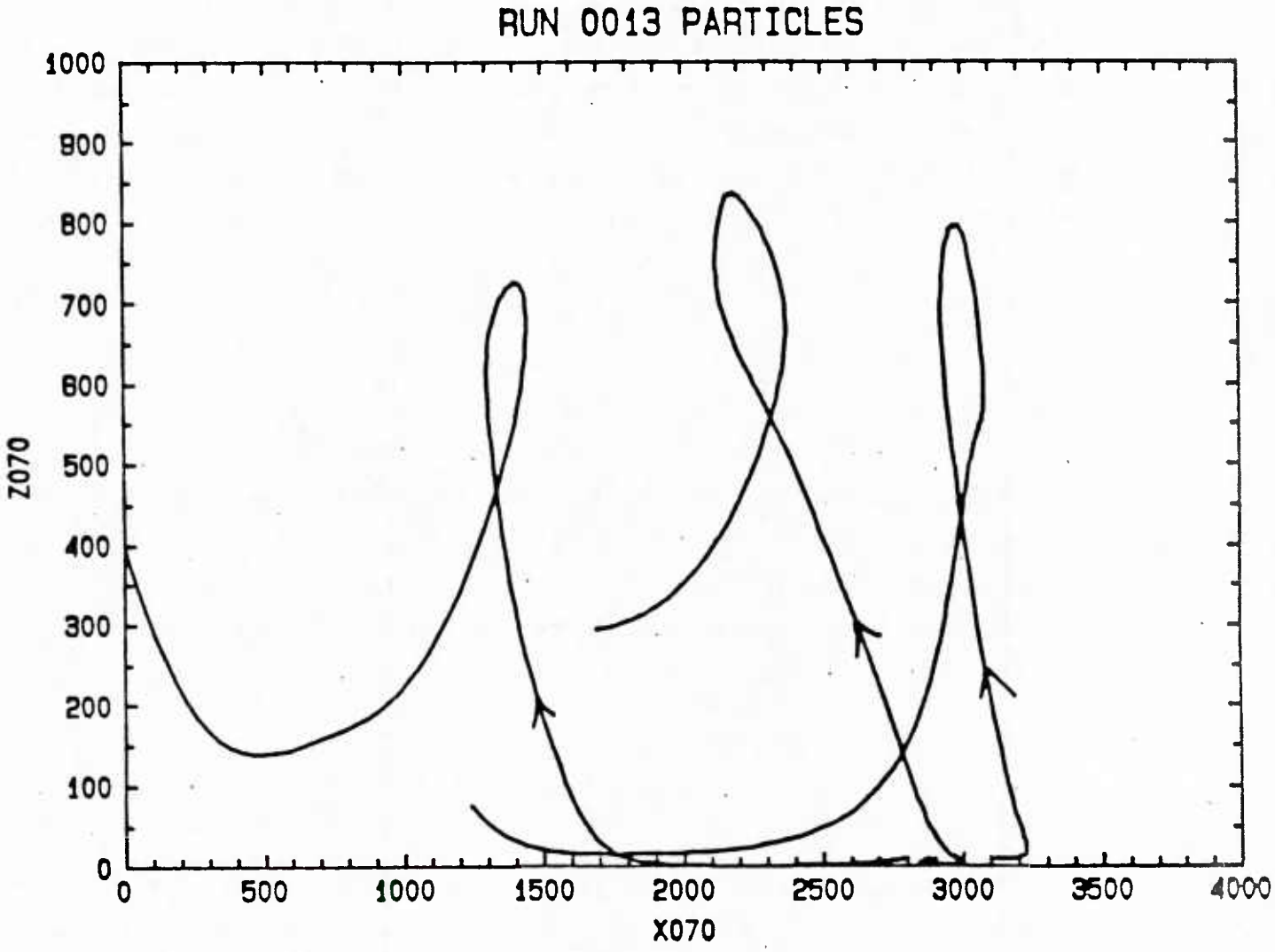

FIGURE C.7: PARTICLE TRAJECTORIES FROM THE l_o = 80m MIXING LENGTH RUN FROM t = 8000s TO t = 12000s

our observations, and so we suggest a model which takes account of the dynamics of the large eddies. If we consider the motion of these eddies, then there is an inviscid force acting at the inversion, namely the dynamic pressure gradient force. The magnitude of this force will be related to w_*^2/z_i where w_* is the convective scaling velocity; which characterizes large eddy velocities. This pressure gradient will act on the overlying stable air, and if we consider a continuous temperature profile, then this force will be capable of dominating the lowest layer whose buoyancy deficit is too small to resist vertical accelerations. If we consider a layer whose temperature excess over the mixed-layer is less than $\Delta\theta$, then this layer will be accelerated by the pressure gradient and can be brought into the mixed-layer provided

$$\frac{w_*^2}{z_i} \sim \frac{g}{T_o} \Delta\theta$$

The downward heat flux carried by large-scale eddies pulling this layer down into the mixed-layer will be roughly $w'\Delta\theta$, where w' is a scaling velocity for the vertical velocities near the inversion. We expect w' to be a fraction of w_* which is roughly proportional to the ratio of the inversion thickness Δh to z_i so that the entrainment flux scales as

$$w_*\Delta\theta \sim \frac{w_*^3}{gz_i} T_o = H_o \quad ,$$

the surface heat flux, from the definition of w_*. We therefore have a simple mechanism whereby large eddies can pull fluid from the base of the inversion by means of pressure gradient forces, and produce plausible estimates of mass and heat entrainment.

REFERENCES

Carson, D. J., 1973: "The Development of a dry inversion-capped convectively unstable boundary layer", Quart. J. Roy. Met. Soc., 99, 450-467.

Carson, D. J. and Smith, F. B., 1974: "Thermodynamic Model for the Development of a Convectively unstable boundary layer." Adv. in Geophys., 18A, 111-124.

Deardorff, J.W., 1979: "Prediction of convective mixed-layer entrainment for realistic capping inversion structure." J. Atmos. Sci., 36, 424-436.

Deardorff, J. W and Willis, G. E., 1982: "Dependence of mixed-layer entrainment on shear stress and velocity jump". J. Fluid Mech., 115, 123-149.

Deardorff, J. W., Willis, G. E. and Stockton, B. H., 1980: "Laboratory studies of the entrainment zone of a convectively mixed layer." J. Fluid Mech., 100, 41-64.

Lewellen, W. S., 1977: "Use of Invariant Modeling." In Handbook of Turbulence, ed. W. Frost and T.H. Moulder, Plenum.

Lewellen, W. S., 1981: "Modeling the lowest 1km of the Atmosphere. AGARD, AG-267.

Mason, P. J. and Sykes, R. I., 1982: "A Two-Dimensional numerical study of horizontal roll vortices in an inversion capped planetary boundary layer". Quart. J. Roy. Met. Soc., 100, 801-823.

Mellor, G. L. and Yamada, T., 1974: "A Hierarchy of turbulence closure models for planetary boundary layers." J. Atmos Sci., 31, 1791-1806.

Pennel, W. T. and LeMone, M. A., 1974: "An experimental study of turbulence structure in the fair-weather trade wind boundary layer." J. Atmos. Sci., 31, 1308-1323.

Stull, R. B., 1973: "Inversion rise model based on penetrative convection." J. Atmos. Sci., 30, 1092-1099.

Teske, M. E. and Lewellen, W. S., 1979: "Horizontal roll vortices in the planetary boundary layer." Proc. AMS Symp. on Turb. Diff. and Air Poll., Reno.

Willis, G. E. and Deardorff, J. W., 1976: "A Laboratory model of the unstable planetary boundary layer." J. Atmos. Sci., 31, 1297-1307.

Zeman, O. and Lumley, J. L., 1976: "Modeling Buoyancy-driven mixed layers", J. Atmos. Sci., 33, 1974-1988.

APPENDIX D

COMMENTS ON SCALAR DIFFUSION IN THE CONVECTIVE BOUNDARY LAYER*

by

W. S. Lewellen, R. I. Sykes and S. F. Parker

Wyngaard (1984) has proposed a relatively simple parameterization of diffusion across the convective boundary layer based on the large eddy simulation (LES) results obtained by him and his colleagues; Wyngaard and Brost (1984), Moeng and Wyngaard (1984). A central feature of this parameterization is the incorporation of the difference between the effective eddy diffusivity for scalar diffusion down from the top of the convective layer and that for diffusion up from the bottom. This asymmetry exhibited by the LES results for the scalar transport in the buoyantly produced turbulence driven by surface heating can not be simulated using first-order K theory.

In this comment we wish to address two questions related to the asymmetric diffusion. First, what level of turbulence closure is required to exhibit the asymmetry between bottom-up and top-down diffusivity? Second, how

*Submitted to J. Atmospheric Sciences for publication

sensitive is Wyngaard's parameterization to the details of the asymmetric diffusion? Not surprisingly, we find that a level of closure which includes some diffusion of the second-order scalar correlations will produce the asymmetry. More surprising, we find that Wyngaard's parameterization is not sensitive to the asymmetric diffusion. In fact, it appears that precise symmetry could be imposed and make little practical difference in his end results.

Under the horizontally homogeneous, quasi-steady conditions assumed for the LES, an expression for K in buoyantly produced turbulence may be written symbolically as:

$$K = - \overline{w'c'} \,/\, (\partial C/\partial z) = \tau_1 \left[\overline{w'w'} - \left(\frac{g}{T} \overline{c'\theta'} - \frac{\partial}{\partial z} \overline{w'^2 c'} \right) \Big/ \partial C/\partial z \right] \qquad (D.1)$$

where the time scale τ_1 is defined equal to

$$\overline{c'w'} \Big/ \overline{\frac{c'}{\rho} \frac{\partial p'}{\partial z}} \; .$$

Under the same conditions the potential temperature-species correlation appearing in Equation D.1 may be written as:

$$\overline{c'\theta'} = \tau_2 \left[- \overline{w'\theta'} \frac{\partial C}{\partial z} + K \frac{\partial \theta}{\partial z} \frac{\partial C}{\partial z} + \frac{\partial}{\partial z} \overline{w'c'\theta'} \right] \qquad (D.2)$$

with τ_2 equal to the ratio of $\overline{c'\theta'}$ to the rate of dissipation of $\overline{c'\theta'}$. When Equations D.1 and D.2 are combined

$$K = \tau_1 \left[\overline{w'w'} + \tau_2 \frac{g}{T_o} \left(\overline{w'\theta'} - \frac{\partial \overline{w'c'\theta'}}{\partial z} \Big/ \partial C/\partial z \right) + \frac{\partial \overline{w'w'c'}}{\partial z} \Big/ \partial C/\partial z \right] \left[1 + \tau_1 \tau_2 \frac{g}{T_o} \frac{\partial \theta}{\partial z} \right]^{-1} \qquad (D.3)$$

Equation D.3 is an exact expression for K for the quasi-steady, horizontally homogeneous, buoyant convective layer as long as the τ's remain exact. If the τ's are taken as properties of the turbulence, independent of the C distribution and the 3rd order diffusion terms are ignored then it is clear that K will also be a property of the turbulence only.

Figures 8 and 10 of Moeng and Wyngaard (1984) for the τ's as given by their LES results suggest that for this problem the τ's may be taken as properties of the turbulence. Thus, the asymmetry appears to be imposed by the turbulent transport of either $\overline{c'\theta'}$ or $\overline{w'c'}$.

The answer to our first question is that a level of closure that incorporates turbulent diffusion of the second-order species correlations is required to produce a proper asymmetry in the top-down-bottom-up diffusion.

Figure D.1 compares Wyngaard and Brost's bottom-up and top-down diffusivities with values we obtain from the second-order closure model of Lewellen (1977) which uses a simple gradient diffusion model for the turbulent transport of both $\overline{c'\theta'}$ and $\overline{w'c'}$. The most obvious difference between the LES results and the second-order closure results is the singularity which appears in K_b near $z = .65z_i$ in the SOC results, but doesn't appear in the LES results. However, this is apparently more a result of uncertainties in the LES result than it is a true difference between the LES and the SOC results. Moeng and Wyngaard (1984), in a recalculation of the LES, present results for the normalized gradient g_b which go thru zero a little above $z = 0.6z_i$. Thus, their more recent results would give a singularity in K_b near the same value of z as given by the SOC results. Since the turbulent transport terms are divided by the concentration gradient in Equation 3, relatively small errors in the turbulent transport can lead to large errors in K in the middle of the convective layer where the gradient is very small. We conclude that the asymmetry between K_b and K_t exhibited by the SOC model is qualitatively similar to that of the LES. Presumably we could use terms of the type proposed by Zeman and Lumley (1976) to adjust the modeled turbulent transport terms and make our profiles of K_t and K_b come closer to the LES. As more detailed LES results become available this may be desirable.

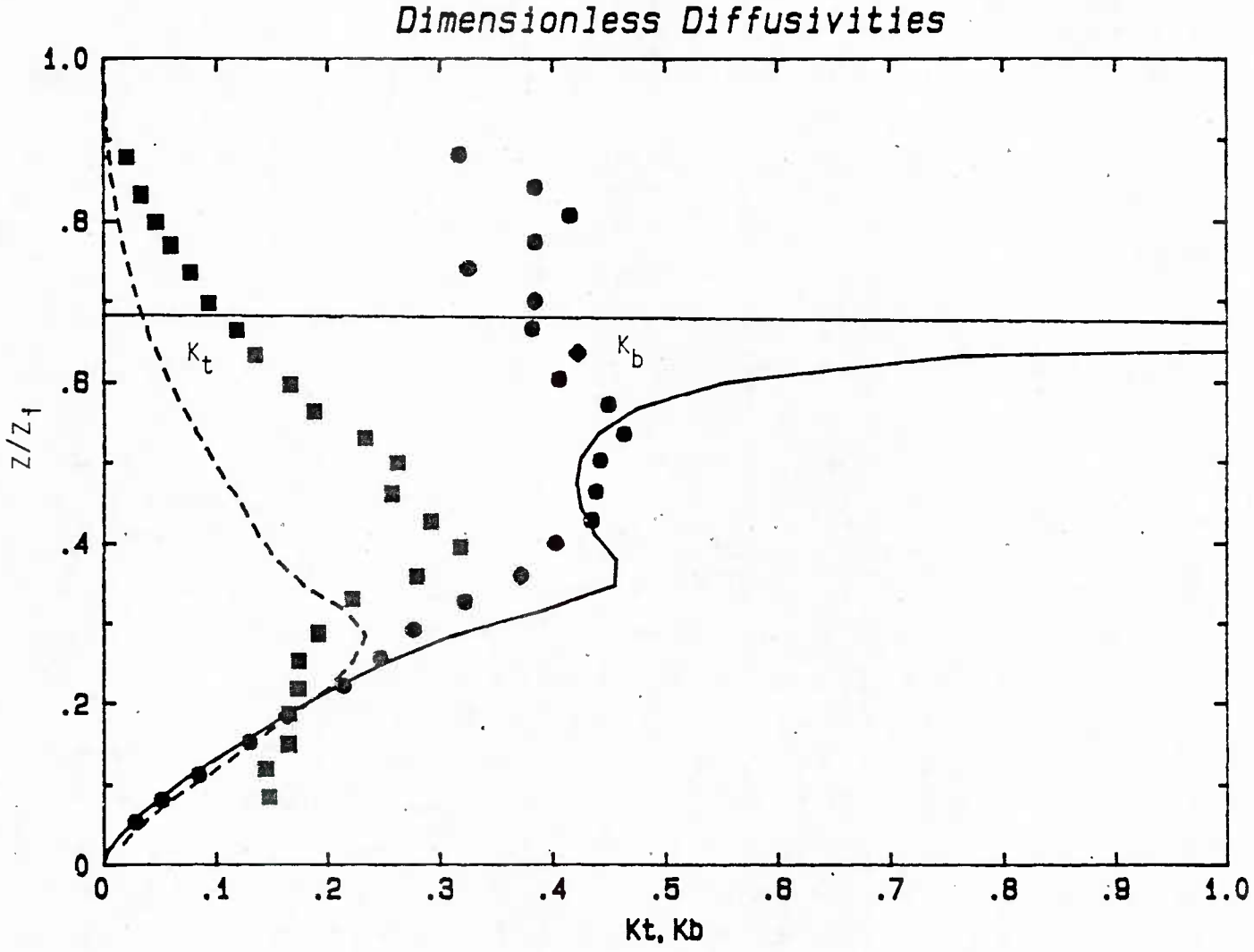

FIGURE D.1: COMPARISON OF THE DIMENSIONLESS SCALAR DIFFUSIVITIES AS OBTAINED BY THE LES OF WYNGAARD AND BROST (1984) WITH THOSE FROM A SIMPLE SECOND-ORDER CLOSURE MODEL.

The next question we address is how important is this K asymmetry in Wyngaard's proposed parameterization. We approach this question by repeating Wyngaard's analysis with the top-down dimensionless gradient, g_t, multiplied by a factor K_1. The parameterizations provided in Equations 21 and 23 are then modified by replacing cw_1 and w_e with cw_1/K_1 and w_e/K_1 respectively. The only other change is Equation 29 for Δ_t. It becomes

$$\Delta_t = \left(2.0/K_1\right)\left[\left(\alpha\, w_e/w_* K_1\right)^{-1/3} - 1\right] \qquad (D.4)$$

These changes force two types of changes in the resulting unmixed layer profile. First, h_1 is moved a little further from z_i as K_1 is decreased, and second the gradient of C in the interfacial region is increased (or decreased) as K_1 is increased (or decreased). To make this sensitivity more specific, consider Wyngaard's boundary conditions for humidity-like scalars. Then his Equations 26 to 31 yield

$$\overline{cw_1} = w_e\left[\left(C_S - C_2\right) - \left(C_S - C_0\right)\left(1 + \frac{\Delta_b w_S}{w_*}\right)\right]\left(1 + \frac{w_e \Delta_t}{w_*}\right) \qquad (D.5)$$

If the top-down and bottom-up diffusivities were made symmetric by making $K_1 \approx 0.4$ then $\overline{cw_1}$ would be decreased by $\approx 20\%$ for typical PBL conditions by virtue of $w_e\Delta_t/w_*$ increasing from ≈ 0.2 to ≈ 0.4. However, since w_e cannot in general be estimated to within an accuracy of 20% this change is of little practical significance until better parameterizations of the entrainment across the inversion are available.

Wyngaard's section 4 is devoted to arguing that his closure is valid for a wide variety of typical conditions. We believe that this is true, but not because the LES results for g_t are valid for all these conditions. It is true because the critical features which allow the parameterization to work are that K go smoothly to a reasonable representation of the surface layer dynamics in the lower part of the layer and that K go smoothly to a small

value within the capping layer. We believe the LES results for g_t in the upper part of the boundary layer are likely to be sensitive to such things as strength of the inversion and non-linearity in the flux profile, but this sensitivity is of little consequence until a much better parameterization of the inversion layer is available.

In Summary, the asymmetry in scalar diffusion within the quasi-steady, homogeneous, convective layer is an interesting feature which can be used to test diffusion models. Second-order closure has a definite advantage over lower level closure in simulating this feature. However, further improvements in the parameterization of entrainment across the inversion are necessary before accurate simulation of this interesting feature is very significant in practical mixed-layer parameterizations such as that proposed by Wyngaard.

REFERENCES

Lewellen, W. S., 1977: "Use of Invariant Modeling", Handbook of Turbulence, (edited by W. Frost and T. H. Moulder), Plenum Publishing Corp., Vol. 1, pp. 237-280.

Moeng, C. H., and Wyngaard, J. C., 1984: "Statistics of Conservative Scalars in the Convective Boundary Layer". Unpublished manuscript.

Wyngaard, J. C., 1984: "Toward Convective Boundary Layer Parameterization: A Scalar Transport Module". J. Atmos. Sci., 41, 1959-1969.

Wyngaard, J. C., and R. A. Brost, 1984: "Top-down and bottom-up scalar diffusion in the convective boundary layer". J. Atmos. Sci., 41, 102-112.

Zeman, O., and Lumley, J. L., 1976: "Modeling Buoyancy-driven Mixed Layers", J. Atmos. Sci., 33, 1974-1988.

DISTRIBUTION

OFFICE OF NAVAL RESEARCH
CODE 420
ARLINGTON, VA 22217-5000

CHIEF OF NAVAL OPERATIONS
(OP-952)
U.S. NAVAL OBSERVATORY
WASHINGTON, DC 20390

CHIEF OF NAVAL OPERATIONS
U.S. NAVAL OBSERVATORY
DR. R. W. JAMES, OP-952D1
34TH & MASS. AVE., NW
WASHINGTON, DC 20390

NAVAL DEPUTY TO THE
ADMINISTRATOR, NOAA
ROOM 200, PAGE BLDG. #1
3300 WHITEHAVEN ST. NW
WASHINGTON, DC 20235

COMMANDING OFFICER
NORDA
NSTL, MS 39529

COMMANDING OFFICER
NAVAL OCEANOGRAPHIC OFFICE
BAY ST. LOUIS
NSTL, MS 39522

COMMANDING OFFICER
FLENUMOCEANCEN
MONTEREY, CA 93943

COMMANDING OFFICER
NAVOCEANCOMFAC
NSTL STATION
BAY ST. LOUIS, MS 39522

DIRECTOR OF RESEARCH
U.S. NAVAL ACADEMY
ANNAPOLIS, MD 21402

NAVAL POSTGRADUATE SCHOOL
METEOROLOGY DEPT.
MONTEREY, CA 93943

NAVAL POSTGRADUATE SCHOOL
PHYSICS & CHEMISTRY DEPT.
MONTEREY, CA 93943-5100

LIBRARY
NAVAL POSTGRADUATE SCHOOL
MONTEREY, CA 93943-5100

COMMANDER (2)
NAVAIRSYSCOM
ATTN: LIBRARY (AIR-723D)
WASHINGTON, DC 20361-0001

COMMANDER
NAVAIRSYSCOM (AIR-330)
WASHINGTON, DC 20361-0001

COMMANDER
AWS/DN
SCOTT AFB, IL 62225

USAFETAC/TS
SCOTT AFB, IL 62225

AFGL/LY
HANSCOM AFB, MA 01731

COMMANDING OFFICER
U.S. ARMY RESEARCH OFFICE
ATTN: GEOPHYSICS DIV.
P.O. BOX 12211
RESEARCH TRIANGLE PARK, NC
27709

COMMANDER & DIRECTOR
U.S. ARMY ATMOS. SCI. LAB.
ATTN: DELAS-AF
WSMR, NEW MEXICO 88002

DIRECTOR (12)
DEFENSE TECH. INFORMATION
CENTER, CAMERON STATION
ALEXANDRIA, VA 22314

ACQUISITIONS SECT. IRDB-D823
LIBRARY & INFO. SERV., NOAA
6009 EXECUTIVE BLVD.
ROCKVILLE, MD 20852

DIRECTOR
OFFICE OF PROGRAMS RX3
NOAA RESEARCH LAB
BOULDER, CO 80302

DIRECTOR
NATIONAL SEVERE STORMS LAB
1313 HALLEY CIRCLE
NORMAN, OK 73069

CHIEF, SCIENTIFIC SERVICES
NWS/NOAA, CENTRAL REGION
ROOM 1836
601 E. 12TH ST.
KANSAS CITY, MO 64106

DIRECTOR
GEOPHYS. FLUID DYNAMICS LAB
NOAA, PRINCETON UNIVERSITY
P.O. BOX 308
PRINCETON, NJ 08540

LABORATORY FOR ATMOS. SCI.
NASA GODDARD SPACE FLIGHT CEN.
GREENBELT, MD 20771

COLORADO STATE UNIVERSITY
ATMOSPHERIC SCIENCES DEPT.
ATTN: DR. WILLIAM GRAY
FORT COLLINS, CO 80523

CHAIRMAN
INSTITUTE OF ATMOS. PHYSICS
UNIV. OF ARIZONA
TUCSON, AZ 85721

ATMOSPHERIC SCIENCES DEPT.
UCLA
405 HILGARD AVE.
LOS ANGELES, CA 90024

CHAIRMAN, METEOROLOGY DEPT.
UNIVERSITY OF OKLAHOMA
NORMAN, OK 73069

CHAIRMAN, METEOROLOGY DEPT.
CALIFORNIA STATE UNIVERSITY
SAN JOSE, CA 95192

NATIONAL CENTER FOR ATMOS.
RSCH., LIBRARY ACQUISITIONS
P.O. BOX 3000
BOULDER, CO 80302

UNIVERSITY OF WASHINGTON
ATMOSPHERIC SCIENCES DEPT.
SEATTLE, WA 98195

CHAIRMAN, METEOROLOGY DEPT.
PENNSYLVANIA STATE UNIV.
503 DEIKE BLDG.
UNIVERSITY PARK, PA 16802

FLORIDA STATE UNIVERSITY
ENVIRONMENTAL SCIENCES DEPT.
TALLAHASSEE, FL 32306

UNIVERSITY OF HAWAII
METEOROLOGY DEPT.
2525 CORREA ROAD
HONOLULU, HI 96822

DIRECTOR
COASTAL STUDIES INSTITUTE
LOUISIANA STATE UNIVERSITY
ATTN: O. HUH
BATON ROUGE, LA 70803

ATMOSPHERIC SCIENCES DEPT.
OREGON STATE UNIVERSITY
CORVALLIS, OR 97331

CHAIRMAN
ATMOS. SCIENCES DEPT.
UNIVERSITY OF VIRGINIA
CHARLOTTESVILLE, VA 22903

CHAIRMAN
METEOROLOGY DEPT.
MASSACHUSETTS INSTITUTE OF
TECHNOLOGY
CAMBRIDGE, MA 02139

CHAIRMAN, METEOROLOGY DEPT.
UNIVERSITY OF UTAH
SALT LAKE CITY, UT 84112

CHAIRMAN
METEOROLOGY & OCEANO. DEPT.
UNIVERSITY OF MICHIGAN
4072 E. ENGINEERING BLDG.
ANN ARBOR, MI 48104

TEXAS A&M UNIVERSITY
METEOROLOGY DEPT.
COLLEGE STATION, TX 77843

ATMOSPHERIC SCIENCES CENTER
DESERT RESEARCH INSTITUTE
P.O. BOX 60220
RENO, NV 89506

ATMOSPHERIC SCI. RSCH. CENTER
NEW YORK STATE UNIV.
1400 WASHINGTON AVE.
ALBANY, NY 12222

METEORO. OFFICE LIBRARY
LONDON ROAD
BRACKNELL, BERKSHIRE
RG 12 1SZ, ENGLAND

EUROPEAN CENTRE FOR MEDIUM
RANGE WEATHER FORECASTS
SHINFIELD PARK, READING
BERKSHIRE RG29AX, ENGLAND

MR. WILLIAM ROGERS
CALSPAN CORP.
BUFFALO, NY 14225

DR. JEROME WEINSTOCK
NOAA
AERONOMY LABORATORY
BOULDER, CO 80303

DR. JAMES DEARDORFF
DEPT. OF ATMOS. SCI.
OREGON STATE UNIV.
CORVALLIS, OR 97331

DR. R. A. ANTONIA
DEPT. OF MECHANICAL ENG.
UNIV. OF NEWCASTLE, NSW 2308
AUSTRALIA

DR. J. C. ANDRE
DIRECTION DE LA METEOROLOGIE
EERM/GMD
92100 BOULOGNE, FRANCE

DR. EARL E. GOSSARD
WAVE PROPAGATION LAB, R45X6
ENVIRONMENTAL RSCH. LABS
BOULDER, CO 80303

DR. G. L. MELLOR
GEOPHYSICAL FLUID DYNAMICS LAB
PRINCETON, NJ 08540

DR. T. YAMADA
LOS ALAMOS NATIONAL LAB
P.O. BOX 1663, MS 466
LOS ALAMOS, NM 87545

DR. J. LUMLEY
SIBLEY SCHOOL OF MECHANICAL &
AEROSPACE ENGINEERING
CORNELL UNIVERSITY
ITHACA, NY 14853

DR. F. NIEUWSTADT
ROYAL NETHERLANDS METEORO.
INSTITUTE
DE BILT, THE NETHERLANDS

DR. W. R. COTTON
DEPT. OF ATMOS. SCIENCES
COLORADO STATE UNIV.
FT. COLLINS, CO 80523

DR. J. WYNGAARD
NCAR
P.O. BOX 3000
BOULDER, CO 80307

DR. B. LAUNDER
DEPT. OF MECHANICAL ENG.
UNIV. OF MANCHESTER
P.O. BOX 88
MANCHESTER M60 1QD ENGLAND

DR. W. C. REYNOLDS
DEPT OF MECHANICAL ENG.
STANFORD UNIVERSITY
STANFORD, CA 94305

DR. P. BOUGEAULT
DIRECTIN DE LA METEOROLOGIE
EERM/GMD
92100 BOULOGNE, FRANCE

DR. J. FERZIGER
MECHANICAL ENGINEERING DEPT.
STANFORD UNIVERSITY
STANFORD, CA 94305

PROFESSOR Y. SASAKI
UNIV. OF OKLAHOMA
ROOM 219
200 FELGAR ST.
NORMAN, OK 73069

DR. ROGER PIELKE
DEPT. OF ATMOS. SCIENCES
COLORADO STATE UNIVERSITY
FT. COLLINS, CO 80523